DYNAMICAL ELECTROMAGNETIC FIELDS NEAR BLACK HOLES

AND

MULTIPOLE MOMENTS OF STATIONARY, GENERAL RELATIVISTIC SYSTEMS

Thesis by

Wai Mo Suen

In Partial Fulfillment of the Requirements

for the Degree of

Doctor of Philosophy

California Institute of Technology

Pasadena, California

1985

(Submitted May 21, 1985)

ACKNOWLEDGEMENTS

I would like to thank my advisor, Kip Thorne, for his support and guidance during my years at Caltech. Part of the work reported in this thesis was done jointly with my officemate Douglas Macdonald, whom I wish to thank for a very pleasant collaboration. My work at Caltech has benefited from the many discussions I have had with the other members of the Paradigm Society. Long live the Society! Also all of my work would not have been possible without the many sacrifices of my wife Wai Man through all these years.

This dissertation was supported in part by the National Science Foundation under Grant Number (AST82-14126).

ABSTRACT

This dissertation contains two works; one on the behavior of dynamical electromagnetic fields in the stationary spacetime generated by a black hole, and the other on the structure of a general stationary vacuum spacetime itself.

The study of electromagnetic field is carried out in terms of the "membrane formalism" for black holes; and it is part of a series of papers with the aim of developing that formalism into a complete, self-consistent description of electromagnetic and gravitational fields in a black hole background. Various model problems are presented as aids in understanding the interactions of electromagnetic fields with a black hole, and special attention is paid to the concept of the "stretched horizon" which is vital for the membrane formalism.

The second work develops a multipole moment formalism for a general stationary system in general relativity. The multipole moments are defined in terms of a general formal series solution of the stationary Einstein equation, in analogy to multipole moments in the Newtonian theory of gravity. These relativistic moments exhibit many desirable properties and are shown to be useful in studying the interactions between a gravitating body and an external gravitational field. A model calculation applying the formalism to a black hole interacting with an external multipole field shows that the interaction can be understood in terms of "elastic moduli" of the black-hole horizon.

TABLE OF CONTENTS

CHAPTER I

INTRODUCTION AND OVERVIEW

The general theory of relativity satisfies one of the requirements to be a great physical theory[1] —it is so simple in form that it can be printed on a T-shirt:

$$\mathcal{G} = 8\pi\mathcal{T}, \tag{1}$$

i.e., the Einstein tensor describing the structure of the spacetime is set equal to 8π times the energy momentum tensor. However in many ways general relativity is one of the hardest, if not the hardest physical theory to work with. It is a 10-component-tensor theory; it is badly nonlinear; it contains a lot of coordinate (gauge) freedom; and, most importantly, it describes at the same time a dynamical field, and the background on which the field exists. Other physical field theories are usually written down in a fixed background, namely a flat 3 dimensional space with a uniformly flowing time; and the physical effects of such theories are described in terms of a preferred set of observers residing in this fixed background, namely the inertial observers. By contrast, in general relativity, the metric tensor $g_{\mu\nu}$ plays both the role of the field and of the background. In general relativity there may not even be a set of background-preferred-observers. This mixing up of dynamical field and background and this losing of a preferred set of observers hinders us a lot in getting a physical feeling for the theory and in borrowing the physical intuition obtained in other theories to understand relativity. This is particularly unfortunate since the mathematical complexity of the theory gives us great need for physical feeling and intuition.

However, in not all physically interesting situations in relativity must we deal with the full problem of dynamical spacetime. There are often situations where the structure of the spacetime separates naturally into a

background plus a dynamical field living in it. This background is often non-flat, and along with it the preferred set of observers to describe the physics is often non-inertial. In these cases, it is possible to reformulate the generally covariant four-dimensional Einstein theory so as to make this separation of background and field explicit. Of course, this reformulation, at the same time, will destroy the explicit four-dimensional covariance of the theory — a price worth paying in return for physical understanding and intuition.

By far the most important case where such a separation comes up is when we have a nearly-stationary spacetime, i.e., a stationary spacetime with either weak or slow changes in "time". In fact, all "everyday physics" which is written down in a background of fixed space and time falls into this category, including the Newtonian theory of gravity, which can be regarded, in the language of general relativity, as a first order, quasi-stationary (both weak and slow) perturbation of a flat background spacetime. In other cases, when gravity cannot be taken as weak but is still nearly stationary, the background appropriate for the study of physical phenomena will no longer be flat, but rather will be curved and may even be topologically non-trivial.

This dissertation will discuss two works, both based on such a separation of a stationary spacetime. The first work is on the membrane formalism for black holes, which studies dynamical fields in a stationary black-hole spacetime; and the second work is on a multipole moment formalism which studies the structure a stationary spacetime itself.

A. The Membrane Formalism for Black Holes

The effects of general relativity have their full strength in the environment of a black hole. A black hole is so clean that it can be fully characterized by only three parameters, its mass, angular momentum and charge. Yet the phenomena associated with it are so rich and exotic (Hawking radiation, superradiance ..., and even a pathway to another world) that it is surely the most interesting of all playgrounds for relativists. However, there is an even more important reason to study black holes: They are nowadays thought to be rather common objects existing in the real universe. Indeed, a wide variety of exotic phenomena are now postulated to be associated with black holes: quasars, jets, Seyfert galaxies, strong X-ray sources.... There is probably even one in the center of our own galaxy[2]. Hence it is important to understand the physics of black holes in astrophysical environments.

The postulated black holes in astrophysical environments share one common property: The strong gravitational field of the hole produces enormous effects on the surrounding material, producing sometimes spectacular phenomena, e.g., the extremely high luminosities (up to 10^{46}erg/sec!) of quasars. However, the surrounding material influences the hole only slightly: the 10^{46}erg/sec luminosity corresponds to an accretion rate of about $0.1M_{\odot}$/yr whereas the central black hole has a mass of order $10^{8}M_{\odot}$ ($M_{\odot}$ denotes the mass of the sun). As a result of this accretion and interaction with the surrounding material, the hole will evolve only quasi-stationarily; and changes in the hole's mass and angular momentum will become significant only after an astronomically long time. In other words, the astrophysically interesting phenomena are taking place on an essential fixed background generated by a stationary black hole.

As was discussed above, it would be advantageous to analyse such situations in terms of a separation of the spacetime physics into a background plus dynamical fields. This separation can be carried out in terms of a 3+1 formulation of general relativity specialized to a stationary black-hole geometry.

When a 4-dimensional spacetime is stationary, it is clear that in some sense we can regard it as a stack of 3-dimensional "space-slices", each with the same geometry and labeled by the parameter "time". However there is more than one way (indeed an infinite number of ways) to choose such identical slices. Arbitrarily picking one way of slicing is not desirable; the resulting description of physics would be entangled with features coming from this artificial choice. Hence it is important to notice that we do require something more for the slicing to produce a good physical picture: the observers who are moving orthogonal (in a 4-dimensional sense) to the spatial slices have to see unchanging geometry. For a general stationary spacetime, it may not be possible to fulfill this requirement. However, due to the additional axial symmetry in a black-hole spacetime, such a choice is possible. After the slicing up of the spacetime, the spaceslices take on a role analogous to that of Galilean absolute space. At each point in the absolute space there resides a fiducial observer (FIDO), with respect to whom the laws of physics are measured and formulated. The only difference between this absolute space and Galilean absolute space is that this one is not flat; and its curvature gives rise to a variety of physical phenomena such as the gravitational deflection of light and a precession of gyroscopes that orbit the hole.

The curvature of absolute space is not the only gravitational effect that FIDOs will experience. The other effects have to do with the way the space slices are stacked up. The slices are labeled with a parameter t, and

naturally this t plays the role of the universal time of the Galilean picture. That is, events occurring at the same value of t, i.e., on the same slice, will be perceived by the FIDOs as simultaneous. However this universal time is not and cannot be the time that the FIDOs' clocks measure. Gravity changes the way the clocks tick; and as the strength of gravity for different FIDOs is different, their clocks tick at different rates and there is no way to match them up to a universal time. This effect is described by a lapse function α, which is the ratio of the ticking rate of universal time t to that of FIDO-measured time τ ($\alpha \equiv d\tau / dt$), and is a function of position in absolute space. Similarly the FIDOs cannot be fixed in position with respect to each other. Rather, they are forced by the hole's "dragging of inertial frames" to shift position with respect to each other as time passes. The effect is described by a shift function $\vec{\beta}$, which is a 3-vector in absolute space.

The full metric describing the geometry of the 4-dimensional spacetime can be expressed in a way which shows these effects explicitly:

$$ds^2 = -\alpha^2 dt^2 + g_{ij}(dx^i + \beta^i dt)(dx^j + \beta^j dt) , \tag{1.2}$$

where Latin indices runs from 1 to 3 and repeated indices are to be summed. Stationarity of the spacetime amounts to the requirement that α, β^i and g_{ij} are functions of x^k only. The absolute space is a t =constant slice; hence the curvature of it is determined by the line element

$$ds^2 = g_{ij} dx^i dx^j , \tag{1.3}$$

where g_{ij} is a 3-tensor (3-metric) living in the absolute space.

Therefore, for a stationary spacetime, after the 3+1 split, gravity is described in terms of $\alpha(x^k)$, $\beta^j(x^k)$ and $g_{ij}(x^k)$. [Of course these α, β^j and g_{ij} are not independent of each other. They are interrelated by the Einstein

equations]. Now this universal time and absolute space form a background for the evolution of dynamical fields. On this background there may be material flowing around; electromagnetic radiation and even gravitational radiation pouring out. However all such physical processes are presumed to have only negligible effects on the properties of the background — unless one integrates over very long time, e.g., $\Delta t \approx 10^8$ years.

From the viewpoint of the FIDOs, the dynamical fields and material flow can be described in a language similar to that of everyday flat-space physics. For example, in an electromagnetic field, a FIDO will measure by his instruments an electric field E^i and a magnetic field B^i, both of which are 3 vectors in absolute space. These measurements of E^i and B^i are of course affected by the state of motion of the FIDOs; and the differential equations relating E^i and B^i at different points in the absolute space, i.e., the "Maxwell equations", will be affected by the motion of the FIDOs with respect to each other and by the curvature of the absolute space. As a result, the Maxwell equations will take up forms analogous to the flat-space equations but will have contributions from the lapse function, shift function and curvature of the background. [For more discussion see Thorne and Macdonald,[3] and chapter II of this dissertation.] Likewise, a weak, dynamical gravitational field evolving on the background is described by an electric type curvature tensor E_{ij} and a magnetic type curvature tensor B_{ij}, both of which are 3-tensors living in the absolute space, which are treated in detail in Refs. 4,5,6.

For the situation of a stationary black hole, our requirements for the choice of the absolute space restrict us to use the "Boyer-Lindquist space slices", i.e., the t=constant slices in the Boyer-Linquist coordinate system (see e.g., MTW[7] Sec. 32.3); and the FIDOs become the zero-angular-momentum observers ("ZAMOs") of Bardeen (1970)[8] (see e.g., MTW Sec.

33.4). In this case, the lapse function, shift function and absolute space line element are given by:

$$\alpha = \frac{\rho}{\Sigma}\sqrt{\Delta}\ ;\ \beta^r = \beta^\theta = 0\ ,\quad \beta^\varphi = -\omega, \tag{1.4}$$

$$ds^2 = (\frac{\rho^2}{\Delta})dr^2 + \rho^2 d\theta^2 + \varpi^2 d\varphi^2\ , \tag{1.5}$$

with

$$\Delta \equiv (r-r_+)(r-r_-)\ ,\quad \rho^2 \equiv r^2+a^2\cos^2\theta\ , \tag{1.6}$$

$$\Sigma^2 \equiv (r^2+a^2)^2-a^2\Delta\sin^2\theta\ ,\quad \varpi\equiv(\Sigma/\rho)\sin\theta\ ,\quad \omega \equiv \frac{2aMr}{\Sigma^2}; \tag{1.7}$$

$$r_+ = m+\sqrt{m^2-a^2}\ ,\quad r_- = m-\sqrt{m^2-a^2}\ , \tag{1.8}$$

where m is the mass and ma is the angular momentum of the black hole. The horizon of the hole is located at $r=r_+$. Immediately we noticed that our absolute-space/universal-time formulation is good only for $r>r_+$. When $r<r_+$, Δ is negative, α becomes imaginary, and the absolute space line element is no longer positive definite [cf. Eq. (1.5)]. Therefore the region inside the black-hole horizon is not included in the formalism, and we have to supply boundary conditions on the horizon for the dynamical fields in our absolute space before a complete picture is obtained.

It has been known for some time that the physical laws on the black-hole horizon can be cast into a form closely analogous to everyday physics [Damour (1978),[9] Znajek (1978)[10]], i.e., in a form where various terms can be identified as representing the effects of an electric conductivity, shear and bulk viscosity, surface pressure , entropy and temperature. Hence in order to obtain a complete Galilean-like picture we must reformulate these horizon equations as boundary conditions for physical fields and matter in

absolute space.

The situation is not as straightforward as one may think at first sight. From Eq. (1.4), we see that when one is far away from the black hole in the absolute space ($r \gg r_+$) the ZAMO-measured-time and the universal time march forward together at the same pace. But as one approaches the horizon, α goes to zero causing universal time to tick slower and slower. Such a situation is illustrated in fig. (1.1) in terms of a spacetime diagram in Eddington-Finkelstein coordinates, (a coordinate system in which the time coordinate is well behaved at the horizon; cf. MTW Box 31.2). [For simplicity the angular momentum of the hole has been set to zero in the figure.] It is seen that the absolute space represented by a t = constant line dips more and more into the past as one approaches the horizon, so that the line and the horizon never intersect.

To properly impose the boundary condition as one approaches the horizon, the concept of a "stretched horizon" is introduced. [See Ref.3 and Sec. 1 of chapter II.] As illustrated by the dotted line in fig. (1.1), we consider the boundary of the absolute space to be located at a radius slightly larger than r_+, i.e., at a stretched horizon so chosen that everywhere on the stretched horizon the lapse function α has a constant value α_H, which is small but non-zero. Then it is easy to show that the horizon equations of Damour and Znajek [9,10] can be translated to this stretched horizon with fractional errors of order $\alpha_H \ll 1$.

This picking-the-boundary-at-finite-α_H throws away the information on the piece of the t =constant slice below the stretched horizon. Indeed, what is recorded in this part of the slice is the past history of the material and field that have fallen into the black hole long ago in the Eddington-Finkelstein time; past history that has no influence on the future evolution

of the dynamical field in the absolute space. The entropy of a black hole can be understood in terms of this throwing away of information.[11]

Now we have a complete picture: In the absolute space there are matter and fields evolving forward in universal time according to field equations closely analogous to their flat space counterparts. The effect of the background gravity is described in terms of a scalar α, a 3-vector β^j and a 3-metric tensor g_{ij}. This background gravity is produced by the central black hole which is a 2-dimensional membrane (the stretched horizon) endowed with everyday physical properties. When perturbed by external fields and matter, this membrane will respond by deformation, vibration, expansion, electric current flow etc.. Hence we call this the "membrane formalism for black holes". Of course, this picture is not expected to be very useful when the external perturbations are large and the whole spacetime becomes dynamical, as then there will be no preferred choice for splitting up the spacetime into background and fields. However, such a picture is useful in actual calculation, and more importantly in providing physical intuition and understanding in physical situations where the black hole is essentially in an equilibrium state, i.e., in nearly all astrophysical situations.

The idea that a black hole behaves in close analogy with an everyday object is not new. In various ways of analysis, a black hole has previously been shown to have a temperature and entropy[12], to spin down due to the tidal effects of an external moon[13], to be torqued by Eddy currents induced by an external magnetic field[14], and to behave in an static external electric field in essentially the same way as a conducting sphere[15]. It was these previous calculations that motivated our Caltech group, led by Kip Thorne, to develop the membrane formalism as a consistent and unified treatment for the description and understanding of black holes in astrophysical

environments.

The foundations of the electromagnetic aspects of the membrane formalism were laid in a paper by Thorne and Macdonald;[3] and Macdonald and Thorne[16] used the resulting formalism to analyse stationary black-hole magnetospheres. Chapter II of this dissertation is a paper by Douglas Macdonald and the present author, in which the membrane formalism is used to study the evolution of dynamical electromagnetic fields in a black hole background. In the first two sections of this chapter, we review the electromagnetic membrane formalism and develop the concept of the stretched horizon introduced in Ref. 3. In Sec. 3, we study in detail the evolution of electromagnetic fields generated by moving charges in the vicinity of a black hole horizon and the effects of these electromagnetic fields on the black hole. In Sec. 4 we study a vibrating magnetic field in the vicinity of a a black hole; this study illustrates the process of settling down of an electromagnetic field to its equilibrium configuration in a black-hole environment. In all these dynamical processes, the concept of stretched horizon is important, and special attention is paid to this concept and the requirements on choosing its location. In the last section of this chapter we discuss how the intuitions gained from our model problems can be used to understand other situations of electromagnetic fields in a stationary background of a black hole.

The gravitational aspect of the membrane formalism are in a series of papers now being written, but are not yet finished, by Price and Thorne[4], Suen, Price and Redmount,[5] and Thorne et al.[6]

B. A Multipole Moment Formalism for Stationary, Asymptotically-Non-Flat Systems

Chapter III of this thesis presents a multipole formalism for stationary, nonasymptotically flat systems in general relativity, developed by the author. Here again we consider a stationary spacetime. But now instead of studying dynamical fields in it, we want to study the structure of the spacetime itself, using the idea of a multipole analysis which is so fruitful in studies of Newtonian gravitational field and the structure of other fields in everyday physics.

Here again in the stationary spacetime we can choose a time coordinate t, such that all the t=constant slices have the same geometry. However for a general stationary spacetime there does not exist the preferred set of observers of the type that we used in the black hole case, who are moving perpendicular (in a 4-dimensional sense) to the t=constant slices and also see unchanged geometry as time goes on. Without this requirement of "preferred-observers" in choosing the 3-dimensional spaceslices, there is ambiguity in the definition of the coordinate t (i.e., we require that $\partial/\partial t$ be the time-like Killing vector of the spacetime, but the zero point of t can be a function of the spatial coordinates). We will leave this freedom unfixed until later.

As before, in our absolute space the effect of gravity is given by the lapse function α, the shift function β^j and the 3-tensor g_{ij}. However they are not the most convenient variables to be used for multipole analysis; instead, we will use a different combination of them. To illustrate this we first briefly review the multipole moment formalism in Newtonian theory.

In Newtonian theory the gravitational field is characterized by a scalar function φ, which satisfies the Laplace equation

$$\nabla^2\varphi = 0 \tag{1.9}$$

in free space. The general solution of this equation is expressible in terms of an expansion in spherical harmonic with appropriate powers of r. The coefficients of the terms in the expansion are the multipole moments. Any φ satisfying (1.9) uniquely determines a set of multipole moments. And given any set of multipole moments, as long as the corresponding series expansion converges, it gives a φ satisfying (1.9). Hence any φ can be considered as a collection of multipole fields, and each piece of it represents a well known structure. Surely a good part of our understanding of the structures of Newtonian gravitational fields (and also of electric and magnetic fields) comes from this multipole analysis.

How can we generalize this analysis to general relativity? Immediately we see many obstacles: (i) The Einstein field equations for α,β^j and g_{ij} are nonlinear and do not satisfy the Laplace equation. (ii) Even when we regard the effects of gravity to be small, i.e., regard $\alpha-1$, β^j and $g_{ij}-\delta_{ij}$ as small and keep them only to linear order, they still do not satisfy in general the Laplace equation. (iii) The identification of the multipole moments in the Newtonian potential depends on an expansion in the spatial coordinates, but now we have complete freedom in choosing our coordinates on the spaceslices. It is absolutely unclear that the multipole expansion resulting from any one choice will be superior *a priori* to that from other choice. (iv) As was discussed above, there is even freedom in the way to slice up spacetime. (v) The Lapse function α, shift function β and 3-metric tensor g_{ij} are interrelated with each other. Therefore if we expand them individually and define separately for each of them a set of multipole moments, those moments will be interrelated and cannot be specified arbitrarily.

Fortunately, all these problems are in fact related to each other, and can be made to disappear all together when we employ the deDonder coordinate formulation of the Einstein equations [see e.g., Landau and Lifshitz[17] and Sec. 2 of Chapter III]. In this formulation the field variables, denoted $\bar{h}^{00}$, $\bar{h}^{0i}$ and $\bar{h}^{ij}$. are the deviations of the metric density $\sqrt{-g}\,g^{\alpha\beta}$ from the Minkowskian metric: $\bar{h}^{\alpha\beta}=\eta^{\alpha\beta}-\sqrt{-g}\,g^{\alpha\beta}$. These quantities are regarded as fields living in a flat Galilean 3 space,and correspondingly their indices are raised and lowered by δ^{ij}. When the $\bar{h}$'s are small, i.e., gravity is weak, to the linear order they satisfy the Laplace equation. At higher orders, the self interactions of the fields produce source terms, and the field equations become Poisson equations. However, multipole moments enter always as the homogeneous parts of the solutions of the Poisson equations. Moreover, by making use of the residual coordinate freedom (still staying within a deDonder coordinate system), we can make the multipole moments appear only in the expansions of $\bar{h}^{00}$ and $\bar{h}^{0i}$; with $\bar{h}^{ij}$ carrying no extra degrees of freedom.

Such a program for multipole analysis in general relativity was developed by Thorne[18], for the special case of asymptotically flat systems. He showed that the expansion of $\bar{h}^{00}$ determines a set of mass multipole moments characterizing the mass distribution of the central gravitating body, whereas the expansion of $\bar{h}^{0j}$ determines a set of current multipole moments characterizing the distribution of material flow of the central body. Subsequently Gursel[19] showed that Thorne's definitions of mass and current moments are identical to those of Geroch and Hansen[21], who developed a multipole formalism using geometric considerations in terms of a compactified conformal space associated with the 3 dimensional family of time-like Killing trajectories of the physical spacetime. For a brief review of

these and other multipole moment formalisms for asymptotically flat systems, see Ref. 20.

What about a general stationary spacetime without the asymptotic flat assumption, i.e., when the central body is subjected to an externally applied gravitational field? Can the interaction between the central body and the applied field be discussed in terms of multipole moments? Indeed, in the Newtonian theory, such interactions give rise to the acceleration, torque, and deformation of the central body — phenomena described elegantly in terms of multipole moments. Chapter III is devoted to a study of these questions in general relativity — a study whose central feature is the development of a Thorne-type multipole formalism for a general, stationary system.

Section 1 of chapter III introduces and briefly reviews multipole moment formalisms in general relativity. Sec. 2 begins by making precise the systems that the new, nonasymptotically flat multipole formalism will be useful for. As in Newtonian theory, the multipole formalism is a useful tool for calculation only when we are not in the immediate vicinity of the central or distant gravitating bodies; where the multipole expansion may not converge fast; i.e., it is useful as a tool for calculation only in a vacuum "buffer zone". Sec. 2A provides an algorithm for constructing the formal general series solution of the stationary vacuum Einstein equations in a deDonder coordinate system in terms of four sets of multipole moments. These moments characterize the mass distribution and material flow of the central body and of the external universe (which generates the external gravitational field). Sec. 2B discusses some general properties of the multipole expansion. Sec. 2C shows that in the present formalism, the spatial coordinates have been restricted to translations of origin and rotations of coordinate axes whereas the time coordinate is fixed up to an overall constant.

In Sec. 3 and Sec. 4 we study the properties of the multipole moments. It is shown that they do have many properties that we expect multipole moments tc have. In Sec. 5 and Sec. 6, we turn to the question of using the multipole moments to describe the gravitational interaction between the central body and the external field it resides in. Sec 5 shows that the force law and torque law in terms of the multipole moments are in exact analogy with their Newtonian counterparts, but now they are valid even for strongly gravitating objects. This result generalizes analogous results of Thorne and Hartle[22] and of Zhang[23]. In Sec. 6 we turn to the third kind of effect, namely, deformation of the central body by external gravity. In the Newtonian theory the change in multipole moments, i.e., the "induced moments", of a body in an external field, are determined not only by the field equations but also by the equation of state of the material making up the body. The same is true in general relativity, except for a black hole, whose mechanical properties must solely be determined by the Einstein equations. Therefore we ask: What is the induced multipole moment when a black hole is put in an external multipole field? In Sec. 6, the model problem of a Schwarzschild black hole in an external quadrupolar gravitational field is studied. It is shown that the response of the black hole to the external field is the same as that of an elastic shell with a surface bulk modulus $\tilde{\kappa}=\infty$, (i.e., the black hole is incompressible); and a surface shear modulus $\tilde{\mu}=-63/(20\pi m)$, where m is the hole's mass, (i.e., a smaller hole is stiffer).

The calculations of Sec. 5 and Sec. 6 reveal that the new multipole moment formalism is a powerful tool for probing the properties of a stationary gravitational field and for understanding the interactions of a body with an external field. Further discussion of the multipole formalism is given in Sec. 7 of the chapter.

REFERENCES

[1] Proclaimed by a distinguished physicist whose name I have forgotten.

[2] See, e.g., R. L. Brown and H. S. Liszt, Ann. Rev. Astron. Astrophys. **22**, 223 (1984).

[3] K. S. Thorne and D. Macdonald, M. N. R. A. S. **198**, 339 (1982)

[4] R. H. Price and K. S. Thorne, Phys. Rev. D. (in preparation).

[5] W. M. Suen , R. H. Price and I. H. Redmount, Phys. Rev. D. (in preparation).

[6] K. S. Thorne, R. H. Price, W. M. Suen, D. A. Macdonald, I. H. Redmount, R. J. Crowley, X. H. Zhang and W. H. Zurek, Rev. Mod. Phys. (in preparation).

[7] C. W. Misner, K. S. Thorne and J. A. Wheeler, *Gravitation* (W. H. Freeman, San Francisco 1973), cited in text as MTW.

[8] J. M. Bardeen, Astrophys. J. **162** 71 (1972).

[9] T. Damour, Phys. Rev. D. **18**, 3598 (1978); see also T. Damour, in *Proceedings of the Second Marcel Grossmann Meeting on General Relativity* ed. R. Ruffini, (Amsterdam: North Holland).

[10] R. Znajek, M. N. R. A. S. **185**, 833 (1978).

[11] W. H. Zurek and K. S. Thorne, Phys. Rev. Lett. submitted.

[12] J. D. Bekenstein, Nuovo Cimento Lett. **4**, 737 (1972); S. W. Hawking, Nature **248**, 30 (1974); S. W. Hawking, Commun. Math. Phys. **43**, 199 (1975).

[13] S. W. Hawking and J. B. Hartle, Commun. Math. Phys. **27**, 283 (1972); J. B. Hartle, Phys. Rev. D. **9**, 2749 (1974).

[14] T. Damour, Phys. Rev. D. **18**, 3598 (1978).

[15] R. S. Hanni and R. Ruffini, Phys. Rev. D. **8**, 3259 (1973).

[16] D. Macdonald and K. S. Thorne, M. N. R. A. S. **198**, 345 (1982).

[17] L. D. Landau and E. M. Lifshitz, *The Classical Theory of Fields* (Pergamon Press, Oxford 1973).

[18] K. S. Thorne, Rev. Mod. Phys. **52**, 299 (1980).

[19] Y. Gürsel, Gen. Rel. & Grav. **15**, 737 (1983).

[20] R. Geroch, J. Math. Phys. **11**, 2580 (1970); R. D. Hansen, J. Math. Phys. **15**, 46 (1974).

[21] A. Ashtekar, in *General Relativity and Gravitation* ed. B. Bertotti, F. de Felice and A. Pascolini, (D. Reidel Company, Dordrecht 1983).

[22] K. S. Thorne and J. B. Hartle, Phys. Rev. D. (in press).

[23] Z. H. Zhang, Phys. Rev. D. (in Press).

FIGURE CAPTION

Fig. 1.1: The surfaces of constant universal time t around a black hole with zero angular momentum ($a=0$), as viewed in Eddington-Finkelstein coordinates. The Eddington-Finkelstein time coordinate $\tilde{t}$ is related to universal time by $\tilde{t}=t+2m\ln(r/2m-1)$, and the Eddington-Finkelstein radial coordinate r is identical to the Boyer-Lindquist or Schwarzschild r. The cones are the radial light cones. A "stretched horizon" H_s located at a small distance outside the true horizon H is denoted by the dotted line.

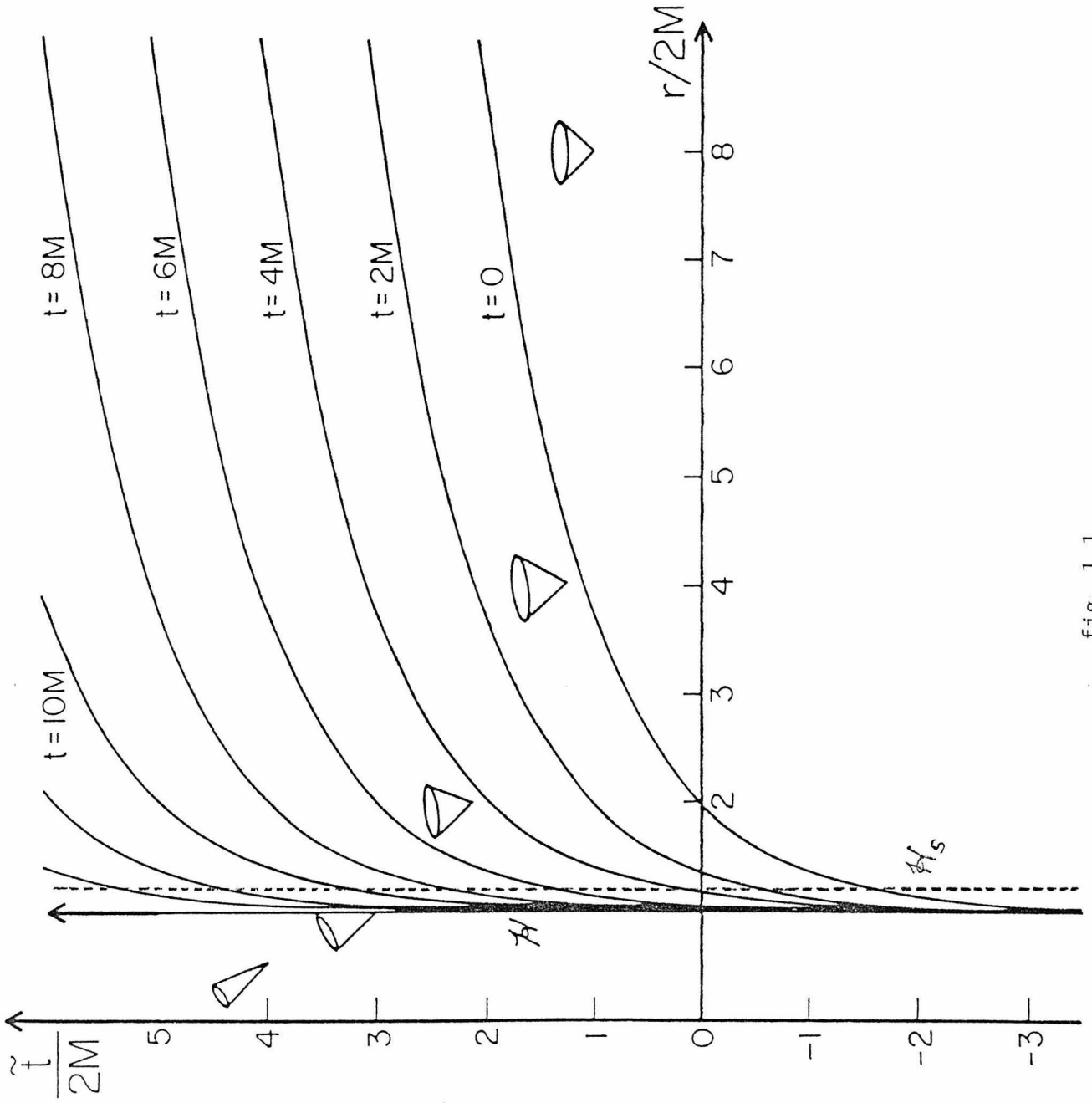

fig. 1.1

CHAPTER II

THE MEMBRANE VIEWPOINT ON BLACK HOLES: DYNAMICAL ELECTROMAGNETIC FIELDS NEAR THE HORIZON

Douglas A. Macdonald and Wai-Mo Suen

Theoretical Astrophysics and Gravitation
California Institute of Technology
Pasadena, California 91125
(received XX December 1984)

ABSTRACT

This paper is part of a series of papers with the aim of developing a complete self-consistent formalism for the treatment of electromagnetic and gravitational fields in the neighborhood of a black-hole horizon. In this *membrane* formalism, the horizon is treated as a closed two-dimensional membrane lying in a curved three-dimensional space, and endowed with familiar physical properties such as entropy and temperature, surface pressure and viscosity, and electrical conductivity, charge, and current. This paper develops the concept of the "stretched horizon" which will be vital for both the electromagnetic and gravitational aspects of the formalism, and it presents several model problems illustrating the interaction of dynamical electromagnetic fields with stationary black-hole horizons: The field of a test charge in various states of motion outside the Schwarzschild horizon is analyzed in the near-horizon limit, where the spatial curvature may be ignored and the metric may be approximated by that of Rindler. This analysis elucidates the influence of the horizon on the shapes and motions of electric and magnetic field lines when external agents move the field lines in arbitrary manners. It also illustrates how the field lines interact with the horizon's charge and current to produce an exchange of energy and momentum between the external agent and the horizon. A numerical calculation of the dynamical relaxation of a magnetic field threading a Schwarzschild black hole is also presented, illustrating the "cleaning" of a complicated field structure by a black-hole horizon, and elucidating the constraints on the location of the stretched horizon.

I. INTRODUCTION

During the 1970's theoretical studies of the physics of black holes showed that black-hole horizons behave as though they were endowed with various physical properties, including entropy and temperature,[1-5] surface pressure and viscosity,[6,7] and electric conductivity, charge, and current.[8-10] Motivated by these studies, in 1978 Damour[10] reformulated the standard theory of black-hole horizons in terms of precise boundary conditions which involve these horizon properties and others. (See also the independent, partial reformulation by Znajek.[8])

Damour's formalism is a powerful foundation on which to build a physically intuitive picture of black-hole physics. But it is only a partial foundation. An intuitive picture of black holes needs, in addition, an intuitively familiar formulation of the laws of physics for the surrounding spacetime, which may contain accretion disks, electromagnetic fields, orbiting stars, etc. The standard generally covariant laws of general relativity do not do the job; but if one performs on them a "3+1 split" (a split of spacetime into space plus time), they acquire an adequately intuitive form.

These considerations have led the authors and their Caltech colleagues to combine Damour's horizon formalism with a 3+1 split of the spacetime around a black hole, thereby obtaining a reformulation of the laws of physics which has intuitive appeal and power. Because this reformulation regards the horizon as a two-dimensional, membrane-like surface residing in a three-dimensional space (and evolving as time passes), we call it the "membrane formalism" for black holes.

Our membrane formalism is completely equivalent, mathematically, to the standard general relativistic black-hole formalism (see, for example, chapters 33 and 34 of MTW[11] and the theoretical sections of Dewitt and

Dewitt[12]); but the mental and verbal pictures associated with the two formalisms are rather different. Our membrane studies (mostly not yet published) suggest that the standard formalism and pictures are the more powerful for studying highly dynamical black holes, but that the membrane formalism and pictures will be more powerful for studying complicated physics around slowly evolving holes. Thus, we regard the membrane formalism as a potentially powerful tool for theoretical astrophysics.

This is the third paper in our research group's series on the membrane formalism. Paper I, by Thorne and Macdonald,[13] constructed the 3+1 split of electromagnetic theory in an arbitrary curved spacetime; then it specialized the 3+1 electromagnetism to the spacetime outside a rotating black hole and there married it to Damour's horizon equations to give the electromagnetic portion of our membrane formalism. Paper II, by Macdonald and Thorne[14] used this membrane formalism to analyze the structure of stationary, axisymmetric black-hole magnetospheres and to study the Blandford-Znajek[15] process, by which such magnetospheres may power quasars and active galactic nuclei.

In this third paper we turn from stationary electromagnetic fields outside black holes to dynamical electromagnetic fields. Our objective is to build up physical intuition by studying a number of idealized thought experiments in which dynamical fields interact with the horizon of a stationary black hole.

In future papers in this series, we and other members of our Caltech group will develop the membrane formulation of gravitational perturbations of a stationary black hole,[16] we will study idealized thought experiments which give physical insight into gravitational perturbations and their effects on the evolution of the hole,[17] and we will present a pedagogical review of the

formalism and its insights.[18]

For the sake of brevity, we assume in this paper that the reader is fully familiar with general relativity theory, at least at the level of track 1 of MTW. However, our future review paper[18] will be written in a form understandable to people who have had only vague contacts with relativity theory.

The structure of this paper is as follows:

In Sec. II, we review the electromagnetic features of the membrane viewpoint and introduce the concept of the *stretched horizon*, which is fundamental to both the electromagnetic and the gravitational aspects of the membrane viewpoint.

In Sec. III, we study electromagnetic fields very near the horizon of a Schwarzschild black hole. We focus attention on a region close enough to the horizon that the curvature of space can be ignored. In this region, the Schwarzschild geometry may be approximated by the algebraically simpler Rindler[19] geometry. We derive the general solution of the electromagnetic field equations in Rindler spacetime and apply it to obtain the fields of charges in various states of motion near the hole's stretched horizon. Those fields (Figs. 3-11) give insight into the electromagnetic properties of the stretched horizon.

Section IV presents a numerical calculation modeling the fully dynamical evolution of a magnetic field in a Schwarzschild background (Figs. 12-15). This example illustrates the "cleaning" of a complicated electromagnetic field by a hole's stretched horizon and also elucidates the constraints on the amount of stretching one should do when passing from the true horizon to the stretched horizon.

Section V describes how the intuition gained from the model problems of Secs. III and IV can be used to understand heuristically other interactions

of black holes with electromagnetic fields.

II. THE 3+1 FORMALISM AND THE STRETCHED HORIZON

In this section, we will briefly review the electromagnetic aspects of the membrane viewpoint, mainly in order to define terms and notation for later use. For further details and derivations, see Thorne and Macdonald[13] (henceforth denoted TM) and Macdonald and Thorne[14] (henceforth denoted MT).

In the 3+1 formalism, we choose a space-filling, rotation-free family of timelike fiducial observers (FIDO's), whose world lines cover the entire spacetime outside the black hole; and we regard the hypersurfaces orthogonal to their world lines as a curved, "absolute" three-dimensional space viewed at different moments of time. (The fact that the congruence is rotation-free guarantees the existence of these hypersurfaces.) We label the hypersurfaces with a parameter t, which we call "universal time." The relation between the proper time τ of the FIDO's and the universal time t is given by the lapse function

$$\alpha = \left.\frac{d\tau}{dt}\right|_{\text{along FIDO world line}} \tag{2.1}$$

The negative four-acceleration of a FIDO $\vec{g} = -\vec{\nabla}\ln\alpha$ lies in the absolute space and plays the role of the "gravitational acceleration measured by the FIDO." (Here and throughout, all vectors and vector operators, e.g., $\vec{g}$ and $\vec{\nabla}$, are three-dimensional and live in the absolute space.) The magnitude of $\vec{g}$ diverges at the horizon, but the "renormalized" quantity $\alpha|\vec{g}|$ has a finite limit at the horizon; this limit is the "surface gravity" g_H of the hole.

The electric and magnetic fields and the charge and current densities are defined physically by measurements made by the FIDO's.

Mathematically this corresponds to the definition

$$E^\alpha = F^{\alpha\beta}u_\beta \quad , \quad B^\alpha = -\frac{1}{2}\varepsilon^{\alpha\beta\gamma\delta}u_\beta F_{\gamma\delta} \quad ,$$
$$\rho_e = -J^\alpha u_\alpha \quad , \quad j^\alpha = (g^{\alpha\beta} + u^\alpha u^\beta)J_\beta \quad , \tag{2.2}$$

where u^α is the FIDO four-velocity, $F^{\alpha\beta}$ is the Maxwell field tensor, and J^α is the four-current density. These E^α, B^α, ρ_e, and j^α are tangent to the hypersurfaces t = constant and thus live as three-vectors and scalars in absolute space. Using these electric and magnetic fields, the curved-space Maxwell equations take a form very similar to their flat-space analogues [see TM Eq. (3.4)].

The 3+1 formalism developed here will be most useful when a particular choice of fiducial observers is singled out by the geometry. For the problems we will study in this paper, namely, Schwarzschild black holes with dynamical electromagnetic "test" fields whose gravitational effects are ignored, such a preferred set of FIDO's is the set of "zero-angular-momentum observers", or ZAMO's.[20] With this choice, the global time parameter t is equal to the standard Schwarzschild time coordinate; the lapse function and the three-metric of absolute space have the form

$$\alpha = (1 - 2M/r)^{1/2} \, , \tag{2.3a}$$

$$ds^2 = (1 - 2M/r)^{-1}dr^2 + r^2(d\theta^2 + \sin^2\theta d\varphi^2) \, ; \tag{2.3b}$$

the horizon's surface gravity is

$$g_H = |\alpha\vec{\nabla}\ln\alpha|_{\alpha=0} = 1/4M \, ; \tag{2.3c}$$

and Maxwell's equations read

$$\begin{aligned} &\vec{\nabla}\cdot\vec{E} = 4\pi\rho_e \, , \\ &\vec{\nabla}\cdot\vec{B} = 0 \, , \\ &\partial\vec{E}/\partial t = \vec{\nabla}\times(\alpha\vec{B}) - 4\pi\alpha\vec{j} \, , \\ &\partial\vec{B}/\partial t = -\vec{\nabla}\times(\alpha\vec{E}) \, , \end{aligned} \tag{2.3d}$$

where M is the mass of the black hole.

Since our absolute three-dimensional space covers only the exterior of the black hole, Maxwell's equations have to be supplemented by a set of boundary conditions on the horizon, $\alpha = 0$, namely the Znajek[8]-Damour[10] horizon equations (TM Sec. 5.4). In attempting to apply these boundary conditions, however, we come up against a pathology of the family of spacetime hypersurfaces t = constant in terms of which the 3+1 split is made. Because the ZAMO world lines become null at the horizon, their orthogonal hypersurfaces also become null there; i.e., they coincide with the horizon as $\alpha \to 0$. They achieve this by extending deep into the past as they approach the horizon. This may be seen from Fig. 1, which shows the t = constant hypersurfaces plotted in spacetime as functions of the Eddington-Finkelstein time coordinate

$$\tilde{t} = t + 2M\ln(r/2M - 1)\,, \tag{2.4}$$

which is well-behaved at the horizon (cf. Box 31.2 of MTW). This ill behavior of the spatial hypersurfaces means that the ZAMO's will never see any infalling particle or any part of the electromagnetic field actually cross the horizon, but rather the ZAMO's will observe them asymptotically approach and hover just above the horizon. If the electromagnetic field is dynamical, the near-horizon fields will form a layered structure reflecting their entire past evolutionary history.

If one (mathematically) approaches the horizon along a particular t = constant hypersurface in order to try to define a horizon boundary condition at that moment of universal time t, one will not see the field settle down to a well-defined value which may be used as a boundary value. Rather, the field will point first one way, and then another, as one examines

the relic fields reflecting more and more ancient eras of the near-horizon region.

A way of avoiding this difficulty in defining boundary conditions at the horizon was suggested briefly in TM, Sec. 5.3, but was not developed there. This method consists of choosing a closed two-dimensional surface just outside the horizon, and applying boundary conditions on this surface rather than on the true horizon. We will call this surface the *stretched horizon*, and for mathematical convenience[16] we will take it to have a fixed (time-independent and angle-independent) location $\alpha = \alpha_H \ll 1$.

By defining boundary conditions on the stretched horizon, we ignore the layered fossil field structure between the stretched horizon and the true horizon. Field boundary values defined at the stretched horizon differ from the values on the true horizon at the same moment of $\tilde{t}$ time by terms of order α_H, so boundary conditions posed on the stretched horizon become increasingly accurate as the stretched horizon is moved closer to the true horizon. In solving a particular problem, the stretched horizon must be chosen so that fractional errors of order α_H are small enough to be tolerated. It also of course must be chosen so that no interesting physics takes place between the stretched horizon and the true horizon.

One purpose of the model problems in this paper is to demonstrate the efficacy of the procedure of stretching the horizon and to determine what constraints exist on the choice of its position.

The "membrane" version of the true horizon's electromagnetic boundary conditions, without an external 3+1 split, has been derived in elegant form by Znajek[6] and Damour[9,10]. Carter[21] reviews that formalism, and TM have translated it into 3+1 language. Although the TM version is not expressed specifically in terms of a stretched horizon, it is trivial to show

that when so expressed it takes the form described below.

The ZAMO-measured field components $\vec{E}_{\|}$ and $\vec{B}_{\|}$ parallel to the horizon diverge as α^{-1} when $\alpha \ll 1$. This is due to the fact that the ZAMO's are accelerating outward to keep from falling into the horizon; they are boosted to almost the speed of light $v \simeq 1$ relative to physically reasonable infalling observers, who see finite fields at the horizon. The horizon-parallel field seen by the ZAMO's thus diverges proportionally to the "gamma factor" $\gamma=(1-v^2)^{-1/2} \propto \alpha^{-1}$ of this boost, while the horizon-normal fields $E_n \equiv (\vec{E}\cdot\vec{n})_{SH}$ and $B_n \equiv (\vec{B}\cdot\vec{n})_{SH}$ remain finite. (Here $\vec{n}$ is the unit outward normal vector at the stretched horizon and the subscript SH denotes evaluation at the stretched horizon.) It is therefore convenient to define "renormalized" parallel fields on the stretched horizon

$$\begin{aligned} \vec{E}_H &\equiv (\alpha\vec{E}_{\|})_{SH} \ , \\ \vec{B}_H &\equiv (\alpha\vec{B}_{\|})_{SH} \ . \end{aligned} \tag{2.5}$$

These renormalized fields have the advantage that they are nearly independent of the location chosen for the stretched horizon. They are equal, to within fractional errors of order α_H, to the true-horizon fields defined by Znajek, Damour, Carter and MT. Since we will often have need of this concept, we will define the notation "$\cong$" to mean "equal, to within fractional terms of order α_H".

In terms of the horizon fields, one may define (imaginary) surface charge and current densities on the stretched horizon:

$$\sigma_H \equiv \frac{E_n}{4\pi} \ , \tag{2.6a}$$

$$\vec{\jmath}_H \equiv \frac{1}{4\pi}\vec{n}\times\vec{B}_H \ . \tag{2.6b}$$

These definitions link the horizon charges and currents to the external fields in the way which would be expected from Gauss's and Ampere's laws. An observer falling through the horizon would not see a charge layer or current sheet on the horizon, of course; but the fields seen by observers who remain outside the hole (e.g., ZAMO's) are accounted for by imagining that the surface charge and current exist on the stretched horizon and ignoring all charge and current, as well as the normal electric field E_n and tangential magnetic field $\vec{B}_{||}$, inside the stretched horizon. For example, the stretched horizon of a Reissner-Nordstrøm black hole with charge Q will have a uniform surface charge density $Q/$(surface area of stretched horizon) in the absence of external sources.

Znajek, Damour, Carter and MT show that one of the standard black-hole-horizon boundary conditions translates into an Ohm's law:

$$\vec{\jmath}_H \cong \frac{\vec{E}_H}{R_H} , \tag{2.7}$$

where $R_H \equiv 4\pi \simeq 377$ ohms is the surface resistivity of the stretched horizon. Moreover, another of the standard boundary conditions translates into the statement that the horizon charge and current densities "close the circuit" of external currents entering the stretched horizon:

$$(\alpha j_n)_{SH} \cong -\frac{\partial \sigma_H}{\partial t} - {}^{(2)}\vec{\nabla}\cdot\vec{\jmath}_H . \tag{2.8}$$

This equation says, more precisely, that whenever electric charge falls into the stretched horizon, it can be regarded as stopping its fall and thereafter moving around on the stretched horizon in a conserved manner, until such a time as it reemerges into the external universe (in the form of opposite charges moving inward, of course). The factor of α in Eq. (2.8) serves to

renormalize $\vec{j}$, the current density measured by ZAMO's, from a "per-unit-ZAMO-proper-time τ" basis to a "per-unit-global-time t" basis—the same kind of time as is used in $\partial\sigma_H/\partial t$ and in $\vec{\mathcal{J}}_H$.

Eqs. (2.6b) and (2.7) imply that

$$\vec{E}_H \cong \vec{n}\times\vec{B}_H \ , \tag{2.9}$$

i.e., the fields at the stretched horizon have the form of ingoing plane waves. This might have been expected from the fact that the horizon's surface resistivity $R_H = 4\pi$ is just the impedance of free space at the end of an open waveguide.

The horizon surface charges and currents enter into dynamical equations in the same way as do ordinary charges and currents. The rate of change of the horizon's momentum density (momentum per unit area) $\vec{\Pi}_H$ with respect to global time t, produced by an electromagnetic field, is given by the expected Lorentz-force law:[10,16]

$$\frac{d}{dt}\vec{\Pi}_H \cong \sigma_H\vec{E}_H + \vec{\mathcal{J}}_H\times B_n\vec{n} \ . \tag{2.10}$$

[If the hole begins precisely nonrotating at $t = 0$, then $\vec{\Pi}_H = 0$ at $t = 0$ and a subsequent growth of $\vec{\Pi}_H$ corresponds to a gradual spinup of the hole. For very slow rotation about the polar ($\theta = 0$) axis, the total angular momentum is[10,21] $J = \int_{SH}(\vec{\Pi}_H\cdot\partial/\partial\varphi)dA \cong I_H\Omega_H$, where $I_H = 4M^3$ is a Schwarzschild hole's moment of inertia[22] and $\Omega_H \ll 1/M$ is the angular velocity.] The fields also increase the black hole's entropy (area) in accord with the Joule-heating relation[8,9]

$$T_H\frac{dS_H}{dt} \cong \int_{SH}\vec{\mathcal{J}}_H\cdot\vec{E}_H dA \ , \tag{2.11}$$

where T_H is the black hole's temperature and S_H is its entropy; and they increase its mass in accord with the first law of black-hole thermodynamics[23] $dM = T_H dS_H + \Omega_H dJ$ ($\simeq T_H dS_H$ for very slow rotation).

The use of "renormalized quantities" on the stretched horizon may generate some initial uneasiness. We have defined all physical quantities living in the absolute space in terms of ZAMO measurements, and we could equally well have used these ZAMO-defined fields ($\vec{E}$, $\vec{B}$, σ, and $\vec{j}$) in defining the boundary conditions on the stretched horizon, without the renormalization factor α_H. The advantage of such an approach would be the simplicity of using a single set of fields in our absolute space and on the stretched horizon; the disadvantage would be that the unrenormalized stretched-horizon fields would depend very sensitively on α_H, i.e., on the location chosen for the stretched horizon, and in general they would diverge as the stretched horizon approached the true horizon. Clearly, since α_H is chosen to be a constant throughout this work, all equations we write down describing the physical properties of the stretched horizon and the relations between its various fields would be valid regardless of which convention was adopted. However, we will choose to present the horizon boundary conditions in terms of the renormalized field quantities in order to maintain notational consistency with Papers I and II and also to enable the formalism to be generalized in our future papers to gravitational interactions with horizons.

The model problems in the following sections will illustrate the utility of the concept of the stretched horizon and will elucidate the constraints which exist on where it may be chosen (i.e., on the value of α_H), and will help the reader develop an intuitive feeling for the membrane view of black holes.

III. ELECTROMAGNETIC FIELDS OF POINT CHARGES NEAR A SCHWARZSCHILD BLACK HOLE

A. The Rindler approximation

In this section we focus our attention on the interaction of a black-hole horizon with the electromagnetic fields of point charges. In order to get maximum insight from a minimum of computational labor, we shall restrict attention to charges that are very close to the horizon and to the near-horizon fields that they produce. This permits us to approximate the Schwarzschild spatial geometry and lapse function by those of Rindler, which cover only the near-horizon region $r - 2M \ll 2M$ and ignore the spatial curvature there.

In the region near the horizon, the Schwarzschild spatial metric (2.3b) may be written in the form [cf. TM, Eq. (5.29)]

$$ds^2 = d\alpha^2/g_H^2 + (2M)^2(d\theta^2 + \sin^2\theta d\varphi^2) ,$$

where α is the lapse function and g_H is the surface gravity of the hole. If one restricts attention to a region of dimensions $\ll M$ centered on the location (θ_0,φ_0) on the horizon, and then defines the variables $x = 2M\sin\theta_0(\varphi - \varphi_0)$, $y = 2M(\theta - \theta_0)$, and $z = \alpha/g_H$, the lapse function and the metric take the Rindler[19] form

$$\alpha = g_H z \ , \quad ds^2 = dx^2 + dy^2 + dz^2 . \tag{3.1}$$

The coordinates (t,x,y,z) will be called Rindler coordinates; in these coordinates the horizon is at $\alpha = z = 0$. Therefore, the Rindler geometry can be considered as an approximation to the metric of a spherically symmetric black hole in the limit as one approaches the horizon. In the Rindler

approximation, z is the proper distance from the horizon, and it is related to the usual Schwarzschild radial coordinate r by

$$\int_{2M}^{r} \frac{dr}{\sqrt{1-2M/r}} \simeq 4M\sqrt{1-2M/r} = \alpha/g_H = z \ . \tag{3.2}$$

Of course, in approximating Schwarzschild space by Rindler space, a certain amount of information is lost. The Rindler approximation neglects the spatial curvature near the horizon; it approximates the lapse function α as linear in the distance z from the horizon; and consequently it characterizes the black hole's gravitational field entirely by the gravitational acceleration $\vec{g} = -\vec{\nabla}\ln\alpha = -(g_H/\alpha)\vec{e}_z$ felt by the ZAMO's. As a result, the Rindler approximation loses sight of the physics associated with spacetime curvature, such as the reflection of electromagnetic waves by the gravitational field, the "tails" of electromagnetic waves,[24] and the Smith-Will electrostatic self-force.[25] on a charge in a curved background. Also, as we restrict ourselves to a region of space of dimensions much less than M, the global structure of the external electromagnetic field is lost.

But the Rindler approximation is nonetheless a valuable tool in studying electromagnetic fields near a black-hole horizon, since the gravitational acceleration $\vec{g}$ is the major influence on the near-horizon field structure of a Schwarzschild black hole. The Rindler approximation combines the kinematic properties of horizons predicted by the membrane formalism (such as electrical conductivity) with an algebraic simplicity lacking in full Schwarzschild. This simplicity permits us to obtain the general analytic solution of the electromagnetic field equations, and thus allows us to develop a detailed understanding of the physics associated with the presence of the horizon. In fact, this consideration is not restricted to electromagnetism; in a future paper, Suen, Price, and Redmount[17] will also use the Rindler

approximation to study the gravitational aspects of the membrane viewpoint. It is also well known that Hawking radiation near a black-hole horizon may be understood in terms of the Rindler approximation's acceleration radiation.[26]

B. Solution of field equations in the Rindler approximation

In order to solve the curved-space Maxwell equations (2.3d) in the Rindler approximation, we note that, since Rindler spacetime is flat, it may be transformed to Minkowski-type coordinates (T,X,Y,Z):

$$\begin{array}{ll} T = z\,\mathrm{sinh} g_H t & Z = z\,\mathrm{cosh} g_H t \\ X = x & Y = y \end{array} \qquad (3.3)$$

These coordinates are associated with a family of observers who are falling freely in the z direction, and who ultimately fall into the horizon. In terms of Minkowski coordinates, the four-metric associated with Eq. (3.1) is

$$^{(4)}ds^2 = -\alpha^2 dt^2 + dx^2 + dy^2 + dz^2 = -dT^2 + dX^2 + dY^2 + dZ^2 \,.$$

To solve for the general electromagnetic field, we will transform the Minkowski-spacetime Liénard-Wiechert potential[27] into Rindler coordinates.

We consider a charge Q moving with four-velocity $u^{\alpha'}(x)$ which is a function of spacetime position x. (Here primed letters will be taken to denote four-vector indices in Minkowski coordinates, while unprimed ones will denote four-indices in Rindler coordinates.) The electromagnetic four-potential $A^{\alpha'}(x)$ at a particular spacetime observation point x will be generated entirely by a single point of the charge's trajectory: the retarded point x_R which lies at the intersection of the particle's trajectory with the past null cone of the observation point. The Liénard-Wiechert potential is

$$A^{\alpha'}(x) = \frac{Qu_R^{\beta'}}{u_{R\beta'}(x_R^{\beta'} - x^{\beta'})} , \tag{3.4}$$

where $|x_R^{\beta'} - x^{\beta'}| \equiv [(x_R^{\beta'} - x^{\alpha'})(x_R^{\beta'} - x^{\beta'})\eta_{\alpha'\beta'}]^{1/2} = 0$ and where $\eta_{\alpha'\beta'} \equiv \text{diag}[-1,1,1,1]$ are the Minkowski metric coefficients.

Transforming this expression to Rindler coordinates yields

$$A^{\alpha}(x) = L^{\alpha}_{O\alpha'}A^{\alpha'} = \frac{QL^{\alpha}_{O\alpha'}L^{\beta'}_{R\beta}u^{\beta}_R}{u_{R\gamma}L^{\gamma}_{R\beta'}(x_R^{\beta'} - x^{\beta'})} , \tag{3.5}$$

where $L^{\alpha}{}_{\alpha'} \equiv \partial x^{\alpha}/\partial x^{\alpha'}$ and $L^{\beta'}{}_{\beta} \equiv \partial x^{\beta'}/\partial x^{\beta}$ are the transformation matrices between Rindler and Minkowski coordinates, the subscripts O and R denote evaluation at the observation point and retarded point, respectively, and $x^{\beta'}(x^{\beta})$ is given by Eq. (3.3). The factors of L_R appear in Eq. (3.5) because u^{β}_R is a vector at the retarded point x_R, not at the observation point.

In the numerator of Eq. (3.5), $L^{\beta'}_{R\beta}u^{\beta}_R$ gives the Minkowski components $u^{\beta'}_R$ of the retarded four-velocity. We parallel-transport it to the observation point by fixing its Minkowski components and then transform to Rindler coordinates using $L^{\alpha}_{O\alpha'}$. The factor $L^{\alpha}_{O\alpha'}L^{\beta'}_{R\beta}$ is the bivector of geodetic parallel displacement defined by Dewitt and Brehme.[24] The potential (3.5) agrees with the Liénard-Wiechert potential given by Dewitt and Brehme as specialized to Rindler space.

Writing out Eq. (3.5) explicitly in terms of Rindler coordinates yields

$$\begin{bmatrix} A^t \\ A^x \\ A^y \\ A^z \end{bmatrix} = \frac{Q}{N} \begin{bmatrix} \frac{z_R}{z}\cosh g_H(t-t_R) & 0 & 0 & \frac{-1}{g_H z}\sinh g_H(t-t_R) \\ 0 & 1 & 0 & 0 \\ 0 & 0 & 1 & 0 \\ -g_H z_R \sinh g_H(t-t_R) & 0 & 0 & \cosh g_H(t-t_R) \end{bmatrix} \begin{bmatrix} u^t_R \\ u^x_R \\ u^y_R \\ u^z_R \end{bmatrix} , \tag{3.6a}$$

where

$$N \equiv g_H z z_R \sinh g_H(t-t_R)u_R^t$$

$$-(z\cosh g_H(t-t_R)-z_R)u_R^z-(x-x_R)u_R^x-(y-y_R)u_R^y \ . \qquad (3.6b)$$

The coordinates t_R, x_R, y_R, z_R of the retarded point are given in terms of those t, x, y, z of the field point by the intersection of the field point's past null cone

$$(x-x_R)^2+(y-y_R)^2+z^2+z_R^2-2zz_R\cosh g_H(t-t_R)=0\ ,\ (t_R<t)\ , \qquad (3.7)$$

with the world line of the charge. Together, Eqs. (3.6), (3.7), and the particle's world line give the complete solution for the field of an arbitrarily moving charge in Rindler space. By linear superposition, we thereby know the general vector potential for an arbitrary distribution of charge and current.

In terms of the four-vector potential, the ZAMO-measured electric and magnetic fields (2.2) are [cf. MT Eq. (2.24)]

$$E^i = -\frac{1}{g_H z}[A^i_{,t}+(g_H^2 z^2 A^t)_{,i}]\ ,$$
$$B^i = \varepsilon^{ijk}A_{k,j}\ , \qquad (3.8)$$

where i,j,k run over x,y,z and ε^{ijk} is the three-dimensional alternating tensor.

In the following subsections, we will discuss the electromagnetic field structure generated by various source motions.

C. "Static" charge in Rindler

For arbitrary motion of the source particle, it is generally not possible to solve Eq. (3.7) explicitly for the retarded coordinates as a function of the coordinates of the observation point. However, when the charged source particle is static in Rindler space, i.e., fixed at a position $(x,y,z) = (0,0,z_0)$, analytic expressions for the retarded coordinates may be derived and Eq. (3.6) may be used to write A^a solely in terms of the observer-point coordinates. In Fig. 2, the trajectory of the accelerated particle is plotted as a dashed line in both the Minkowski and Rindler spacetime coordinate systems.

Substituting $x_R = 0$, $y_R = 0$, and $z_R = z_0$ in Eq. (3.7) and adopting the cylindrical coordinates $\rho \equiv (x^2 + y^2)^{1/2}$ and $\varphi \equiv \tan^{-1}(y/x)$, we find

$$t_R = t - \frac{1}{g_H}\cosh^{-1}\left(\frac{z^2 + \rho^2 + z_0^2}{2zz_0}\right). \tag{3.9}$$

Eq. (3.6) then yields[28]

$$\begin{aligned} A^t &= \frac{Q}{g_H z^2}\frac{z^2 + \rho^2 + z_0^2}{\xi}, \quad A^z = -\frac{Q}{z}, \\ \xi &\equiv \sqrt{[z^2 + \rho^2 - z_0^2]^2 + 4\rho^2 z_0^2}, \end{aligned} \tag{3.10}$$

From Eq. (3.8), the only nonvanishing physical components of the electromagnetic field are

$$\begin{aligned} E_\rho &= \frac{8Qz_0^2\rho z}{\xi^3}, \\ E_z &= \frac{4Qz_0^2}{\xi^3}[z^2 - \rho^2 - z_0^2]. \end{aligned} \tag{3.11}$$

As might be expected, this field is stationary in the sense that it does not depend on the Rindler time t and it is purely electric. It should also be

noted that it is normal to the horizon at $z = 0$. The electric field lines are plotted in the lower right corner of Fig. 3. It is a major advantage of the 3+1 viewpoint that field lines may be used to describe the field. The Gaussian Maxwell equations $\vec{\nabla}\cdot\vec{B} = 0$ and $\vec{\nabla}\cdot\vec{E} = 4\pi\rho_e$ say, just as they do in flat-space electrodynamics, that magnetic field lines never end and that electric field lines end only on electric charge.

The horizon charge density Eq. (2.6a), which terminates the normal electric field of Eq. (3.11) at the horizon, is

$$\sigma_H = \left.\frac{E_z}{4\pi}\right|_{z=0} = -\frac{Qz_o^2}{\pi(\rho^2 + z_o^2)^2} \; ; \tag{3.12}$$

and by integrating σ_H over the horizon, one can verify that the total charge induced on the horizon is equal to $-Q$. The horizon surface current density defined in Eq. (2.6b) vanishes, so there is no dissipation of energy in the horizon. The stretching of the horizon described in Sec. II is not necessary in this example since the field is stationary and therefore has none of the layered horizon-field structure described there.

It is important to note that, although the horizon surface charge density (3.12) was not explicitly included as a source in deriving the electric field (3.11) from Eqs. (3.6) and (3.8), its inclusion would not change the exterior field in any way. The reason for this is the defined role of the horizon surface charge: it terminates the normal electric field in the region exterior to the horizon, and annuls it in the interior region. Indeed, by substituting zero for z_o in Eqs. (3.11), it may be seen that a hypothetical charge on the horizon $z = 0$ produces no field in the exterior region. For the more general case (considered in the following sections) where the horizon must be stretched, the exterior fields produced by the induced charge and current densities on the stretched horizon may be shown to be of order α_H,

the lapse-function value at the stretched horizon, and thus will vanish in the limit as the stretched horizon approaches the true horizon.

The same conclusion holds for a Schwarzschild black hole, which has zero net charge. As shown by Hanni and Ruffini[29], a hypothetical charge on the horizon produces a radial electric field centered on the center of the hole. If the total charge on the horizon is zero, then no matter what its distribution, it will produce no external electric field. For a Reissner-Nordstrøm black hole with total charge Q, the surface charge density σ_H consists of a total charge Q distributed over the horizon. Although this charge distribution may be distorted away from uniformity by the fields of external sources, the field generated by the horizon charge will remain the same as that of the Reissner-Nordstrøm hole, i.e., $\vec{E} = Q/r^2$, $\vec{B} = 0$.

The solution (3.11) might alternatively have been derived from the Copson-Linet[30] solution for a point charge at rest outside a Schwarzschild black hole by applying the change of variables and the limiting process (Rindler approximation) described in Eq. (3.2) and the preceding paragraph. The Copson-Linet solution is summarized in 3+1 form in TM, Sec. 6.1. The field lines were first plotted by Hanni and Ruffini[29] and an example is shown in Fig. 4. For a point charge Q at rest above the north pole of the hole at $r = b$, $\theta = 0$, the horizon surface charge density for the Copson-Linet solution is [cf. TM Eq. (6.4)]

$$\sigma_H = \frac{Q[M(1 + \cos^2\theta) - 2(b - M)\cos\theta]}{8\pi b[b - M(1 + \cos\theta)]^2} . \qquad (3.13)$$

This charge density yields a total induced surface charge of zero. As shown in Fig. 6 of Ref. 29, the horizon is polarized, with a total charge $-2Q[b - M - \sqrt{b(b-2M)}]/b$ north of the critical colatitude $\theta = \theta_{crit} \equiv \cos^{-1}\{[b - M - \sqrt{b(b-2M)}]/M\}$, and a like charge of the opposite sign

distributed south of this latitude. When one applies the Rindler approximation to Eq. (3.13), the critical radius where the sign of the polarization charge changes is moved out to $\rho = \infty$, so the charge density (3.12) is of the opposite sign to Q over the entire Rindler horizon.

Thus, we have verified that Eq. (3.6) gives the previously-known field of a Rindler-static charge; and we have shown explicitly that this field is a valid approximation to the field of a charge static outside Schwarzschild in the near-horizon limit. We now turn to the study of the fields of charges in motion above the Rindler horizon.

D. Infalling charge

Another simple source configuration which yields an explicit analytic solution for the fields is that of a charge $-Q$ stationary in Minkowski coordinates at position $Z = Z_o$, so that its trajectory in Rindler coordinates is

$$z = \frac{Z_o}{\cosh g_H t} . \tag{3.14}$$

As seen in Rindler coordinates, this particle emerges from the past horizon at $t = -\infty$, reaches a maximum distance Z_o from it, and then falls into the future horizon at $t = +\infty$. In Fig. 2, the trajectory of this charge is shown as a dotted line in the two different coordinate systems. The physical components of the particle's field as seen by Minkowski observers (who are falling into the hole with the particle) are

$$E_{\rho'} = -\frac{Q\rho}{r^3} , \quad E_{Z'} = -\frac{Q(Z - Z_o)}{r^3} , \tag{3.15}$$

where $r \equiv \sqrt{\rho^2 + (Z - Z_o)^2}$. In Rindler coordinates the nonvanishing physical components are

$$E_\rho = -\frac{Q\rho}{r^3}\cosh g_H t \ ,$$
$$E_z = -\frac{Q}{r^3}[z\cosh g_H t - Z_o] \ , \qquad (3.16)$$
$$B_{\hat{\varphi}} = \frac{1}{\rho}B_\varphi = \frac{Q\rho}{r^3}\sinh g_H t \ ,$$

where $r \equiv \sqrt{\rho^2 + [z\cosh g_H t - Z_o]^2}$ in terms of Rindler coordinates. These are the fields seen by static observers (ZAMO's) outside the horizon, i.e., the fields which are used in our membrane viewpoint of black holes.

The definition of the horizon charge and current densities in this case is trickier than in the case of the Rindler-stationary charge. In attempting to calculate them, one evaluates E_ρ and E_z at the horizon ($z = 0$, $t = \infty$), which leads to indeterminate results. The reason for this is the infinite gravitational redshift at the horizon. As described in Sec. II, the field structure associated with the infalling charge only asymptotically approaches the horizon, and the tangential field strength at $z = 0$ diverges exponentially with universal time t. To get meaningful results, it is necessary to define the charge and current densities on a stretched horizon as discussed in Sec. II. We choose it at the location $\alpha = \alpha_H \ll 1$, or $z = z_H \equiv \alpha_H / g_H$, where $0 < z_H \ll Z_o$. The charge and current densities on the stretched horizon produced by the infalling charge are

$$\sigma_H = \left.\frac{E_z}{4\pi}\right|_{z=z_H} = \frac{-Q(z_H\cosh g_H t - Z_o)}{4\pi[\rho^2 + (z_H\cosh g_H t - Z_o)^2]^{3/2}} \ ,$$
$$\vec{\jmath}_H = \left[\frac{\alpha}{4\pi}\vec{e}_z \times \vec{B}_{||}\right]_{z=z_H} = \frac{-Qg_H\rho z_H\sinh g_H t}{4\pi[\rho^2 + (z_H\cosh g_H t - Z_o)^2]^{3/2}}\vec{e}_\rho \ , \qquad (3.17)$$

respectively, where $\vec{E}_{||}$ is the component of E parallel to the horizon. As the particle descends toward the stretched horizon, the charge density becomes more and more sharply peaked at the position $\rho = 0$ directly under the particle; the integral of σ_H over the stretched horizon, however, remains

constant at the value $Q/2$ during the descent. In the limit as the particle approaches the stretched horizon, the charge density approaches the functional form

$$\sigma_H \to \frac{Q\delta(\rho)}{4\pi\rho} . \tag{3.18}$$

The surface current density feeds the growing concentration of charge at $\rho = 0$.

As in the case of the Rindler-stationary charge treated in Sec. III.C, the present problem is the near-horizon limit of a Schwarzschild problem: that of a charge which emerges from the horizon and falls back into it. As before, the charge simply polarizes the surface of the Schwarzschild hole, leaving it with zero net charge; but the Rindler approximation moves the neutral point where the polarization charge changes sign out to $\rho = \infty$, so that the charge density on the entire stretched Rindler horizon has the opposite sign to Q.

According to Eq. (2.11), the rate that energy is dissipated in a unit area of the stretched horizon is just $\vec{\jmath}_H \cdot \vec{E}_H$, and the rate of increase of the hole's mass-energy may be obtained by integrating this quantity over the stretched horizon:

$$\frac{dM}{dt} = T_H \frac{dS_H}{dt} \cong \int_{SH} \vec{\jmath}_H \cdot \vec{E}_H dA = \frac{Q^2 g_H^2 z_H^2 \sinh g_H t \cosh_H t}{8(z_H \cosh g_H t - Z_0)^2} . \tag{3.19}$$

The integral of this function over time, which should give the total mass-energy absorbed by the horizon, diverges due to an infinite contribution at the point at which the particle crosses the stretched horizon. This is not unexpected, however, since the particle is assumed to be pointlike and thus has an infinite amount of energy in its near field.

In contrast to the case of the Rindler-stationary charge, only half of the field lines of the infalling charge intersect the stretched horizon; the rest extend to spatial infinity. It may be seen by comparing Eqs. (3.14) and (3.16) that the electric field lines in Rindler coordinates emanate radially from the charge, just as they do in Minkowski coordinates. But unlike in Minkowski space, the field lines in Rindler space do not emerge from the charge isotropically. As the particle falls in, its field lines (even the ones that eventually extend to spatial infinity), are flattened down near the horizon within an ever-widening circle of radius $\Delta\rho \sim z_H \cosh g_H t$ on the stretched horizon. If its electric field lines were plotted, the entire field out to any chosen radius ρ would ultimately seem to disappear beneath the stretched horizon. Therefore, in plotting the field, it is convenient to add an oppositely charged particle, stationary outside the horizon, with field given by Eq. (3.11), to "hold the field lines up" and to illustrate the approach of the field toward stationarity.

Since we are considering Rindler space as an approximation to Schwarzschild, it is not physically realistic to consider the full trajectory of the Minkowski-stationary particle. Although the full analytic continuation of the Schwarzschild geometry has a past horizon, an astrophysical black hole does not. Therefore, we choose to consider the example of a neutral particle which splits into two parts at $t = 0, z = z_0$: a charge $+Q$ which continues along the uniformly accelerated trajectory $z = z_0$, and a charge $-Q$ which falls freely into the hole along the trajectory $Z = z_0$. Thus, we set $Z_0 = z_0$ in Eqs. (3.16) and then superpose the fields (3.11) and (3.16). The electromagnetic field will be given by this superposition inside the future light cone of the spacetime point $(t,x,y,z) = (0,0,0,z_0)$, and will vanish outside it. Likewise, the surface currents and charges (3.12) and (3.17) are valid at points

on the stretched horizon within the future light cone of the splitting point, and vanish outside it. That is, currents flow only within the ever-widening circle $\rho = \sqrt{2z_H z_o \cosh g_H t - z_H^2 - z_o^2}$ on the stretched horizon. If the charge densities corresponding to the static and infalling particles are summed and integrated over this circle on the stretched horizon, it may be verified explicitly that the resulting total charge has the expected behavior: it vanishes for time $t < g_H^{-1}\cosh^{-1}(z_o / z_H)$ when the infalling charge is still above the stretched horizon, and is equal to $-Q$ after the charge falls through the stretched horizon.

Figure 3 shows the electric field lines resulting from this superposition at several representative times. It may be seen that the effects of the field of the infalling particle rapidly vanish, and that by about $t = 6/g_H$, the field has very nearly settled down to the stationary form which would be produced by the static charge alone. All of the effects of the infalling particle's field become flattened into a thin layer just above the true horizon, the thickness of which decreases at a rate proportional to $1/\cosh g_H t \sim e^{-g_H t}$; thus all effects of the infalling charge disappear beneath the stretched horizon in a time of order $g_H^{-1}\ln(z_o / z_H)$.

E. Charge in uniform motion parallel to the horizon

In this subsection, we shall study the case of a charge sliding at constant height and with constant velocity above the Rindler horizon. We will analyze in detail the electric and magnetic fields, the work done on the charge, and the horizon heating.

We consider a charge Q which is located at $(x,y,z) = (0,0,z_o)$ at $t = 0$ and which moves in the $+x$ direction with constant velocity $d\vec{x}/d\tau \equiv \vec{v} = \beta\vec{e}_x$, as seen by the ZAMO's, for all time $-\infty < t < \infty$. Thus, its

velocity with respect to universal time t is $d\vec{x}/dt = \alpha\vec{v} = g_H z_o \beta \vec{e}_x$. If we set $\alpha_o \equiv g_H z_o$ and

$$\begin{aligned} x_R^\beta &= (t_R, \alpha_o \beta t_R, 0, z_o) , \\ u_R^\beta &= (\gamma/\alpha_o, \gamma\beta, 0, 0) , \end{aligned} \tag{3.20}$$

where $\gamma \equiv (1-\beta^2)^{-1/2}$, then Eqs. (3.6) and (3.8) yield

$$\begin{aligned} E_x &= \frac{Q\gamma^3 z_o}{N^3}[D(\tilde{\alpha} + \beta SD - \beta^2 C) + \beta S(\beta^2 - \tilde{\alpha}C)] , \\ E_y &= \frac{Q\gamma^3 z_o}{N^3}\tilde{y}(\tilde{\alpha} + \beta SD - \beta^2 C) , \\ E_z &= \frac{Q\gamma^3 z_o}{N^3}[\tilde{\alpha}\beta SD - (1+\beta^2)\tilde{\alpha}C + \tilde{\alpha}^2 + \beta^2] , \\ B_x &= \frac{Q\gamma^3 z_o}{N^3}\beta\tilde{y}(CD - \beta S) , \\ B_y &= \frac{Q\gamma^3 z_o}{N^3}\beta[\beta SD - CD^2 - C(\tilde{\alpha}^2 + \beta^2) + \tilde{\alpha}(C^2 + \beta^2)] , \\ B_z &= \frac{Q\gamma^3 z_o}{N^3}\beta\tilde{y}(\tilde{\alpha}C - \beta^2) , \end{aligned} \tag{3.21}$$

where we have used coordinates normalized by z_o: $\tilde{y} \equiv y/z_o$, $\tilde{\alpha} \equiv \alpha/\alpha_o = z/z_o$, and a "lagging-comoving" x-coordinate: $\tilde{x} \equiv x/z_o - g_H\beta t - \beta\ln(z/z_o)$. We also define $D \equiv (x - x_R)/z_o = \tilde{x} + \beta\ln[\tilde{\alpha}(C+S)]$ where $C \equiv \cosh g_H(t - t_R) = (\tilde{\rho}^2 + \tilde{\alpha}^2 + 1)/2\tilde{\alpha}$, $S \equiv \sinh g_H(t - t_R) = \sqrt{(C^2 - 1)}$, and $\tilde{\rho}^2 \equiv D^2 + \tilde{y}^2$. The quantity N of Eq. (3.6b) can be expressed as $N = \gamma z_o\{\tilde{\alpha}S - \beta[\tilde{x} + \beta\ln(\tilde{\alpha}(C+S))]\}$. Note that $\tilde{\rho}^2$ is defined implicitly in terms of the observer-point coordinates through C and S; only in the limit $\beta \to 0$ can it be expressed explicitly as $\tilde{\rho}^2 = \tilde{x}^2 + \tilde{y}^2$, and thus only in this limit can the electric and magnetic fields be expressed completely explicitly in terms of the observer-point coordinates.

Figure 5a shows the electric field lines in the $x-z$ plane for a charge moving with $\beta = 0.5$. Figure 5b is a 3-dimensional plot, as viewed from the side, for the same situation. The solid field lines are those which emerge

from the charge at the polar angle $\theta = 90°$, measured from the vertical z axis; the dotted lines are those field lines coming out at $\theta = 120°$. All of the field lines curve down toward the horizon. Figures 5c and 5d show the same plots for the case $\beta = 0.1$.

In the region close to the charge, the electric field lines go out radially with an excess concentration factor γ in directions perpendicular to the motion, just as for a uniformly moving charge in Minkowski space. For $\beta = 0.1$, the field structure resembles that of the Rindler-static charge (last diagram of Fig. 3) in a large region around the charge.

In the region close to the horizon, both the $\beta = 0.1$ and $\beta = 0.5$ cases show a similar tangential structure with diverging tangential field strength, although the $\beta = 0.1$ case shows this structure much closer to the horizon, so close that it cannot be resolved in the figure. The field in the tangential structure is complicated, varying rapidly in strength and direction as a function of α near the horizon. But any field line followed far enough toward the horizon will eventually point in the $+x$ direction, essentially because this part of the field was generated by the charge at early times when it was far to the left in the figure. Near the horizon, the tangential field structure is sinking slowly down toward the horizon at a rate $dz/dt = \alpha$, i.e., it is approaching the horizon asymptotically along the trajectory $z = \text{const.} \times e^{-g_H t}$. (Note that the descent is slow relative to universal time t, but at the speed of light as measured locally by the ZAMO's.) The separation between neighboring field lines goes as α and the field-line density as measured by the ZAMO's thus diverges as α^{-1}, indicating a diverging tangential field strength near the horizon. However, the details of this near-horizon tangential field have no effect on the structure of the external field and thus may be conveniently ignored by stretching the horizon. A possible choice of

the stretched horizon is shown as a dotted line in Fig. 5a.

It may be seen from Fig. 5 that the largest normal field at the stretched horizon, and thus the largest concentration of horizon surface charge (2.6a), occurs at a position lagging behind the charge. The tangential fields drive a surface current (2.6b), which moves the surface charge concentration along the stretched horizon at a constant distance behind the charge. By evaluating E_z from (3.21), taking α_H to be small, and using Eq. (2.6a), we find the induced charge density on the stretched horizon to be

$$\sigma_H = \left.\frac{E_z}{4\pi}\right|_{SH} = -\frac{Q}{\pi z_o^2}\,\frac{\tilde{\rho}^2 + 1 + (\tilde{\rho}^2 - 1)\beta^2 - (\tilde{\rho}^2 + 1)\beta D}{(\tilde{\rho}^2 + 1 - 2\beta D)^3}\,, \qquad (3.22)$$

where $\tilde{\rho}$ is given implicitly by $\tilde{\rho}^2 = D^2 + \tilde{y}^2$, $D = \tilde{x} + \beta\ln(\tilde{\rho}^2 + 1)$. When $\beta = 0$, this is easily seen to reduce to the static form Eq. (3.12). The variation of the charge density (3.22) along the x axis is shown in Fig. 6 for two different choices of stretched-horizon location: $\alpha_H^{(1)} = 10^{-2}\alpha_o$ and $\alpha_H^{(2)} = 10^{-4}\alpha_o$. It may be seen that in each case the charge is concentrated around $\tilde{x} = 0$, i.e., $x = x^* \equiv \alpha_o\beta t + (\alpha_o\beta/g_H)\ln(\alpha_H/\alpha_o)$. The quantity $\alpha_o\beta t - x^* = (\alpha_o\beta/g_H)\ln(\alpha_o/\alpha_H)$ is the amount by which the induced charge distribution lags behind the source; it is given by the velocity of the source multiplied by the time required for the field to propagate from the position of the charge down to the stretched horizon. The size of the lag increases as α_H is made smaller, i.e., as the stretched horizon is moved closer to the true horizon. The qualitative features on the stretched horizon are independent of the value of α_H we choose (see also Fig. 7). They are just shifted in the x direction by an amount $(\beta/g_H)\ln(\alpha_H^{(1)}/\alpha_H^{(2)})$, since the field at $\alpha_H^{(2)}$ is laid down a time $(1/g_H)\ln(\alpha_H^{(1)}/\alpha_H^{(2)})$ earlier than the corresponding field on $\alpha_H^{(1)}$. As was stressed in Sec. II, we look at earlier epochs in the history of the field evolution as we look closer to the true horizon. We can understand the lag

physically either by saying that there are strong retardation effects near the stretched horizon, or by noting that the stretched horizon has a finite resistivity which gives rise to a frictional force on the moving induced charges. This behavior is qualitatively the same as for the flat-space case of an external charge moving past a conducting surface with finite resistivity and dragging its induced charge behind itself.

Substituting the tangential electric field given by Eq. (3.21) into the definition (2.6b), we obtain the induced surface current density

$$\begin{aligned} \vec{J}_x &= -\frac{\alpha_H B_y}{4\pi}\bigg|_{SH} = \frac{Q\alpha_o}{2\pi z_o^2}\,\frac{\beta(\tilde{\rho}^2+1)[2D^2-2\beta D+2\beta^2-(\tilde{\rho}^2+1)]}{(\tilde{\rho}^2+1-2\beta D)^3}\,, \\ \vec{J}_y &= \frac{\alpha_H B_x}{4\pi}\bigg|_{SH} = \frac{Q\alpha_o}{\pi z_o^2}\,\frac{\beta\tilde{y}(\tilde{\rho}^2+1)(D-\beta)}{(\tilde{\rho}^2+1-2\beta D)^3}\,. \end{aligned} \tag{3.23}$$

Eqs. (3.22) and (3.23) can be combined to verify that

$$^{(2)}\vec{\nabla}\cdot\vec{J} + \frac{\partial\sigma_H}{\partial t} = 0\,,$$

which is the charge conservation equation, as there is no external charge entering the stretched horizon. This current distribution is shown in Fig. 7 for $\beta = 0.5$, $t = 0$, with $\alpha_H^{(1)} = 10^{-2}\alpha_o$ and $\alpha_H^{(2)} = 10^{-4}\alpha_o$.

The distribution of induced charge and current gives us immediate information on the energy and momentum transfer between the hole and the charge. The direction of the momentum transfer is evident from the fact that the induced charges on the stretched horizon suffer an Ohmic resistance as they move in the $+x$ direction; thus, momentum in the $+x$ direction will be transferred to the hole. Also, from Eq. (2.11), Joule heating of the horizon dissipates the Maxwell field energy at the rate

$$\frac{dM}{dt} = T_H\frac{dS_H}{dt} \cong \int_{SH}\vec{J}_H\cdot\vec{E}_H\,dA\,. \tag{3.24}$$

Using the definitions (2.5) and (2.6) along with Ohm's law (2.7) and the zero-reflection boundary condition (2.9), this may be written as

$$\frac{dM}{dt} \cong \alpha_H^2 F_E = \alpha_H^3 \int_{SH} T^{tz}\, dx dy \ , \tag{3.25}$$

where F_E is the ZAMO-measured energy flux into the stretched horizon and where one factor of α_H multiplying it comes from converting $d/d\tau$ to d/dt on the stretched horizon, and the other comes from redshifting the energy. The Maxwell energy flux density in the z direction measured by ZAMO's on the stretched horizon is given by $\alpha_H T^{tz} = \alpha_H (E_y B_x - E_x B_y)/4\pi$. The heating rate dM/dt could be found explicitly by substituting the fields from Eq. (3.21) into Eq. (3.25) and performing the integral. However, it may be found much more easily by the following consideration.

The field energy dissipated in the horizon must be provided by the agent which keeps the charge in uniform motion. By considering the power supplied to the charge as measured by the local ZAMO at the position of the charge, the power flowing into the horizon can be easily evaluated (see Appendix) to be

$$\frac{dM}{dt} = \frac{2}{3} Q^2 g_H^2 \frac{\beta^2}{(1-\beta^2)^2} \ . \tag{3.26}$$

Next we look at the momentum transfer between the charge and the horizon. In the membrane language, the momentum transfer is produced by a frictional force on the flowing induced charge in the stretched horizon; from Eq. (2.10) the x component of this force is

$$\frac{dp_H^x}{dt} \cong \int_{SH} (\sigma_H \vec{E}_H + \vec{J}_H \times B_n \vec{n})_x \, dA \ . \tag{3.27}$$

Thus, from Eqs. (2.5) and (2.6), the torque on a Schwarzschild hole due to a

charge moving in the φ direction at polar angle $\theta = \theta_o$, very close to the horizon, is

$$\frac{dJ}{dt} \cong 2M\sin\theta_o \frac{dp_H^{\vec{}}}{dt} = -2M\alpha_H \sin\theta_o \int_{SH} T^{xz}\, dxdy \ , \tag{3.28}$$

where $2M\sin\theta_o$ is the "lever arm" for converting force to torque, and where $\alpha_H T^{xz} = -\alpha_H(E_x E_z + B_x B_z)/4\pi$ is the Maxwell flux density of x-momentum in the z direction, as measured by ZAMO's on the stretched horizon. The torque dJ/dt can be evaluated either by computing T^{xz} from Eqs. (3.21) for $\vec{E}$ and $\vec{B}$ and then performing the surface integral (3.28), or by the following consideration.

The momentum imparted to the horizon must be supplied by the agent which keeps the charge in uniform motion; in the Appendix, by computing the force on the charge, we obtain

$$\frac{dJ}{dt} = (2M\sin\theta_o)\frac{2}{3}\frac{Q^2 g_H^2}{\alpha_o}\frac{\beta}{(1-\beta^2)^2} \ . \tag{3.29}$$

Note that since (power supply)=β(momentum supply), as measured by the ZAMO's at the position of the charge, then dJ/dt and dM/dt are very simply related: $dM/dt = \alpha_o \beta (2M\sin\theta_o)^{-1} dJ/dt$.

It is also informative to look at the actual distribution of energy and momentum inflow on the stretched horizon, as given by T^{tz} and T^{xz} [cf. Eqs. (3.25) and (3.28)]. Figure 8 shows these distributions along the x axis, after integration over all y values. As may be readily seen by comparing Fig. 8 to Figs. 6 and 7, the region of greatest energy and momentum inflow coincides with the region of strongest induced charge and current.

Figure 8 shows that, from the viewpoint of our membrane formalism, the region of maximum inflow of energy and momentum lags behind the

motion of the charge above the horizon. The question of whether this region lags or leads the charge is not completely unambiguous, however. It has been pointed out by Hartle[7] that an alternative, natural way to compare the transverse positions of points at different values of α (different distances from the horizon) is by means of a zero-angular-momentum light ray. This corresponds to a slicing of spacetime different from our choice: A coordinate change $\tilde{t} = t + (1/g_H)\ln\alpha$ brings the spacetime metric into the form

$$ds^2 = -\alpha^2 d\tilde{t}^2 + 2\alpha d\tilde{t} dz + dx^2 + dy^2 . \qquad (3.30)$$

(The coordinate $\tilde{t}$ and the Minkowski time coordinate T are the Rindler-approximation limits of the infalling Eddington-Finkelstein time coordinate, Eq. (2.4), and the Kruskal-type time coordinate $4M(r/2M - 1)^{1/2}\sinh(t/4M)$, respectively.) In the metric (3.30), a zero-angular-momentum null ray has the trajectory $\tilde{t}$ = const., x = const., y = const., and hence, in a constant-$\tilde{t}$ slice, a zero-angular-momentum null ray starting from the charge will strike the stretched horizon directly underneath it. Such a position, after transforming back to the membrane viewpoint's t-slicing, is marked as x^* in Fig. 8. We can clearly see that, from the "zero-angular-momentum-light-ray viewpoint," the location of maximum input of energy and momentum occurs at a position on the stretched horizon where the charge is not yet "overhead." The same kind of phase-lead phenomenon was observed by Hartle[7] when he studied the tidal bulge on the horizon due to an orbiting moon. However, when observed in a slice of constant t (the absolute space of our membrane viewpoint), the position of maximum energy and momentum input (or tidal bulge) will lag behind the source on the stretched horizon, which is much more suggestive to physical intuition.

F. Charge in nonuniform motion near the horizon

To obtain a better feeling for the evolution of field lines near the horizon, we consider charges that move only for a finite period of time.

We first consider a charge which stays at $(x,y,z) = (0,0,z_0)$ for all $t < 0$, then moves with constant velocity $dx/d\tau = \alpha_0^{-1}dx/dt = \beta$ in the $\vec{e}_x$ direction until $t = 1/g_H = z_0/\alpha_0$, and then stops again for all $t > 1/g_H$ at $x = \beta z_0$. (We again set $\alpha_0 \equiv g_H z_0$.) For $t > 1/g_H$, the structure of the electric field lines is divided into three regions. Figure 9a shows the field lines for $t = 2/g_H$, $\beta = 0.5$. Near the charge there is a region centered at $x = \beta z_0$, $y = 0$ where the field configuration has settled down to the static Coulomb field. In the region far away from the charge, we also have a static Coulomb field. This is the region where the charge's "start-to-move" signal has not yet arrived, i.e., the region where the spacetime separation from the point $t = 0$, $x = 0$, $y = 0$, $z = z_0$ is spacelike. Sandwiched between the near and far zones is the transition region, where the field is given by Eq. (3.21). (We idealize the charge's acceleration as being instantaneous and ignore the field generated at these instants. If this assumption were not made, there would be two shells of radiative field corresponding to retarded times during which the particle was accelerated. But the same conclusions would apply to these shells as to the transition region, so we will not consider them here.) As time progresses (Fig. 9b), those parts of the transition region propagating towards the horizon approach it asymptotically along a trajectory $z = \text{const.} \times e^{-g_H t}$. Hence the transition region gets thinner and the field lines become more and more tangential. The field-line density increases as $1/\alpha$ and hence the tangential electric field grows. This tangential structure finally sinks down to the stretched horizon and drives a current which transports the surface charge from the region near $x = 0$ to the region under

the source's new position. There is also some surface charge attracted in from the region $x \gg 0$ to settle under the charge, while some excess charge near $x = 0$ flows off in the $-x$ direction. The current flow produces Joule heating and a Lorentz force in the horizon, which dissipate the energy and momentum carried by the field in the transition region. For times $t \gg 1/g_H$, the field on and above the stretched horizon returns to a fully static configuration (last diagram of Fig. 3).

The qualitative features of the tangential field structure observed in the above problem are not special to it, but rather they are a general feature of any field lines that move in the vicinity of a horizon.

For example, consider a problem where we move an initially static charge perpendicular to the horizon with constant ZAMO-measured velocity β during the time interval $0 < t < 1/g_H$. In this interval, the charge has a trajectory $z = z_o e^{g_H \beta t}$ (upward motion) and a four-velocity $u^\alpha = (\gamma/\alpha, 0, 0, \gamma\beta)$ where $\gamma \equiv (1-\beta^2)^{-1/2}$. Putting this into Eqs. (3.6) and (3.8), we have the electric field:

$$E_\rho = \frac{Q\tilde{\rho}}{z_o^2} \frac{(1-\beta^2)(\tilde{\alpha}e^{-g_H\beta t_R} - \beta S)}{[\tilde{\alpha}(S-\beta C) + \beta e^{g_H\beta t_R}]^3},$$
$$E_z = \frac{Q}{z_o^2} \frac{\tilde{\alpha}(1-\beta^2)(\tilde{\alpha}e^{-g_H\beta t_R} - \beta S - C)}{[\tilde{\alpha}(S-\beta C) + \beta e^{g_H\beta t_R}]^3}, \qquad (3.31)$$

where $\tilde{x} \equiv x/z_o$, $\tilde{y} \equiv y/z_o$, $\tilde{\alpha} \equiv z/z_o$, $\tilde{\rho} \equiv \sqrt{(\tilde{x}^2 + \tilde{y}^2)}$, $S \equiv \sinh g_H(t - t_R)$, $C \equiv \cosh g_H(t - t_R)$, and the retarded time t_R is defined implicitly by $\tilde{x}^2 + \tilde{y}^2 + \tilde{\alpha}^2 + e^{2g_H\beta t_R} - 2\tilde{\alpha}e^{g_H\beta t_R}\cosh g_H(t - t_R) = 0$.

Figures 10a and 10b show the field lines at $t = 2.5/g_H$ and $t = 3.5/g_H$, respectively. The qualitative features are clearly the same as in the case of the charge moved parallel to the horizon, and again we see a tangential structure traveling down to the stretched horizon. In this case, the current

flows radially outward and distributes the induced charge over a larger region in the new static situation.

For further insight into the evolution of the electric field, we show in Fig. 11a the evolution of the direction of a particle's electric field as the field "propagates" near the horizon. More specifically, we consider the particle of Figs. 5a, 5b, 6, 7, and 8, which is moving parallel to the horizon (x-direction) with a locally measured velocity $\beta = 0.5$. The particle's field, as described by the Liénard-Wiechert potential (3.5), propagates away from the particle with the speed of light. (Of course, this is strictly true only close to the horizon where the spacetime curvature and its scattering effects are negligible.) In Fig. 11a, we study the propagation in the $x-z$ plane of that piece of the electric field which is emitted by the particle at time $t = 0$, when the particle is at the point from which the curved lines diverge. These curved lines are the spatial tracks of the null geodesics along which that bit of field propagates. Each short segment, or arrow, depicts the direction that the field points when it has reached the location, on its propagation geodesic, where the arrow's tail sits. Thus, the first set of arrows in Fig. 11a (those nearest the particle's position) constitute a snapshot of the field at a time $t = 0.3/g_H$ after the emission event—when the particle has moved to the location of the first cross. The second set of arrows is a snapshot of the field at $t = 0.6/g_H$, when the particle has reached the cross marked 0.6. Each successive snapshot and particle location is at a subsequent time interval $\Delta t = 0.3/g_H$. When the fields generated are still in the region close to the charge, they behave essentially in a Minkowskian way, except that those parts that travel upward move faster as α gets larger and those parts traveling downward toward the horizon move more slowly as α get smaller. Recall that in flat-space electrodynamics, the electric field lines of a

uniformly moving charge always point toward the present position of the charge. For the case of a particle near the Schwarzschild or Rindler horizon, however, the parts of the field traveling away from the horizon point in front of the present position of the charge, while those parts traveling downward toward the horizon point to the rear of it and eventually become tangential to the horizon.

Had we chosen to take snapshots at constant intervals of $\tilde{t}$ [Eq. (3.30)], the field propagating on the null trajectories would march through the horizon without hesitation; but since we use constant intervals of universal time t, we take an infinite number of snapshots of the field in the region just outside the horizon. Therefore, we see an unchanging field structure as t progresses: the fossil field structure described in Sec. II. The introduction of the stretched horizon simply cuts off the redundant taking of snapshots at a convenient surface outside the horizon.

All of the above figures and conclusions have pertained to the electric field of a moving charge. It is of interest also to investigate the evolution of a magnetic field near a black-hole horizon. From the curved-space Maxwell equations (2.3d), it is seen that, in regions of space with no sources, the duality transformation $\vec{E} \to \vec{B}$ and $\vec{B} \to -\vec{E}$ preserves the form of the equations and hence their solutions, just as in flat-space electrodynamics. Therefore all of the qualitative conclusions reached above for an electric field will hold also for a magnetic field.

More specifically, for a static magnetic field, as for a static electric field, the field lines will intersect the stretched horizon orthogonally, so that by Eq. (2.6b) there is no surface current to produce dissipation. If the magnetic field is disturbed, the disturbance will propagate down toward the horizon and form a tangential structure. This assertion is supported by Fig.

11b, which shows the magnetic field generated by the uniformly moving particle of Fig. 11a propagated along null trajectories in the $y-z$ plane, in the same manner as was done for the electric field in Fig. 11a. Note here, as for the electric field, that the field structure becomes tangential near the horizon. When this structure sinks through the stretched horizon, a current is induced which dissipates the Maxwell field energy and momentum. The effect of this process is to "clean" the magnetic field by removing complicated tangential structure near the horizon. This process might be important in models of quasars which involve large magnetic fields in the neighborhoods of black-hole horizons.[15] A model problem relevant to this process will be considered in the next section.

IV. Relaxation of a Magnetic Field in Schwarzschild Spacetime

The previous section considered electromagnetic model problems in Schwarzschild spacetime in a region close enough to the horizon that the Rindler approximation could be adopted. If the Rindler approximation is dropped, the mathematics of these problems generally becomes more difficult. The spatial curvature which was ignored in the transition from Schwarzschild to Rindler makes the three-space vector operators, and thus Maxwell's equations, considerably more complicated in the full Schwarzschild spacetime. However, it is instructive to investigate a model problem in the full Schwarzschild black-hole background to verify that the models we have made using the Rindler approximation have not omitted any important features of the interaction of electric and magnetic fields with a horizon and also to develop intuition concerning the effect of spatial curvature on those fields.

We consider the problem of a Schwarzschild black hole of mass M, surrounded by a perfectly conducting concentric sphere of radius $R > 2M$ into which an axially symmetric magnetic field is frozen. At time $t = 0$, the magnetic field lines are momentarily static and purely radial, pointing into the hole below the equator and out of the hole above it, as shown in Fig. 12. Immediately after time $t = 0$, this initial configuration is released and allowed to evolve dynamically in accord with the vacuum Maxwell equations, except that the field lines continue to be held fixed in the conducting sphere at radius R. We shall study the dynamical evolution of this field.

In Schwarzschild coordinates (t,r,θ,φ), where the lapse function is $\alpha = \sqrt{1 - 2M/r}$, the initial electric and magnetic fields are

$$\begin{aligned} \vec{E} &= 0 , \\ \vec{B} &= B_0 \alpha \left(\frac{R}{r}\right)^2 \cos\theta \frac{\partial}{\partial r} = B_0 \left(\frac{R}{r}\right)^2 \cos\theta \vec{e}_{\hat{r}} , \end{aligned} \tag{4.1}$$

and the corresponding initial vector potential is purely toroidal:

$$\vec{A} = \frac{B_0 R^2}{2r} \sin\theta \vec{e}_{\hat{\varphi}} , \tag{4.2}$$

where B_0 is the magnetic field strength on axis at the outer sphere and $\vec{e}_{\hat{\varphi}} \equiv (1/r\sin\theta)\partial/\partial\varphi$. [Throughout this section, carats will be used to denote the orthonormal basis $(\vec{e}_{\hat{r}},\vec{e}_{\hat{\theta}},\vec{e}_{\hat{\varphi}})$.]

The field lines are fixed at their outer ends because they are frozen into the perfectly conducting outer sphere, but they are free to slip through the stretched horizon since it has a finite conductivity. Qualitatively, one would expect the field lines to pull themselves into a more vertical orientation due to their tension.

The symmetries of the problem, along with Maxwell's equations, ensure that all components of the four-vector potential except $A_\varphi(t,r,\theta)$ will remain zero. This component may be written in terms of the "magnetic flux function" $\psi(t,r,\theta) \equiv 2\pi A_\varphi(t,r,\theta)$ which, as shown in MT, is equal to the total magnetic flux through the circle of constant radius and latitude (r,θ) = constant. The expressions for the electric and magnetic fields in terms of ψ are

$$\begin{aligned} \vec{E} &= -\frac{1}{\alpha}\dot{\vec{A}} = -\frac{\dot{\psi}\vec{e}_{\hat{\varphi}}}{2\pi\alpha r\sin\theta} , \\ \vec{B} &= \vec{\nabla}\times\vec{A} = \frac{\vec{\nabla}\psi\times\vec{e}_{\hat{\varphi}}}{2\pi r\sin\theta} , \end{aligned} \tag{4.3}$$

where the overhead dot denotes time differentiation. The only nonvacuous Maxwell equation is Ampere's law [MT Eq. (2.17c)], which, specialized to vacuum Schwarzschild spacetime and expressed in terms of ψ, may be written as

$$\vec{\nabla}\cdot\left(\frac{\alpha}{r^2\sin^2\theta}\vec{\nabla}\psi\right) - \frac{1}{\alpha r^2\sin^2\theta}\ddot{\psi} = 0 . \tag{4.4}$$

The covariant three-space derivatives in the vector operators in this equation may be expanded in terms of ordinary derivatives, with the result

$$-\frac{\psi_{,tt}}{1-2M/r} + \left(1-\frac{2M}{r}\right)\psi_{,rr} + \frac{2M}{r^2}\psi_{,r} + \frac{\psi_{,\theta\theta}}{r^2} - \frac{\cot\theta}{r^2}\psi_{,\theta} = 0 . \tag{4.5}$$

By introducing the "tortoise coordinate" r^* of Regge and Wheeler[31] defined by

$$\begin{aligned} dr^* &= \frac{dr}{1-2M/r} , \\ r^* &= r + 2M\ln\left(\frac{r}{2M}-1\right) , \end{aligned} \tag{4.6}$$

Eq. (4.5) can be put into the form

$$-\psi_{,tt} + \psi_{,r^*r^*} + \frac{1}{r^2}\left(1 - \frac{2M}{r}\right)\left[\psi_{,\theta\theta} - \cot\theta\psi_{,\theta}\right] = 0 . \tag{4.7}$$

In this equation, r is to be thought of as an implicitly defined function of r^*.

The boundary condition of "no outgoing waves at the horizon" [Eq. (2.9)] requires

$$[\vec{E}_{\|} - \vec{n}\times\vec{B}_{\|}]_{r\to 2M} \to 0 , \tag{4.8}$$

where $\vec{n}$ is the unit normal vector $\vec{e}_{\hat{r}}$ to the horizon and $\vec{E}_{\|}$ and $\vec{B}_{\|}$ are the field components tangential to the horizon. The tangential fields may be expressed in terms of the potential ψ as

$$\begin{aligned} \vec{E}_{\|} &= -\frac{1}{2\pi\alpha r\sin\theta}\frac{\partial\psi}{\partial t}\vec{e}_{\hat{\varphi}} , \\ \vec{B}_{\|} &= \frac{[\vec{\nabla}\psi\times\vec{e}_{\hat{\varphi}}]_{\|}}{2\pi r\sin\theta} = -\frac{\alpha}{2\pi r\sin\theta}\frac{\partial\psi}{\partial r}\vec{e}_{\hat{\theta}} , \end{aligned} \tag{4.9}$$

so the horizon boundary condition (4.8) becomes

$$\left[\frac{\partial\psi}{\partial t} - \frac{\partial\psi}{\partial r^*}\right]_{r\to 2M} \to 0 . \tag{4.10}$$

The initial field $\vec{A} = (2\pi r\sin\theta)^{-1}\psi(0,r,\theta)\vec{e}_{\hat{\varphi}} = B_0(R^2/2r)\sin\theta\vec{e}_{\hat{\varphi}}$ has the angular dependence of the $l = 1, m = 0$ vector spherical harmonic[27] $\vec{X}_{1,0}(\theta,\varphi) = i\sqrt{3/8\pi}\sin\theta\vec{e}_{\hat{\varphi}}$; and since neither the differential equation (4.7) nor the boundary conditions mix different multipoles, the field will remain proportional to this harmonic as it evolves. It is thus convenient to separate variables by defining a new field variable $u(t,r)$:

$$\psi(t,r,\theta) = \pi B_0 R^2 u(t,r)\sin^2\theta . \tag{4.11}$$

Then the wave equation (4.7) for ψ takes the form

$$-u_{,tt} + u_{,r^*r^*} - \frac{2}{r^2}\left(1 - \frac{2M}{r}\right)u = 0 . \tag{4.12}$$

This equation describes a one-dimensional wave subject to a potential $V(r^*) \equiv 2(1 - 2M/r)/r^2$. This potential goes to zero at the horizon proportionally to $\alpha^2 \simeq e^{2g_H r^*}$, goes to zero as $r^{-2} \simeq (r^*)^{-2}$ at large r, and has a global maximum at $r = 3M$ ($r^* \simeq 1.61M$): $V_{\max} = 2/(27M^2)$. The inner boundary condition (4.10) written in terms of $u(t,r)$ is just

$$\left[\frac{\partial u}{\partial t} - \frac{\partial u}{\partial r^*}\right]_{r \to 2M} \to 0 . \tag{4.13}$$

which has the form of a "perfectly absorbing" boundary condition for the one-dimensional wave equation (4.12). The outer boundary condition is $u(t,R) = 1$, and the initial conditions are $u(0,r) = 1$ and $u_{,t}(0,r) = 0$.

The wave equation (4.12) was integrated numerically subject to these initial and boundary conditions, and the structure of the magnetic field lines was then reconstructed from $u(t,r)$ using the relation (4.11) and the definition of $\psi(t,r,\theta)$ as the magnetic flux function (Eq. 4.9). The inner boundary condition (4.13) was applied not at the actual horizon $r^* = -\infty$, but at a slightly stretched horizon $r^* = -20M$, which corresponds to the Schwarzschild radius $r = (2 + 3.3\times10^{-5})M$ and $\alpha_H = 4.1\times10^{-3}$. (Although this horizon stretching is motivated by numerical considerations, it is the same stretching as occurs in the membrane viewpoint.) Representative plots of the magnetic field line structure are shown in Figs. 13a and 13b for the cases $R = 3M$ and $R = 10M$, respectively.

The qualitative behavior of the solutions, as depicted in $r-\theta$ coordinates, is that the field oscillates for a time before settling down to a final

static configuration consisting of precisely vertical field lines. The final static configuration could be derived directly by setting the time derivatives in Eq. (4.12) to zero, and solving it subject to the boundary conditions $u(r=R) = 1$ and $u_{r*}(r=2M) = 0$; it is the solution $\psi(r,\theta) = \pi B_0 r^2 \sin^2\theta$ found by Wald[32] and by Hanni and Ruffini.[33]

As the field lines oscillate, they leave behind disconnected field-line loops near the horizon, such as those shown in the diagram for $t/M = 28$ in Fig. 13b. These loops drop toward the horizon at the locally measured speed of light, $dr^*/dt \sim 1$ or $dr/dt \sim \alpha^2$. Thus, as described qualitatively in Sec. II, the field has a layered structure at the horizon which reflects the entire past history of its evolution. However, these layered horizon fields do not affect the overall large-scale structure of the field outside the horizon; the position of the stretched horizon in the numerical integration could be moved outward considerably without changing the diagrams in Fig. 13 in any noticeable way.

The complex, multilayered nature of the near-horizon fields is illustrated graphically in Fig. 14. In the top part of this figure, the magnetic field lines are plotted on an embedding diagram for Schwarzschild spacetime, which consists of a paraboloid of revolution.[11] In this part of the diagram, the Schwarzschild radial coordinate r is measured radially outward from the axis of cylindrical symmetry of the embedding diagram, and the angular coordinate θ is measured around this axis. The ignorable coordinates t and φ are suppressed. The diagrams in Fig. 13 are what one would see if one were looking down into the paraboloid along the axis of symmetry. The paraboloid of the embedding diagram is cut off at a stretched horizon which is taken to be at a radius $r = 2.15M$. (As will be explained later, this would be a poor choice of stretched horizon at which to apply the boundary

condition (4.13), but it is chosen here for illustrative purposes.) In order to make the fields between the stretched horizon and the true horizon visible, they are plotted on a cylinder matched to the paraboloid at the stretched horizon. In this part of the diagram, the vertical distance, i.e., the cylindrical "z-coordinate," is equal to the tortoise coordinate r^*; and the previous identification of θ with the cylindrical angular coordinate is maintained. Plotting the near-horizon fields in this way as functions of r^* has the effect of expanding the radial scale so that the field structure is visible.

The data plotted in Fig. 14 show the field-line structure at the time $t = 92M$ for the case $R = 10M$. At this time, the field lines have sprung outward and snapped back inward four times and are beginning to spring outward for a fifth time. The relic field line loops left by each of these oscillations are visible running down the cylinder, and the partially formed loops at the top of the cylinder may be seen to connect to field lines outside the stretched horizon. The field lines are vertical in the lowermost region of the diagram due to the fact that the field was held stationary until its release at $t = 0$. As one proceeds up the cylinder, one finds successively fewer concentric loops in each set of field lines since the oscillations are dying out and fewer field lines snap back to the stretched horizon with each oscillation.

Two criteria need to be considered in choosing the position of the stretched horizon in a problem of this sort. The potential $V(r^*)$ in Eq. (4.12) acts as a barrier to incoming waves, partially transmitting them and partially reflecting them. Application of the "perfectly absorbing" boundary condition at the stretched horizon rather than at the true horizon is equivalent to neglecting waves reflected from the part of the potential barrier (spacetime curvature) between the two horizons. Since $V(r^*)$ goes to zero proportionally to α^2 near the true horizon, this approximation becomes

better and better as the stretched horizon is moved inward toward the true horizon. In the problem at hand, it was found that moving the stretched horizon from its original location $r^* = -20M$ out to $r^* = -10M$ or $r = (2 + 4.9\times10^{-3})M$ made no noticeable difference in the numerical solutions obtained. On the other hand, putting the stretched horizon at $r = 2.15M$, as was done in Fig. 14 for illustrative purposes, should not be done in the numerical solution of the problem since $V(r^*)$ still has 41% of its maximum value there.

The other criterion affecting the choice of the stretched horizon is the requirement that it be close enough to the true horizon that important features of the field are not neglected below the stretched horizon. More specifically, we demand that α_H be small enough that the field does not evolve substantially along any null ray between $\alpha = \alpha_H$ and $\alpha = 0$. In terms of the Eddington-Finkelstein time coordinate $\tilde{t}$ of Eq. (2.4), the equation of such a null ray is $dr / d\tilde{t} = -1$. If Δt is the (universal) timescale of evolution of the field, the above criterion translates into the requirement that $\alpha_H \lesssim \sqrt{2g_H\Delta t}$. This condition is certainly satisfied in the present problem for either of the choices of the stretched horizon mentioned above, since the timescale of variation of the field is $\Delta t \sim M$.

The only dissipation in this problem comes from the horizon boundary condition. If the stretched horizon had a surface resistivity of either zero or infinity, rather than presenting incoming waves with the vacuum impedance $R_H = 4\pi = 377$ ohms, the field lines would oscillate forever. The damping timescale of the oscillations is determined by the size of the horizon relative to the perfectly conducting outer sphere: for the case $R = 3M$, the field lines almost settle down to the static configuration after springing outward just once, while for the case $R = 10M$, they oscillate many times.

The magnetohydrodynamical decay time of a field slipping through a conducting medium with surface resistivity R_H may be shown[34] to be roughly equal to $4\pi L/R_H$, where L is a length comparable with the dimensions of the region where current flows. For the present problem, where $L \sim 2M$, this timescale is just $2M$, the light-travel time across the hole (which, as claimed in Sec. 7.5 of MT, is the approximate annihilation time for a field loop with both feet in the hole). Not all of the field lines are dissipating their vibrational energy in the hole at a particular time, however. One would therefore expect the timescale t_* of the relaxation of the field lines to be roughly equal to $2M$ divided by the time-averaged fraction of field lines which thread the horizon, which is approximately $4M^2/R^2$; that is

$$t_* \sim 2M\left(\frac{R^2}{4M^2}\right) = \frac{R^2}{2M} \ . \tag{4.14}$$

The time t_* is the timescale of the loss of magnetic field energy into the hole, so it will be instructive to elaborate further on the nature of the transfer of electromagnetic energy into the hole.

Following MT, one may define a density ε_E and flux density $\vec{S}_E$ of "redshifted energy" or "energy-at-infinity:"

$$\varepsilon_E \equiv (\alpha/8\pi)(\vec{E}^2 + \vec{B}^2) = \frac{\alpha}{32\pi^3 r^2 \sin^2\theta}\left[\frac{\dot{\psi}^2}{\alpha^2} + (\vec{\nabla}\psi)^2\right] , \tag{4.15a}$$

$$\vec{S}_E \equiv (\alpha/4\pi)\vec{E}\times\vec{B} = -\frac{\dot{\psi}\vec{\nabla}\psi}{16\pi^3 r^2 \sin^2\theta} \ . \tag{4.15b}$$

These satisfy the conservation law

$$\frac{d}{dt}\int_V \varepsilon_E dV + \int_{\partial V} \alpha \vec{S}_E \cdot d\vec{A} = 0 \ , \tag{4.16}$$

for any time-independent three-dimensional region V lying entirely exterior

to the horizon and having the two-dimensional boundary surface ∂V. Here $d\vec{A}$ is the outward-pointing normal area element vector.

One may also write down the charge and current densities on the stretched horizon as defined in Sec. II. If we take the stretched horizon to be at r_H, the charge density vanishes and the current density (2.6b) is

$$\vec{\mathcal{J}}_H = \frac{1}{4\pi}\vec{e}_{\hat{r}}\times\vec{B}_H = -\frac{1}{8\pi^2 r_H \sin\theta}\frac{\partial\psi}{\partial r^*}\vec{e}_{\hat{\varphi}} , \tag{4.17}$$

where $\vec{B}_H$, the stretched-horizon magnetic field, is defined by Eq. (2.5). The stretched-horizon current density is thus purely toroidal, and from Eq. (4.11) one may see that it varies with latitude proportionally to $\sin\theta$.

If we take the region V in Eq. (4.16) to be the spherical shell between the stretched horizon and the outer radius $r = R$, then the only contribution to the surface integral in Eq. (4.16) comes from the stretched horizon, since there is no energy flux through the perfectly conducting sphere at $r = R$. The rate of mass increase of the hole per unit universal time is equal ("$\cong$", in the sense of Sec. II) to the rate of energy flow, per unit universal time t, through the stretched horizon. Using Eqs. (4.6), (4.9), (4.15b), and (4.17), this may be expressed as

$$\frac{dM}{dt} \cong \int_{SH} \alpha\vec{S}_E\cdot d\vec{A} = \int_{SH} \vec{\mathcal{J}}_H\cdot\vec{E}_H dA , \tag{4.18}$$

in agreement with Eq. (2.11). Here the area element vector $d\vec{A}$ points along the outward normal to the region V and hence along the *inward* normal to the horizon. By integrating Eq. (4.16) over time, one may obtain the difference between the total energies of the field in the initial (E_i) and final (E_f) configurations:

$$E_f - E_i = \Delta\int_V \varepsilon_E dV = -\int_0^\infty \left[\int_{SH} \vec{\mathcal{J}}_H\cdot\vec{E}_H dA\right]dt \cong -(M_f - M_i) , \tag{4.19}$$

where M_i and M_f are the initial and final masses, respectively, of the hole.

The quantities E_i and E_f may be obtained explicitly by integrating the energy density ε_E over the region V using the initial and final fields: $\psi_i = \pi B_0 R^2 \sin^2\theta$ and $\psi_f = \pi B_0 r^2 \sin^2\theta$, respectively. The results are

$$\begin{aligned} E_i &\cong \frac{B_0^2 R^4}{12M}\left(1 - \frac{2M}{R}\right), \\ E_f &\cong \frac{B_0^2 R^3}{6}\left(1 - \frac{2M}{R}\right). \end{aligned} \tag{4.20}$$

The rate of energy flow through the stretched horizon can be calculated from Eqs. (4.11), (4.13), (4.17), and (4.18) to be

$$\frac{dM}{dt} \cong \int_{SH} \vec{\mathcal{P}}_H \cdot \vec{E}_H dA \cong \frac{B_0^2 R^4}{6}\left(\frac{\partial u}{\partial r^*}\right)^2_{SH}. \tag{4.21}$$

The quantity $(\partial u / \partial r^*)^2_{SH}$, which by Eq. (4.21) is proportional to the energy flux through the stretched horizon, is plotted in Fig. 15 for the cases $R = 3M$, $R = 10M$, and $R = 100M$. The displacement of the first peak from the origin in these diagrams is due to the finite time required for the waves to propagate down to the stretched horizon. It has been verified numerically that the area under these curves satisfies the energy balance condition, Eq. (4.19), i.e.,

$$\begin{aligned} E_f - E_i = -\frac{B_0^2 R^4}{6}\int_0^\infty \left(\frac{\partial u}{\partial r^*}\right)^2_{SH} dt &\cong -\frac{B_0^2 R^4}{12M}\left(1 - \frac{2M}{R}\right)^2 \\ \Longleftrightarrow \int_0^\infty \left(\frac{\partial u}{\partial r^*}\right)^2_{SH} dt &\cong \frac{(1 - 2M/R)^2}{2M}. \end{aligned} \tag{4.22}$$

The curve for $R = 100M$ in Fig. 15 seems to be a superposition of two oscillations of distinct periods, a fact which may be confirmed by Fourier

transforming it. The period of the longer-term oscillation is approximately twice the radius R of the outer shell, i.e., roughly the light-travel time across the shell. This just corresponds to the time necessary for a particular field line to spring outward and then back inward.

The period of the shorter-term oscillation is roughly equal to $10M$. This value may be justified by an argument similar to that used by Press[35] for gravitational waves. An argument precisely analogous to that given by Press predicts that $u(t,r)$ should have a peak in its frequency spectrum corresponding to a period

$$T \sim \frac{2\pi}{V_{\max}^{1/2}} = 3\pi\sqrt{6}M \sim 23M \ . \tag{4.23}$$

Since the energy flux curves in Fig. 15 are proportional to the squares of $\partial u / \partial r^*$, they should have roughly half this period, or about $10M$ as observed. This argument could also be couched in terms of the gradual decay of a packet of electromagnetic waves in spiral orbits close to the unstable photon orbit at $r = 3M$, as Goebel[36] does for gravitational waves.

Thus, the short period might be characterized as the "sticking time", during which the oscillating field lines are caught and held by the effective potential, while the long period is the natural vibration time of the field lines.

The double periodicity noticeable in the $R = 100M$ curve of Fig. 15 is not evident in the $R = 3M$ and $R = 10M$ cases since the two periods are too close together in the $R = 10M$ case and the oscillations die out too soon in the $R = 3M$ case.

This double periodicity somewhat complicates the task of finding an "experimental" relationship between the damping timescale t_* and the

cavity radius R to compare with the "theoretical" relationship (4.14). The curves consist of periods of oscillation interspersed with periods of quiescence, so a good fit to an exponential decay is impossible. However, rough fits to the envelopes of the curves yield decay times which conform approximately to a power law relationship of the form $t_*/M = \beta(R/M)^\gamma$. The values of γ given by a least squares log-log fit ranged from 1.6 to 1.8 depending on the assumptions made in the fits to the envelopes, and the values obtained for β ranged from 0.4 to 0.6. The theoretical relationship (4.14) would predict the values $\beta = 0.5$ and $\gamma = 2$.

The results of this model problem and those considered in Sec. III suggest some very general conclusions concerning the nature of a stationary electromagnetic field outside a black hole. In paper II of this series (MT Sec. 7.5), an analysis of the equations of structure for a stationary, force-free black-hole magnetosphere showed that no magnetic field loops can extend out of the horizon and then back in. King, Lasota, and Kundt[37] showed that a stationary magnetic field in a vacuum cavity between a black hole and a surrounding plasma shell must be "nearly uniform," i.e., similar to the final configuration of the field in this section. These results all suggest that, in stationary situations, regardless of the complexity of the electromagnetic fields produced by external (accretion disk) currents in the vicinity of a black hole, the field which actually threads the horizon will be "clean;" it will have no loops or complicated tangential structure near the horizon, and no localized concentrations of magnetic field will exist on any region of the horizon.

Insight gained from the above model problems suggests the mechanism by which a black hole gets rid of such structures (i.e., cleans its field) if they try to form. Fig. 16 shows two examples based on the scenario of a magnetic

field threading a black hole and held on it by an accretion disk.[15] The material of the disk is slowly spiraling into the hole and dragging its imbedded field, which may be chaotic, onto the hole. In Fig. 16a (top), a localized concentration of magnetic flux has formed at a particular point on the horizon. As was observed in the model problem of this section, the field lines will spring outward, driving toroidal currents (shown by arrows on middle diagram) in the stretched horizon which dissipate the electromagnetic field energy. The field lines may oscillate several times, but within a timescale of order M, the complex, dynamical tangential field will disappear beneath the stretched horizon, leaving just the uniform field shown in the bottom illustration. In Fig 16b (top), a loop of magnetic field (labeled "L") has been carried onto the horizon. Tension along the field lines will cause the loop to shorten, bringing itself close to and parallel to the stretched horizon (middle diagram). The loop will then sink into the stretched horizon, driving currents as shown in the middle diagram to dissipate its field energy, until it is completely gone (bottom).

V. DISCUSSION AND CONCLUSION

One of the main strengths of the membrane view of black-hole horizons is the cogent and self-consistent mental picture it provides of the interactions of a horizon with an electromagnetic field. As demonstrated by the model problems in this paper, the membrane viewpoint often allows the qualitative results of calculations to be guessed before they are done. It is important to emphasize, though, that the membrane viewpoint is completely consistent with other viewpoints of black holes, the "black-hole viewpoint" based on Penrose and Eddington-Finkelstein spacetime diagrams, for example. But the membrane viewpoint emphasizes those phenomena which are

important in the electromagnetic interaction of a horizon with the exterior universe, and deemphasizes those phenomena, such as the relic tangential horizon field, which are not.

Since the membrane viewpoint is based on a 3+1 split of spacetime, it is particularly well suited to calculations in static or stationary spacetimes. If the spacetime is highly dynamical, however, it loses much of its power since there is then no preferred family of spacelike hypersurfaces with respect to which to make the 3+1 split. In this case, it is more efficacious to view physics in terms of the spacetime diagrams of the black-hole viewpoint. The class of problems for which the membrane formalism is most useful, however, includes most problems of real astrophysical interest. Astrophysical models involving black holes usually assume a nearly stationary and axisymmetric hole interacting electromagnetically, gravitationally, and materially with a complex astrophysical environment (accretion disks, magnetized plasmas, stellar companions, etc.); and for these types of situations the membrane viewpoint is ideally suited. See Ref. 18 for a fuller comparison of the membrane viewpoint with other viewpoints.

In Sec. III, we studied the interaction of external electromagnetic fields with a Schwarzschild horizon in the Rindler approximation. In Sec. IV, a dynamical magnetic field problem in the full Schwarzschild geometry was solved and studied in detail. In both cases, we have illustrated the evolution of the electric and magnetic fields with field-line diagrams. It is the 3+1 formulation in terms of which the membrane formulation is couched which enables such field line diagrams to be drawn, and this feature contributes greatly to an intuitive understanding of the fields. It was also emphasized in both problems that the concepts of the stretched horizon and its surface charge and current were very helpful in understanding how the presence of

the black-hole horizon affects the electromagnetic fields in its vicinity, and in understanding the entropy, energy, and momentum transfer between the field and the hole. In the model problem done in Sec. IV, the criteria governing the choice of the stretched horizon were elucidated: the desire to ignore the relic, near-horizon tangential electromagnetic field, the necessity of making reflection from the electromagnetic potential barrier negligible, and the requirement that the evolution of the field during its propagation from the stretched horizon to the true horizon be negligible. These criteria, although they were derived from consideration of a very specific problem, do not depend on the precise details of that model. This of course is to be desired if the concept of the stretched horizon is to have applicability beyond this limited problem.

The stretched-horizon charges and currents, even though they are entirely imaginary, enter as source terms into Maxwell's equations in exactly the same way as do ordinary charges and currents (although, in the model problems of Secs. III and IV, they turned out to give no contribution to the external field since the black holes under consideration were uncharged). We have seen from the model problems that these concepts facilitate an intuitive understanding of the interactions of a black-hole horizon with external electromagnetic fields. By use of the membrane formalism, both the distortion of an electromagnetic field by the presence of a horizon and the field's effect on the dynamics of the black hole can be understood in close analogy with flat-space electrodynamics.

To elucidate these points more explicitly, we will briefly discuss several black-hole electromagnetic problems in terms of the surface charges and currents. (For further detail on these problems see Ref. 18.) First, we consider the question of how the electric field of a charge very close to, and

stationary outside, the Schwarzschild horizon will be distorted by the gravitational field of the hole. This problem was considered in mathematical detail in Sec. III.C, but here we are interested in the qualitative features of the solution which can be derived intuitively. Immediately we see that, since the stretched horizon behaves like a conductor, the horizon will be polarized so that charges of the opposite sign are induced in the region under the charge, and the electric field lines will bend to strike the stretched horizon normally.

It is as an aid to intuition rather than as an explicit calculational tool that the membrane viewpoint may find its greatest utility. Although this paper has done no calculations in Kerr spacetime, it is possible to guess the qualitative features of some results which have been derived in the past:

Consider a Kerr hole immersed in a uniform magnetic field aligned with its spin axis. It is natural to regard the stretched horizon of a Kerr black hole as behaving essentially like a rotating conducting surface. A spinning conducting sphere in a magnetic field will develop a charge separation, as shown in Fig. 17a, which by Eq. (2.6a) tells us that there will be a normal electric field coming out of the equatorial region and going into the polar regions. Hence we see that the rotation of the Kerr hole couples with the magnetic field to produce a quadrupolar electric field structure as shown in Fig. 17a. This is verified by the field explicitly calculated by Wald[32]; and the analogy is discussed further by Phinney[38] and in Ref. 18.

As another example, one which enables us to examine the effect of an electromagnetic field on the dynamics of a black hole, we consider a Kerr hole immersed in a magnetic field inclined obliquely to its spin axis (Fig. 17b). For a rotating conducting sphere in an oblique magnetic field, we know that the electromagnetic torque on eddy currents in the sphere would

tend to slow the spin of the sphere and also to align the spin with the field. Hence we would expect the spinning hole to line up gradually with the magnetic field and the entropy of the black hole to be increased by the Joule heating due to the stretched-horizon currents. This result was conjectured by Press[39] and proven by King and Lasota[40] and interpreted in terms of horizon currents by Damour.[9]

The interaction of rotating holes with electromagnetic fields is treated in considerable detail in other papers of our series: Paper II (MT) and the review paper[18] which our group is now writing.

This paper has tried to motivate the adoption of the membrane viewpoint not only as a calculational tool in solving problems, but also as an aid to intuition in thinking about these problems. As was emphasized above, there is no difference in the physical predictions of the membrane viewpoint and other viewpoints; they are both consequences of General Relativity and are thus mathematically equivalent. They differ solely in the aspects of the physics which they emphasize and in the array of mental pictures they present as aids to intuitive understanding of physical problems. This paper has attempted to show that, for problems involving dynamical electromagnetic fields around black holes, the mental pictures conjured up by the membrane viewpoint are much more apt for a physical description of the problem than are those conjured up by older viewpoints of black-hole horizons.

ACKNOWLEDGEMENTS

We are indebted to Kip S. Thorne for many helpful suggestions during the course of this work and the preparation of the manuscript. We also thank the other members of the Caltech Paradigm Society: Richard Price, Thibaut Damour, Ronald Crowley, Wojciech Zurek, Ian Redmount, Sam Finn, and Xiao-He Zhang. This work was supported by the National Science Foundation under Grant No. AST82-14126.

APPENDIX

For a point particle of charge Q and mass m moving in flat space with four-velocity u^μ, the equations of motion including radiation reaction are[41]

$$F^\mu_{\text{ext}} \equiv \frac{Dp^\mu}{ds} = ma^\mu - \frac{2}{3}Q^2(\dot{a}^\mu - u^\mu a^\nu a_\nu) , \tag{A1}$$

where F^μ_{ext} is the external four-force, p^μ is the total four-momentum of the particle and its electromagnetic field $a^\mu = Du^\mu / ds$ is the four-acceleration, and the overhead dot indicates differentiation with respect to the charge's proper time s. Since Eq. (A1) is generally covariant, it must be valid in Rindler coordinates. We choose kinematic quantities appropriate to a charge moving with constant ZAMO-measured velocity $d\vec{x} / d\tau = \beta \vec{e}_x$:

$$\begin{aligned} u^\mu &= (\gamma / \alpha_o , \gamma\beta, 0, 0) , \\ a^\mu &= (0, 0, 0, g_H \gamma^2 / \alpha_o) , \\ \dot{a}^\mu &= (g_H^2 \gamma^3 / \alpha_o^3, 0, 0, 0) , \end{aligned}$$

where $\gamma \equiv (1 - \beta^2)^{-1/2}$, and where α_o is the value of the lapse function at the position of the particle. When converted to a per-unit-universal-time basis, $d / dt = (\alpha_o / \gamma) d / ds$, the rate of change of the x-momentum of particle plus field as computed from Eq. (A1) is

$$\frac{dp^x}{dt} = \frac{\alpha_o}{\gamma}\frac{dp^x}{ds} = \frac{\alpha_o}{\gamma}F^x = \frac{2}{3}Q^2 g_H^2 \frac{\gamma^4 \beta}{\alpha_o} ; \tag{A2}$$

and the rate of change of "energy-at-infinity" $-p_t$ of particle plus field is

$$\frac{-dp_t}{dt} = -\frac{\alpha_o}{\gamma}\frac{dp_t}{ds} = \frac{\alpha_o^3}{\gamma}\frac{dp^t}{ds} = \frac{\alpha_o^3}{\gamma}F^t = \frac{2}{3}Q^2 g_H^2 \gamma^4 \beta^2 . \tag{A3}$$

By conservation of momentum, Eq. (A2) gives the rate of flow of x-momentum into the horizon; and the corresponding rate of flow of angular

momentum into the horizon is

$$\frac{dJ}{dt} = (2M\sin\theta_o)\frac{dp^z}{dt} = (2M\sin\theta_o)\frac{2}{3}\frac{Q^2 g_H^2}{\alpha_o}\gamma^4\beta \qquad \text{(A4)}$$

[Eq. (3.29)]. By conservation of energy-at-infinity, $-dp_t/dt$ is the rate of flow of energy-at-infinity into the horizon, i.e., the rate of increase dM/dt of the hole's mass [Eq. (3.26)]. The results derived here agree with the results obtained from explicit evaluation of the surface integrals (3.25) and (3.28).

REFERENCES

[1] J. D. Bekenstein, Ph.D. thesis, Princeton University, 1972.

[2] S. W. Hawking, Commun. Math. Phys. 25, 152 (1972).

[3] S. W. Hawking and J. B. Hartle, Commun. Math. Phys. 27, 283 (1972).

[4] J. D. Bekenstein, Phys. Rev. D 7, 2333 (1973).

[5] S. W. Hawking, Commun. Math. Phys. 43, 199 (1975).

[6] J. B. Hartle, Phys. Rev. D 8, 1010 (1973).

[7] J. B. Hartle, Phys. Rev. D 9, 2749 (1974).

[8] R. L. Znajek, Mon. Not. R. Astron. Soc. 185, 833 (1978).

[9] T. Damour, Phys. Rev. D 18, 3598 (1978).

[10] T. Damour, in *Proceedings of the Second Marcel Grossman Meeting on General Relativity*, edited by R. Ruffini (North Holland, Amsterdam, 1982); also for more detail, T. Damour, these de doctorat d'etat (Ph.D. thesis), l'Universite Pierre et Marie Curie, Paris, 1979.

[11] C. W. Misner, K. S. Thorne, and J. A. Wheeler, *Gravitation*, (W. H. Freeman, San Francisco, 1973); cited in text as MTW.

[12] C. Dewitt and B. Dewitt (editors), *Black Holes*, (Gordon and Breach, New York, 1973).

[13] K. S. Thorne and D. A. Macdonald, Mon. Not. R. Astron. Soc. 198, 339 (1982); cited in text as TM.

[14] D. A. Macdonald and K. S. Thorne, Mon. Not. R. Astron. Soc. 198, 345 (1982); cited in text as MT.

[15] R. D. Blandford and R. L. Znajek, Mon. Not. R. Astron. Soc. 179, 433 (1977).

[16] R. H. Price and K. S. Thorne, in preparation, to be submitted to Phys. Rev. D.

[17] W.-M. Suen, R. H. Price, and I. H. Redmount, in preparation, to be submitted to Phys. Rev D.

[18] K. S. Thorne, R. H. Price, W.-M. Suen, D. A. Macdonald, I. H. Redmount, R. J. Crowley, and X.-H. Zhang, in preparation, to be submitted to Rev. Mod. Phys.

[19] W. Rindler, Am. J. Phys. 34, 1174 (1966).

[20] J. M. Bardeen, W. H. Press, and S. A. Teukolsky, Astrophys. J. 178, 347 (1973).

[21] B. Carter, in *General Relativity, An Einstein Centenary Survey*, edited by S. W. Hawking and W. Israel (Cambridge University Press, Cambridge, 1979).

[22] D. Christodoulou and R. Ruffini, in *Black Holes*, edited by C. Dewitt and B. Dewitt, (Gordon and Breach, New York, 1973).

[23] J. M. Bardeen, B. Carter, and S. W. Hawking, Commun. Math. Phys. 31, 161 (1973).

[24] B. S. Dewitt and R. W. Brehme, Ann. Phys. (N.Y.) 9, 220 (1960).

[25] A. G. Smith and C. M. Will, Phys. Rev. D 22, 1276 (1980).

[26] W. G. Unruh, Phys. Rev. D 14, 870 (1976).

[27] See, for example, J. D. Jackson, *Classical Electrodynamics*, 2nd ed. (Wiley, New York, 1975).

[28] T. C. Bradbury, Ann. Phys. (N.Y.) 19, 323 (1962); D. G. Boulware, Ann. Phys. (N.Y.) 124, 169 (1980); M. Soffel, B. Müller, and W. Greiner, Gen. Relativ. Gravit. 12, 287 (1980).

[29] R. S. Hanni and R. Ruffini, Phys. Rev. D 8, 3259 (1973).

[30] E. T. Copson, Proc. R. Soc. London, Ser. A 118, 184 (1928); B. Linet, J. Phys. A 9, 1081 (1976).

[31] T. Regge and J. A. Wheeler, Phys. Rev. 108, 1063 (1957).

[32] R. M. Wald, Phys. Rev. D 10, 1680 (1974).

[33] R. S. Hanni and R. Ruffini, Lett. Nuovo Cimento 15, 189 (1976).

[34] See, for example, T. G. Cowling, *Magnetohydrodynamics*, (Interscience, New York, 1957).

[35] W. H. Press, Astrophys. J. 170, L105 (1971).

[36] C. J. Goebel, Astrophys. J. 172, L95 (1972).

[37] A. R. King, J. P. Lasota, and W. Kundt, Phys. Rev. D 12, 3037 (1975).

[38] E. S. Phinney, in *Proceedings of the Torino Workshop on Astrophysical Jets*, edited by A. Ferrari and A. G. Pacholczyk (D. Reidel, Dordrecht, Holland, 1983).

[39] W. H. Press, Astrophys. J. 175, 243 (1972).

[40] A. R. King and J. P. Lasota, Astron. Astrophys. 58, 175 (1977).

[41] P. A. M. Dirac, Proc. R. Soc. London, Ser. A 167, 148 (1938); also problem 17.4 of Ref. 27.

FIGURE CAPTIONS

FIG. 1. The surfaces of constant universal time t around a Schwarzschild black hole, as viewed in Eddington-Finkelstein coordinates. The Eddington-Finkelstein time coordinate $\tilde{t}$ is related to universal time by $\tilde{t} = t + 2M\ln(r/2M - 1)$, and the Eddington-Finkelstein coordinate r is identical to the Schwarzschild r. The cones are the radial light cones as given by the metric in Eddington-Finkelstein coordinates: $ds^2 = -d\tilde{t}^2 + dr^2 + (2M/r)(d\tilde{t} + dr)^2 + r^2(d\theta^2 + \sin^2\theta d\varphi^2)$.

FIG. 2. The world lines of the Minkowski-stationary (dotted line) and Rindler-stationary (dashed line) charges, as seen in Minkowski (a) and Rindler (b) coordinates. The Minkowski-stationary charge is fixed at $Z = z_0$, while the Rindler-stationary charge is fixed at $z = z_0$. In diagram (a), the lower and upper 45° lines represent the past and future event horizons, respectively. In diagram (b), the intersection of the horizons is represented by the solid vertical line $z = 0$, to which the dotted line asymptotes.

FIG. 3. Electric field lines for two opposite charges which split at $t = 0$, $z = z_0$: one remaining stationary in Rindler coordinates, and the other stationary in Minkowski coordinates and thus falling into the horizon. The field line diagrams are shown at different values of Rindler-time t. By $t = 6/g_H$, the field geometry has become almost indistinguishable from the field of the stationary charge alone, which is shown in the lower right-hand diagram.

FIG. 4. Electric field lines of a charge at rest outside a Schwarzschild black hole ("Copson-Linet" solution[29]).

FIG. 5. Electric field lines for a charge moving with uniform velocity in the $+x$ direction in Rindler space at a distance z_0 above the horizon. Part (a) shows the field lines in the $x-z$ plane for $\beta = 0.5$. A possible choice of the

stretched horizon is shown as a dotted line. Part (b) is a three-dimensional plot as viewed from the side, showing the field lines which emerge from the charge at polar angles of $\theta = 90°$ (solid lines) and $\theta = 120°$ (dotted lines), with respect to the vertical z axis. Parts (c) and (d) are similar plots for the case $\beta = 0.1$.

FIG. 6. The stretched-horizon surface charge density $\sigma_H(x,0,0)$ along the x axis (directly below the track of the particle), as induced by a charged particle in uniform motion parallel to the horizon at a height z_o above it (same particle as in Figs. 5a and 5b). The charge density is plotted in units of Q/z_o^2 and is shown for two different choices of stretched horizon location: $\alpha_H^{(1)} = 10^{-2}\alpha_o$ and $\alpha_H^{(2)} = 10^{-4}\alpha_o$. Both are shown at time $t = 0$ for $\beta = 0.5$. The points marked x^* are defined by $x^* = (\alpha_o\beta/g_H)\ln(\alpha_H/\alpha_o)$. Both plots go slightly positive in the region to the right of their large negative peaks.

FIG. 7. The stretched-horizon surface current density induced by the moving charged particle of Figs. 5a, 5b, and 6 for $\beta = 0.5$, $t = 0$. Part (a) shows the distribution on a stretched horizon at $\alpha_H^{(1)} = 10^{-2}\alpha_o$, and part (b) for $\alpha_H^{(2)} = 10^{-4}\alpha_o$. Values of x/z_o are indicated by the scale next to each figure, showing that the lag of the current distribution increases as α_o is made smaller.

FIG. 8. The flux of energy and angular momentum carried into the stretched horizon by the electromagnetic field of the charged particle of Figs. 5a, 5b, 6, and 7. The solid line (scale on left) shows the energy flux per unit x-length $(1/Q^2g_H^2)(dM/dtdx)$ into the stretched horizon as a function of x, obtained by integrating the energy flux density over y. The dotted line (scale on right) shows the flux of x-momentum per unit x-length $(1/2M\sin\theta_o)(\alpha_o/Q^2g_H^2)(dJ/dtdx)$ into the stretched horizon. Both are shown at time $t = 0$ for the choice of parameters $\beta = 0.5$ and $\alpha_H = 10^{-4}\alpha_o$

and both are plotted in units of z_0^{-1}. The point labeled x^* is the location where a zero-angular-momentum light ray from the charge's retarded position strikes the stretched horizon: $x^* = \beta z_0 \ln(\alpha_H / \alpha_0) = -4.6 z_0$. The momentum plot goes slightly negative in the region to the left of the peak.

FIG. 9. Electric field lines of the temporarily moving charge which moves with constant velocity parallel to the horizon, $d\vec{x} / d\tau = \beta \vec{e}_x$, from $t = 0$ to $t = 1/g_H$ and is static before and after this motion. In both diagrams, $\beta = 0.5$; diagram (a) shows the field at $t = 2/g_H$, and diagram (b) shows it at $t = 3.5/g_H$.

FIG. 10. Electric field lines of the temporarily moving charge which moves with constant velocity perpendicular to the horizon, $d\vec{x} / d\tau = \beta \vec{e}_z$, from $t = 0$ to $t = 1/g_H$ and is static before and after this motion. In both diagrams, $\beta = 0.5$; diagram (a) shows the field at $t = 2.5/g_H$, and diagram (b) shows it at $t = 3.5/g_H$.

FIG. 11. Constant-time-interval snapshots of the field of a charge moving with $\beta = 0.5$ in the x direction, parallel to the horizon (charge of Figs. 5a, 5b, 6, 7, and 8). The figure shows the directions of those bits of field (indicated by the short segments, or arrows) that were "emitted" by the particle when it was at the point to which the curved lines converge. The curved lines are the spatial tracks of the null geodesics along which the field propagates, and the direction of the field is indicated by the arrows on them. Part (a) shows the electric field in the $x-z$ plane with a snapshot interval $\Delta t = 0.3/g_H$. Also shown are the positions of the particle (crosses) at the times of the successive snapshots, labeled by the time t in units of $1/g_H$. Part (b) shows the magnetic field in the $y-z$ plane with a snapshot interval $\Delta t = 0.3/g_H$.

FIG. 12. Initial geometry of magnetic field lines in Schwarzschild space, shown in $r-\theta$ coordinates with φ = constant. The outer boundary, at which a

perfectly conducting sphere resides, is at radius $r = R \equiv 10M$; the inner sphere is the horizon. The arrows show the direction of the field. This is the view which would be seen by looking down into the paraboloidal embedding diagram of Schwarzschild space. The field lines are frozen into the outer sphere, but are free to slip through the horizon since its conductivity is finite. The tension of the field lines will tend to straighten them out.

FIG. 13. The vibratory time evolution of the field whose initial conditions (for $R = 10M$) are shown in Fig. 12. Part (a) shows representative magnetic-field-line diagrams in the evolution of the case $R = 3M$. Since most of the field lines thread the horizon at all times, the field settles down quickly to its final static configuration. Part (b) shows representative magnetic-field-line diagrams in the evolution of the case $R = 10M$. Since the horizon is small relative to the outer sphere, the field lines oscillate for a long time before reaching their final static configuration. The diagrams shown cover only the first oscillation in detail, and the beginning of the second oscillation at $t/M = 28$. The last two diagrams are much further in the future and show that the oscillations have died out substantially by $t/M = 155$ and almost completely by $t/M = 500$. The kinks in the field lines for the case $t/M = 12$ are due to the finite grid used in the numerical integration.

FIG. 14. Embedding-diagram view of the vibrating magnetic field of Figs. 12 and 13 at time $t = 92M$ for the case $R = 10M$, with the near-horizon fields expanded for visibility. In the top part of the figure, the magnetic field lines are plotted on the paraboloidal embedding diagram of Schwarzschild space. The paraboloid is cut off at a stretched horizon which is taken to be at a radius $r = 2.15M$, and a cylinder is matched onto it there. In order to make the near-horizon fields visible, the distance along this cylinder is measured by the tortoise coordinate r^*. We view the diagram from an elevation angle

of 18° and a rotation angle of 45°. At the time shown, the field lines have sprung outward and snapped back inward four times and are beginning to spring outward for a fifth time. The relic field-line loops left by each of these oscillations are visible running down the cylinder, and the partially formed loops at the top of the cylinder may be seen to connect to field lines outside the stretched horizon. In the lowermost region of the diagram, the field lines are vertical due to the fact that the field was held stationary until its release at $t = 0$. As one proceeds up the cylinder, one finds successively fewer concentric loops in each set of field lines, since the oscillations are dying out and fewer field lines snap back to the stretched horizon with each oscillation.

FIG. 15. The rate of flow of magnetic energy through the horizon as a function of time for the vibrating magnetic field of Figs. 12, 13, and 14. Plots are shown for three different values of the radius of the outer conducting sphere: $R = 3M$, $R = 10M$, and $R = 100M$. Plotted vertically is the dimensionless quantity $M^2(\partial u / \partial r^*)^2_{SH}$ which, as shown in Eq. (4.21), is proportional to the energy flux through the horizon. The curve for $R = 100M$ shows a clear double periodicity corresponding to the two different length scales in the problem: R and M.

FIG. 16. Qualitative illustrations of the "cleaning" of a complex electromagnetic field by a black-hole horizon. Part (a) shows the dispersal of a localized concentration of magnetic flux threading the horizon. Part (b) shows the annihilation of a field-line loop, marked "L", with both feet embedded in the horizon. In both cases, the horizon currents, which dissipate excess field energy, are indicated by arrows on the horizon.

FIG. 17. Part (a) shows a Kerr black hole immersed in a uniform magnetic field aligned with its spin axis. The polarization of surface charge produced

by the field leads to a quadrupolar electric field structure. Part (b) shows a Kerr black hole in a magnetic field inclined obliquely to its spin axis. Electromagnetic forces on the hole's surface currents will tend to align the hole's spin with the magnetic field and to increase its entropy.

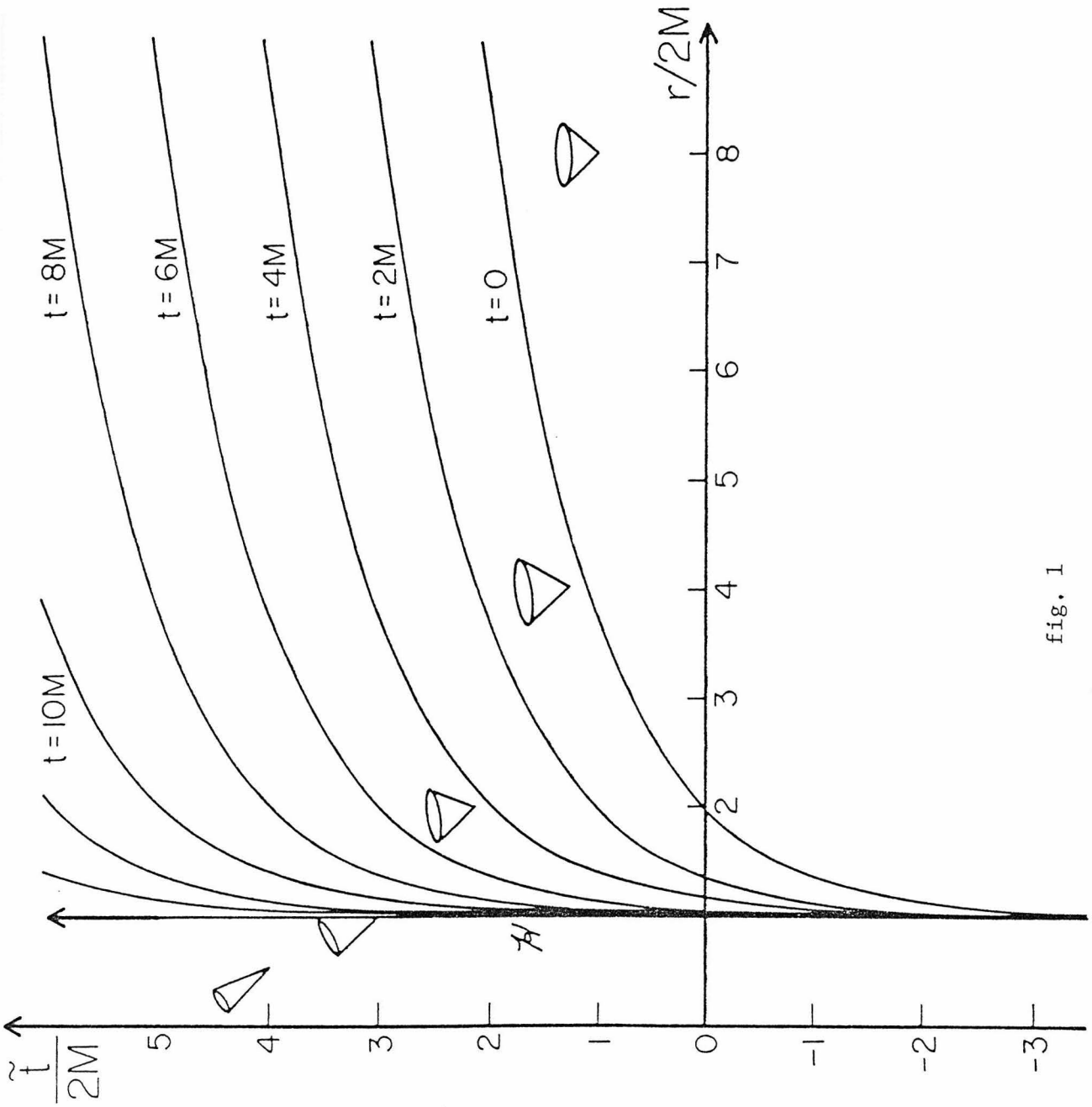

fig. 1

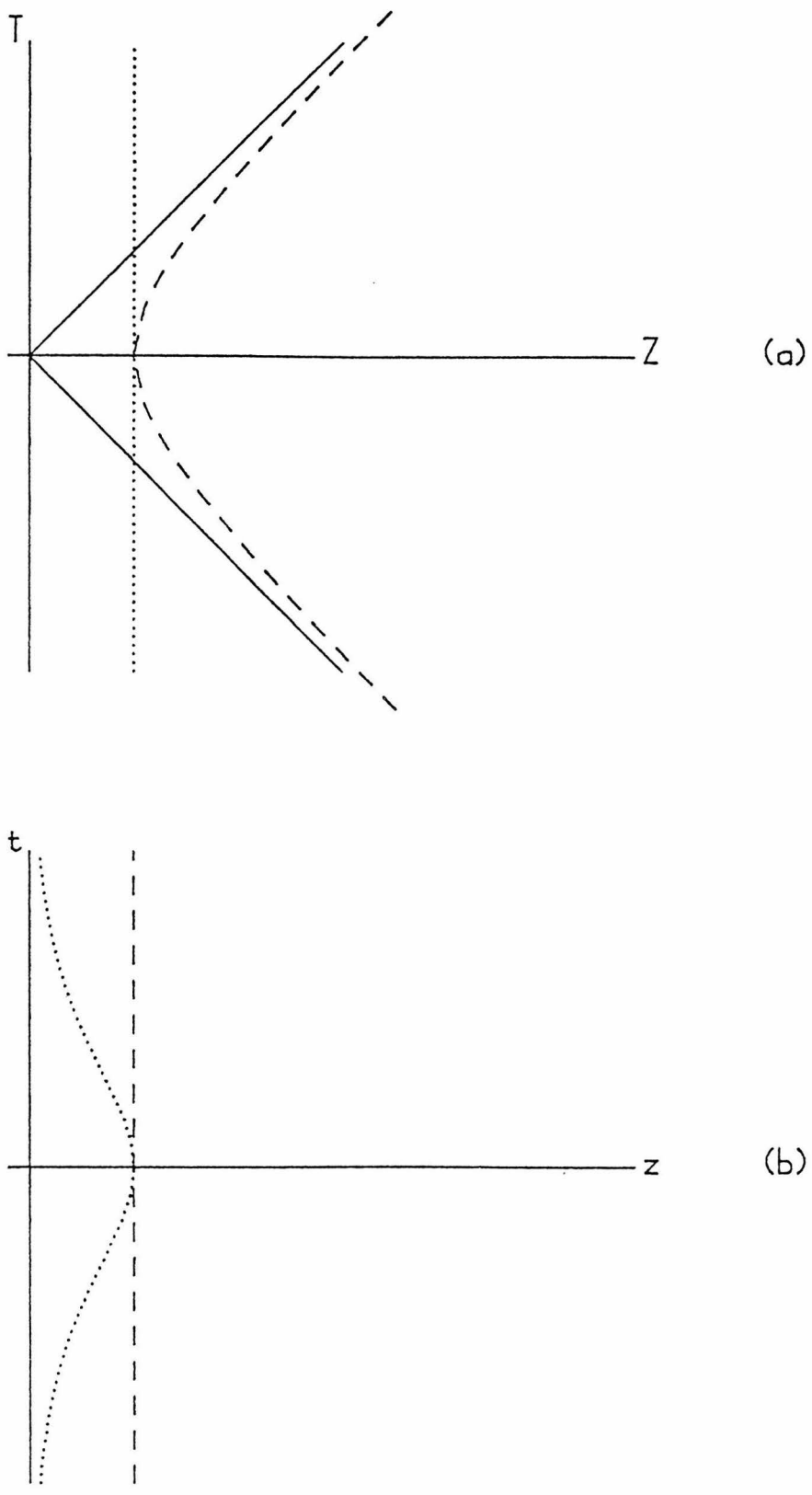

fig. 2

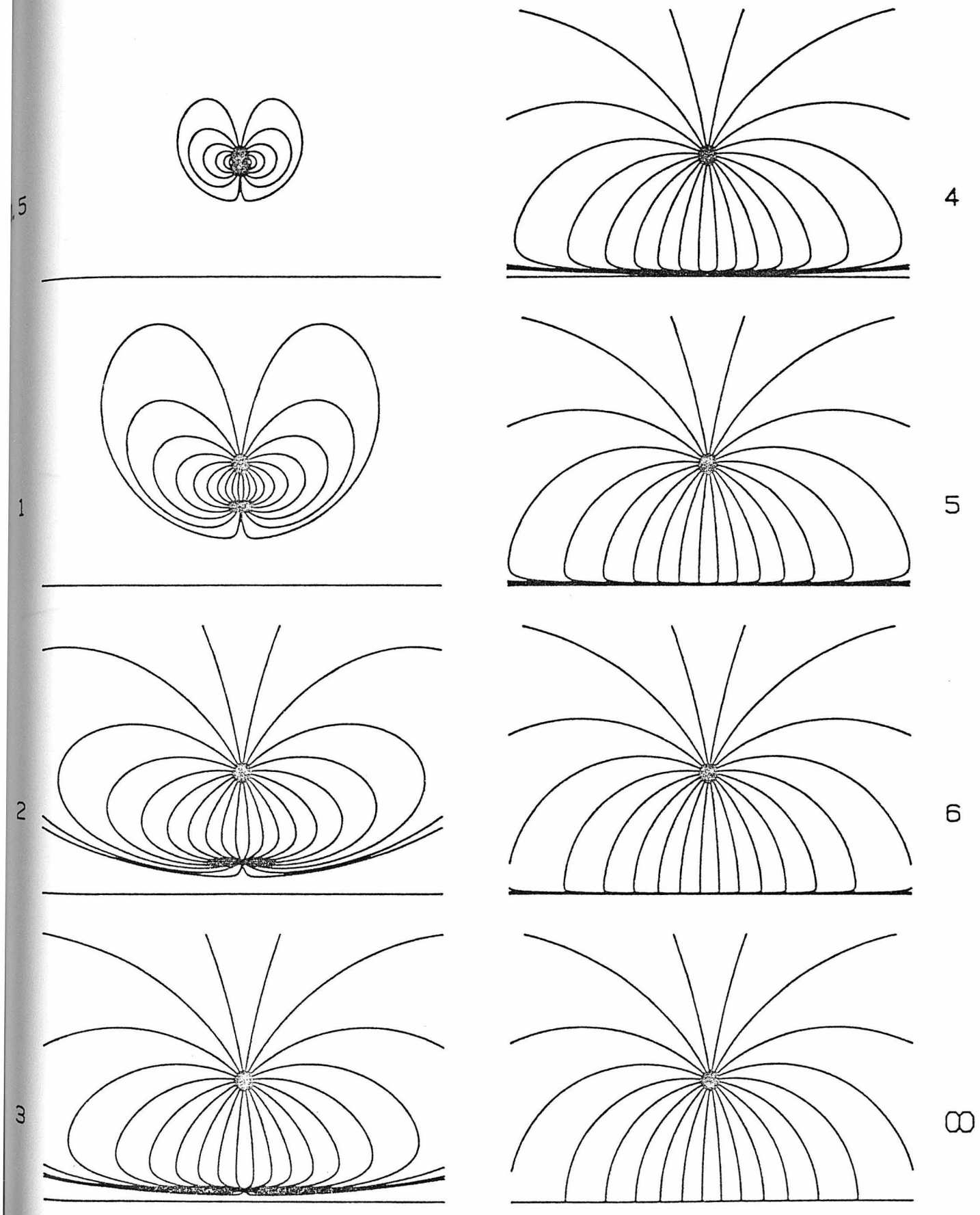

fig. 3

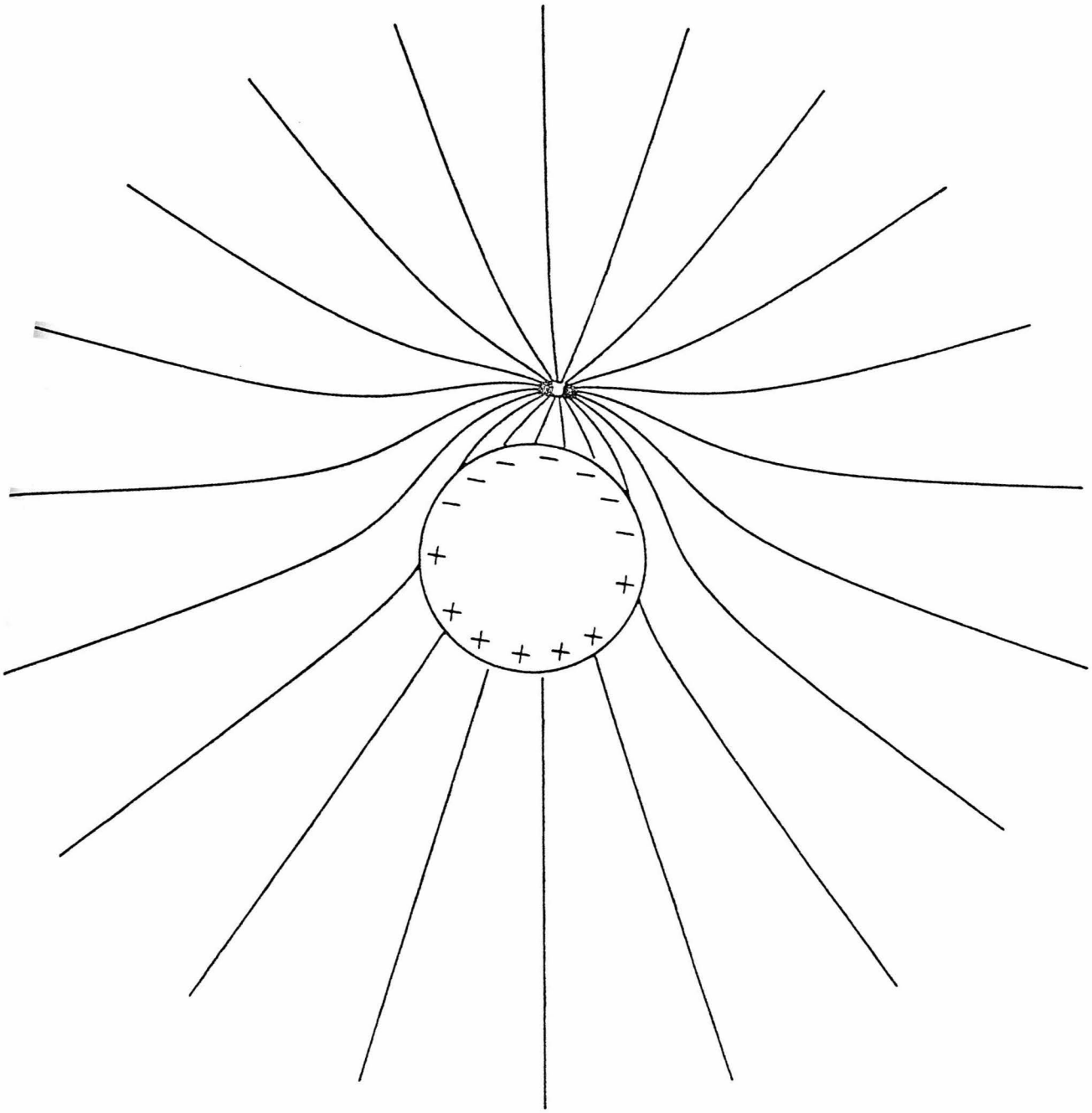

fig. 4

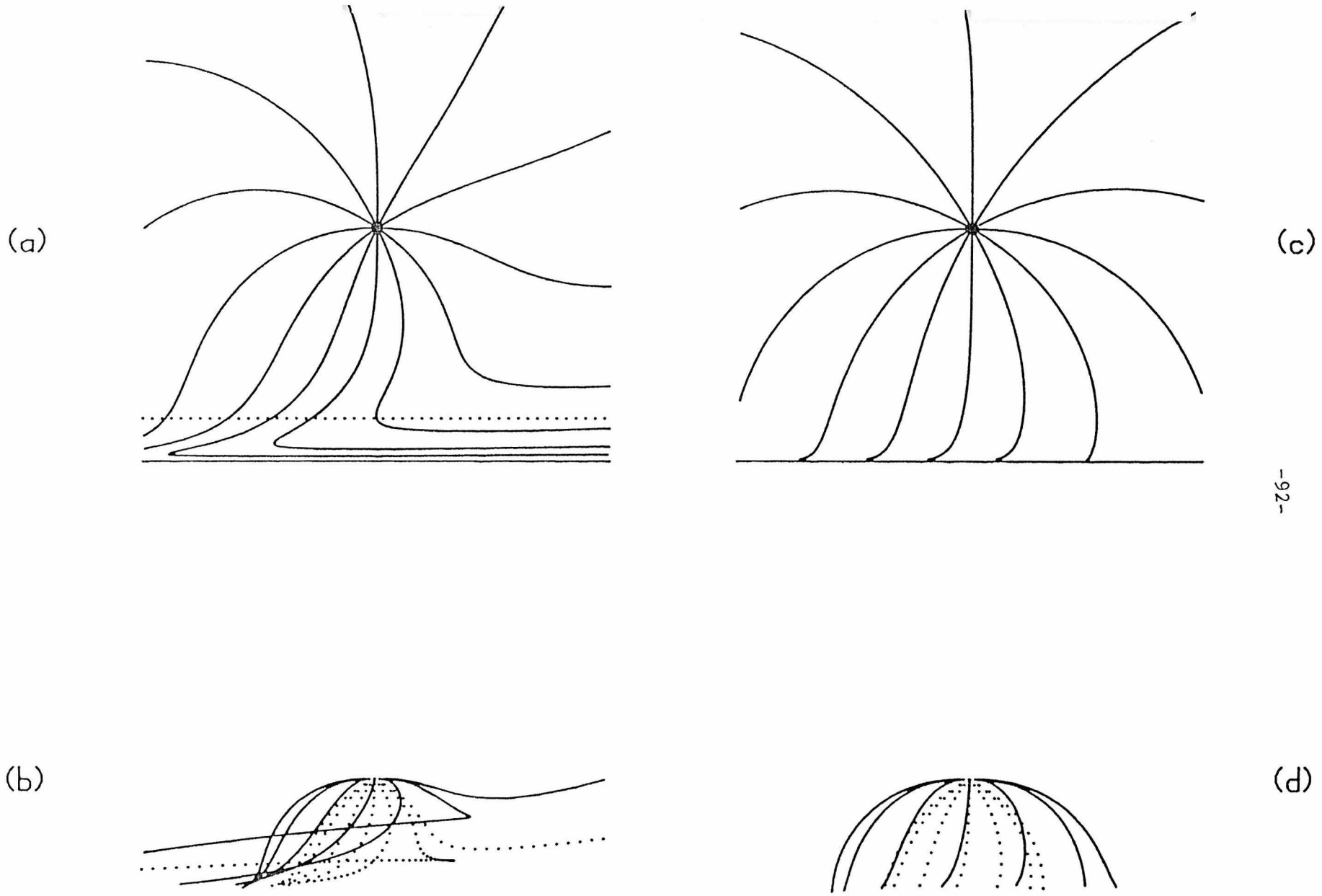

fig. 5

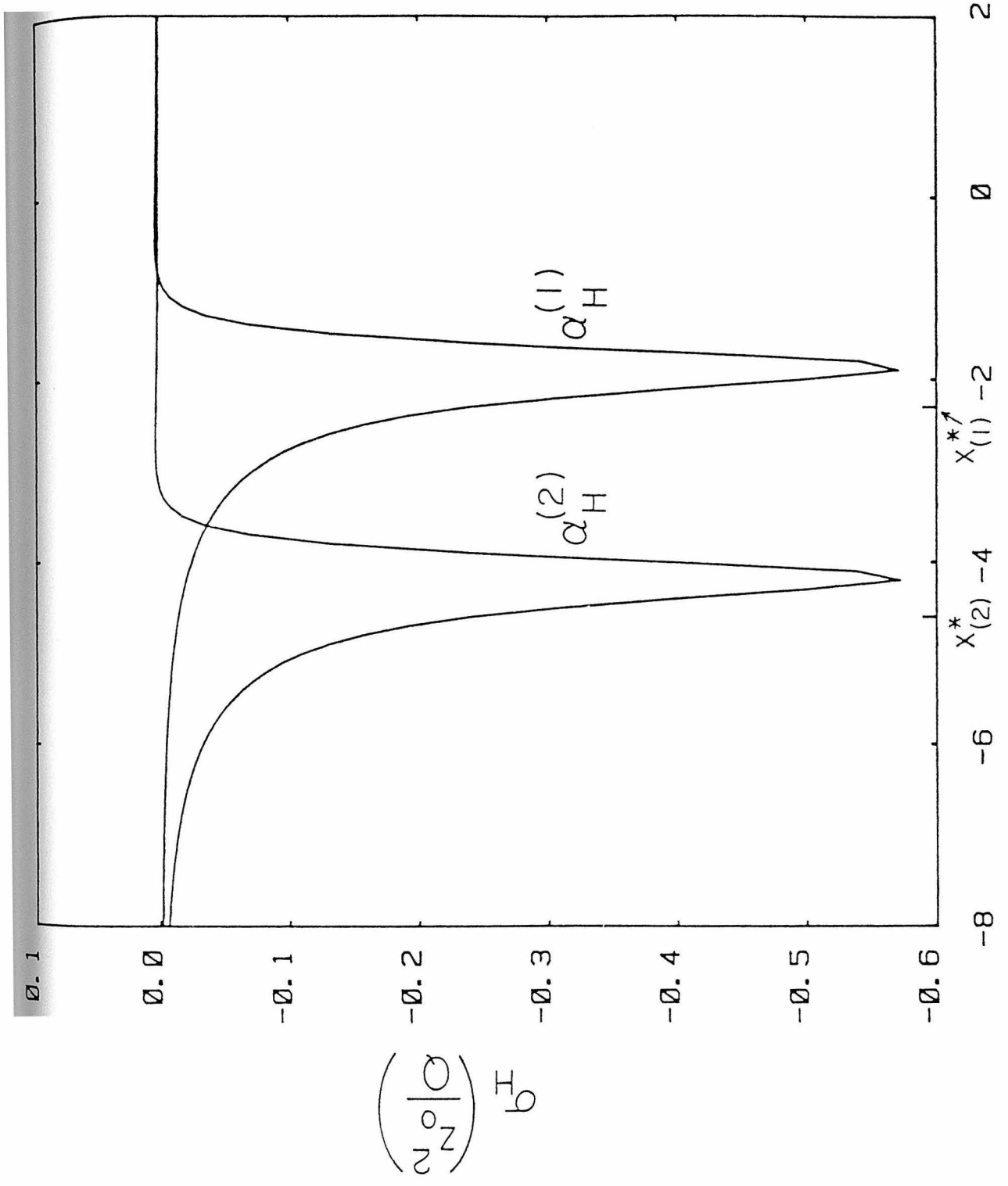
Ø.1
0.0
-0.1
-0.2
-0.3
-0.4
-0.5
-0.6
-8
-6
-4
-2
Ø
2
$\left(\frac{Q}{N_o R}\right) q_H$
$Q_H^{(1)}$
$Q_H^{(2)}$
$X^*_{(2)}$
$X^{*\prime}_{(1)}$
X/Z_o

fig. 6

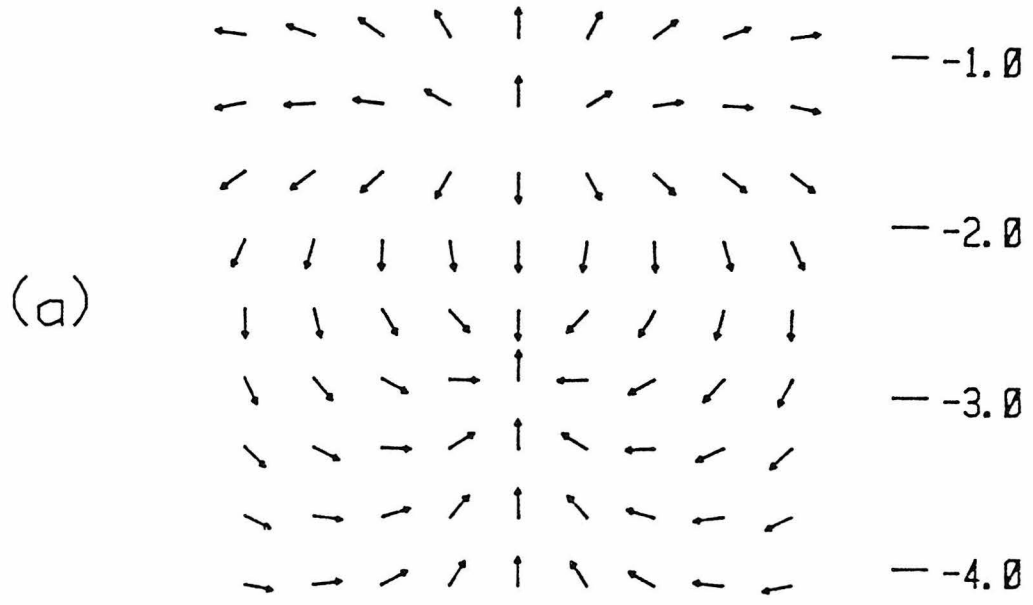

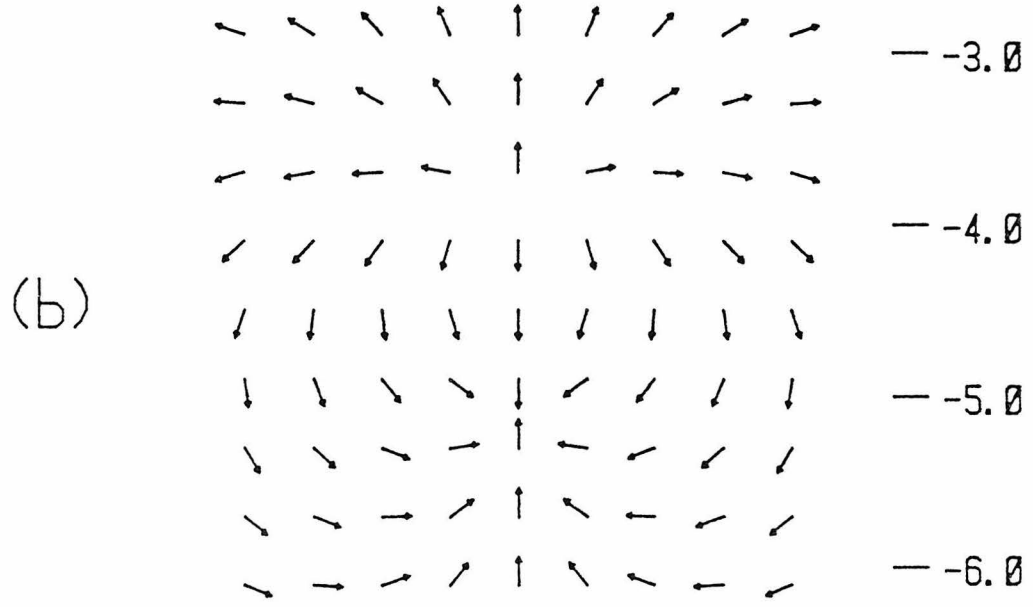

fig. 7

$\frac{z_o}{Q^2 g_H^2} \frac{dM}{dt\,dx}$
0.5
0.4
0.3
0.2
0.1
0.0
-7
-6
-5
-4
-3
-2
-1
x^*
X/Z_o
1.5
1.2
0.9
0.6
0.3
0.0
$\frac{z_o}{2M \sin\theta_o} \frac{\alpha_o}{Q^2 g_H^2} \frac{dJ}{dt\,dx}$

fig. 8

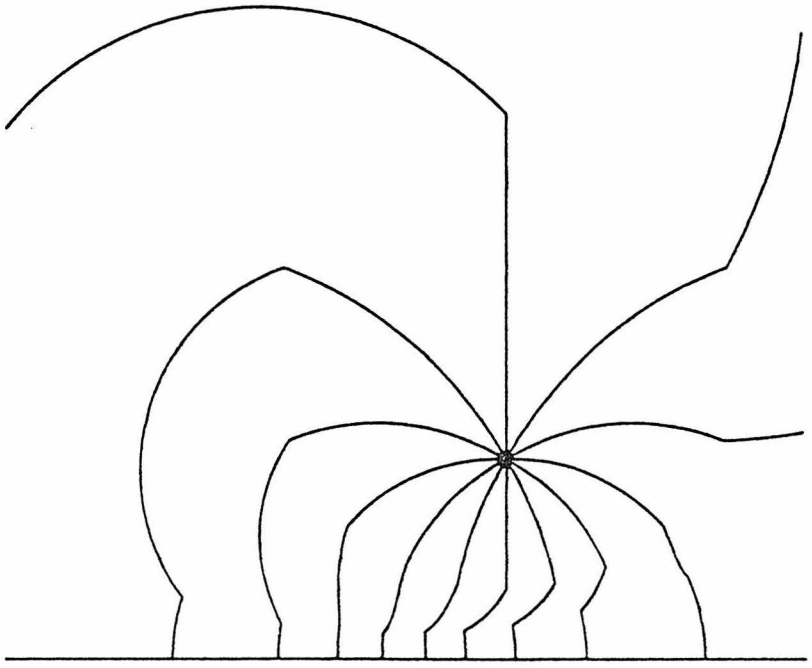

(a)

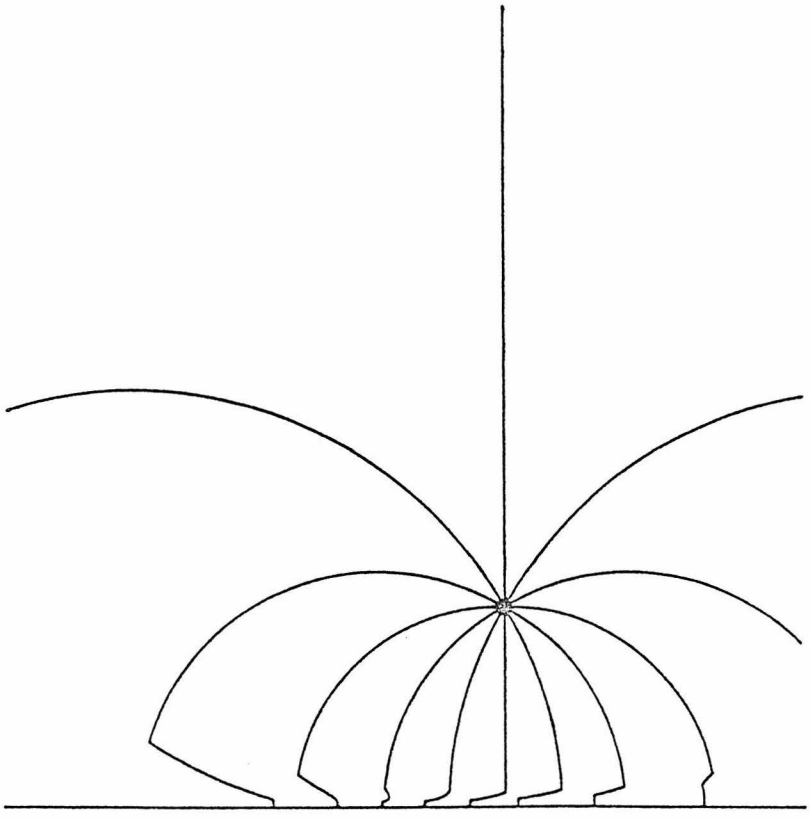

(b)

fig. 9

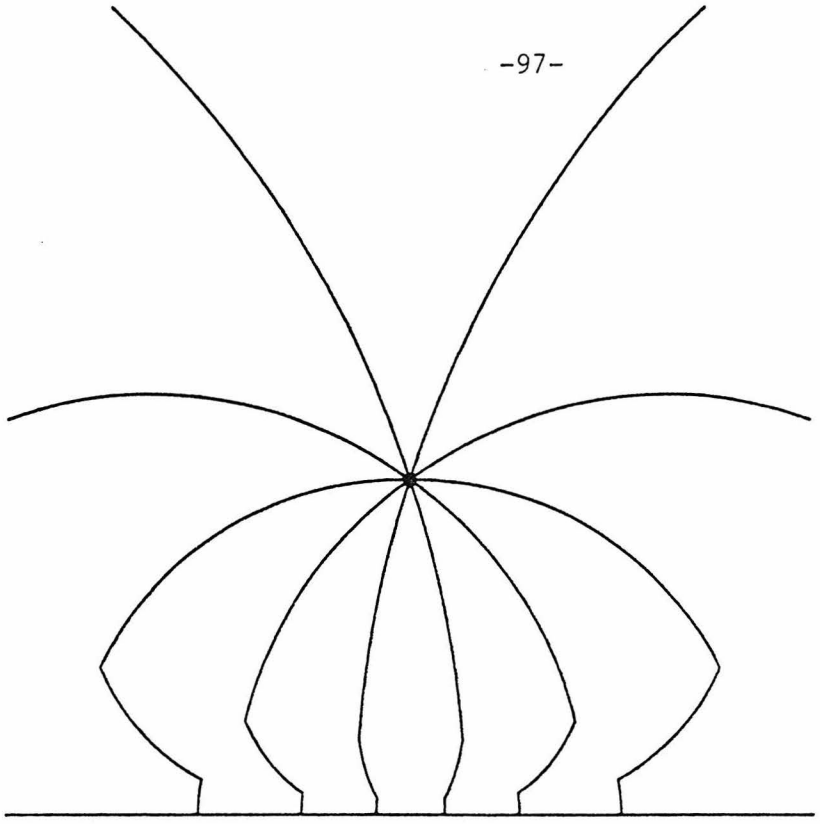

(a)

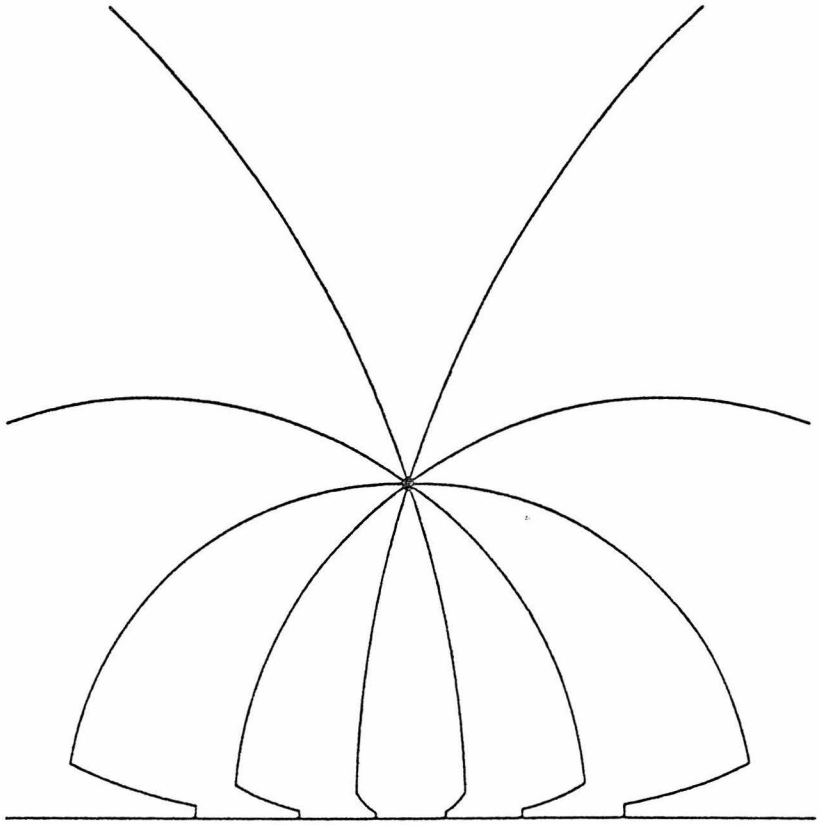

(b)

fig. 10

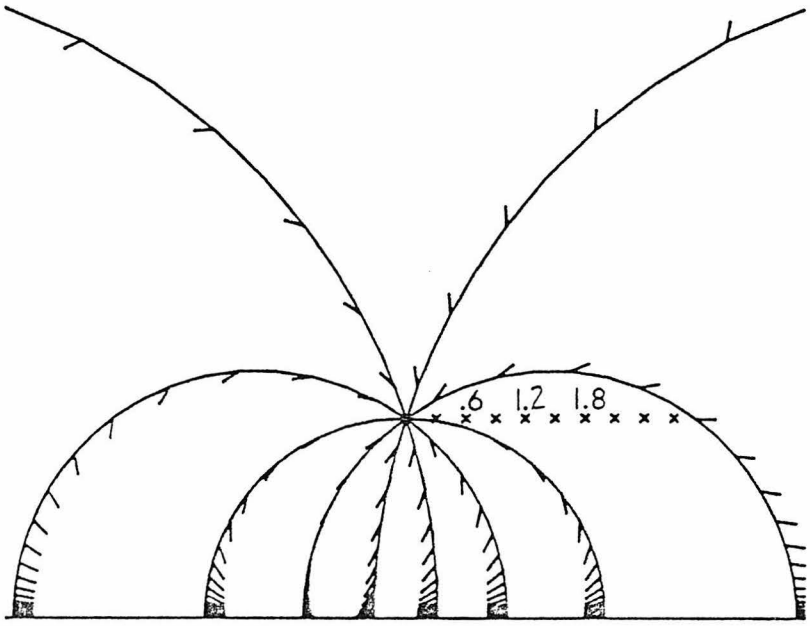

(a)

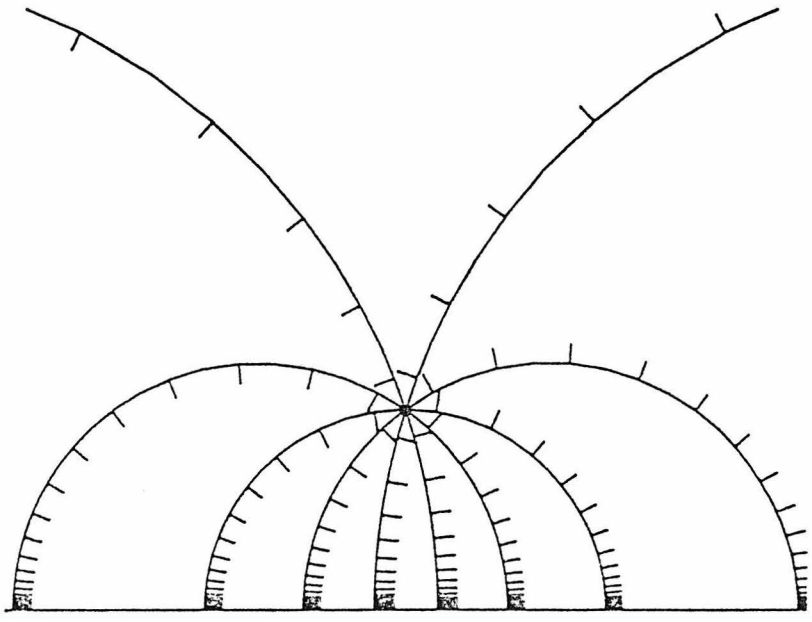

(b)

fig. 11

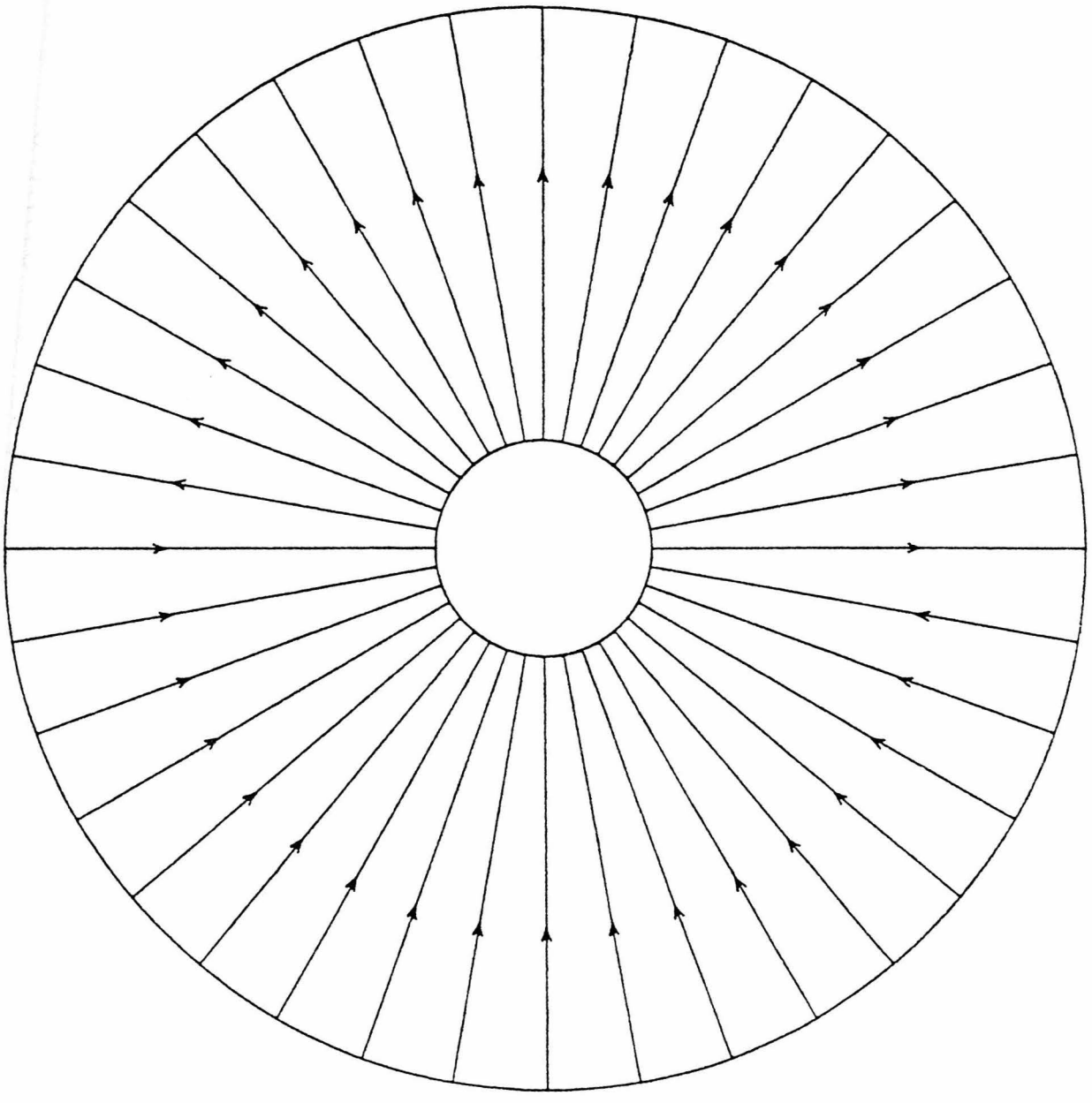

fig. 12

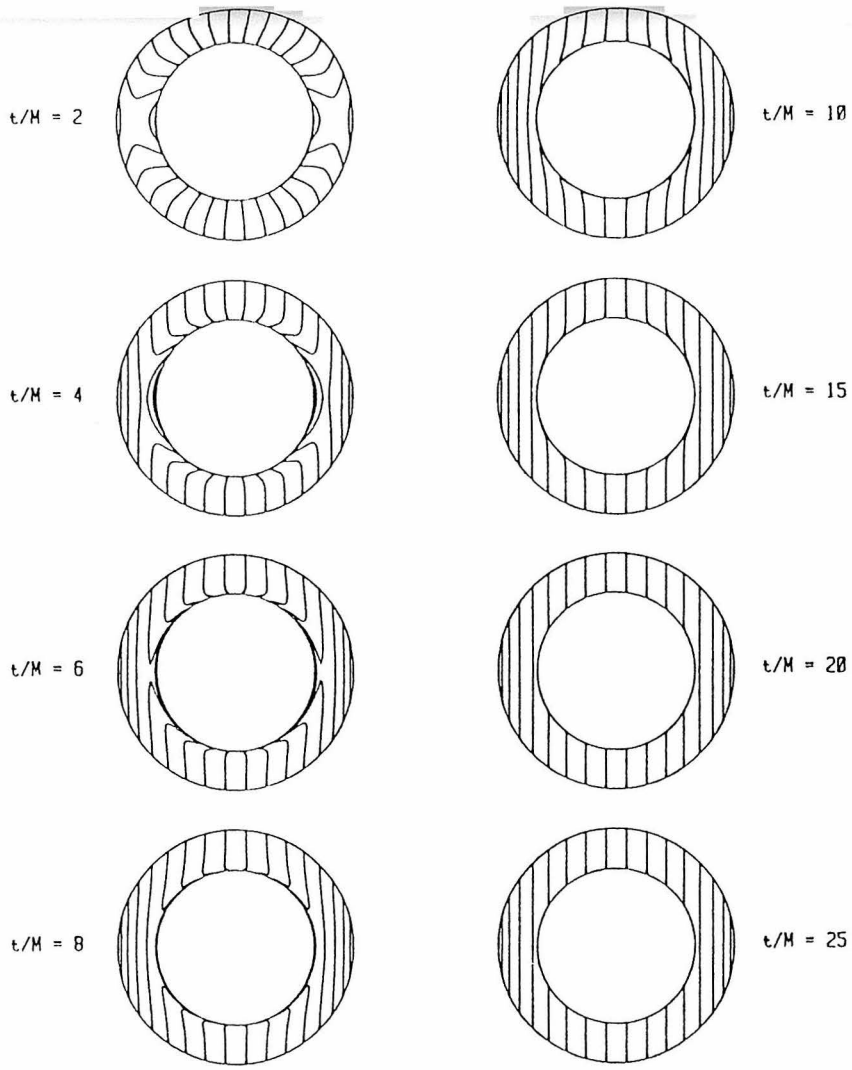
t/M = 2
t/M = 4
t/M = 6
t/M = 8
t/M = 10
t/M = 15
t/M = 20
t/M = 25
(a)

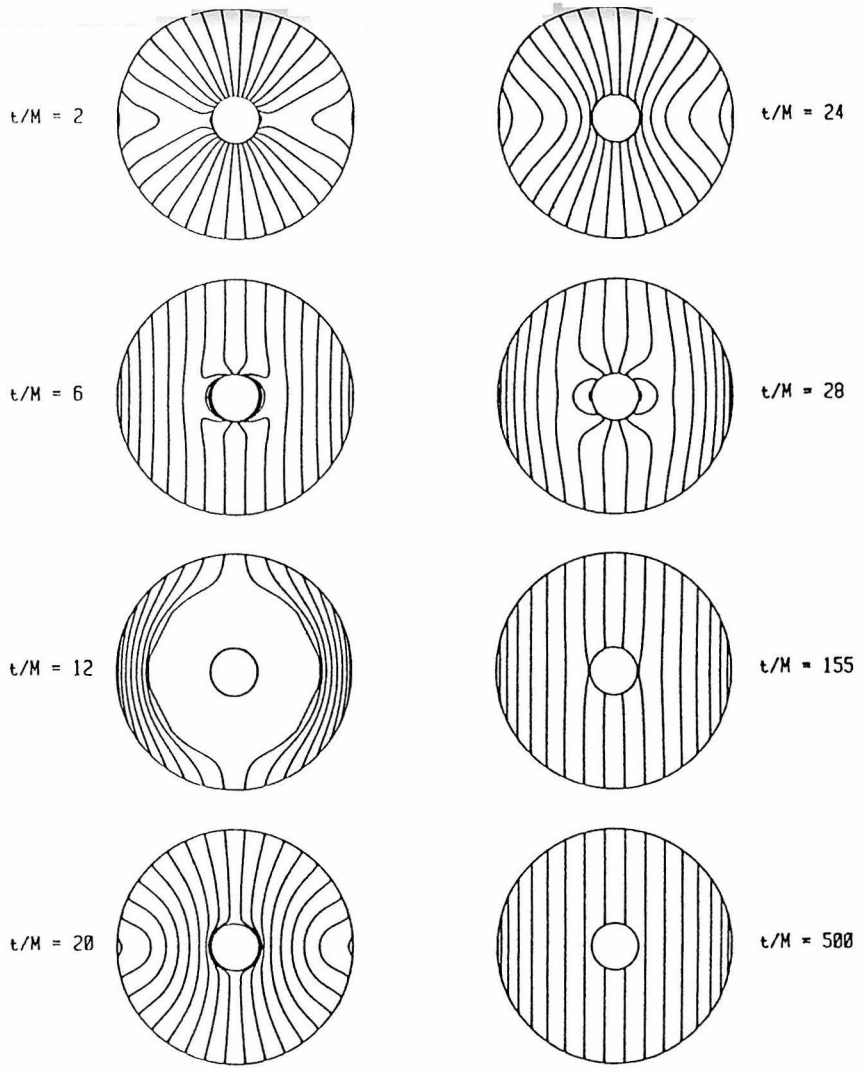
t/M = 2
t/M = 6
t/M = 12
t/M = 20
t/M = 24
t/M = 28
t/M = 155
t/M = 500
(b)

fig. 13

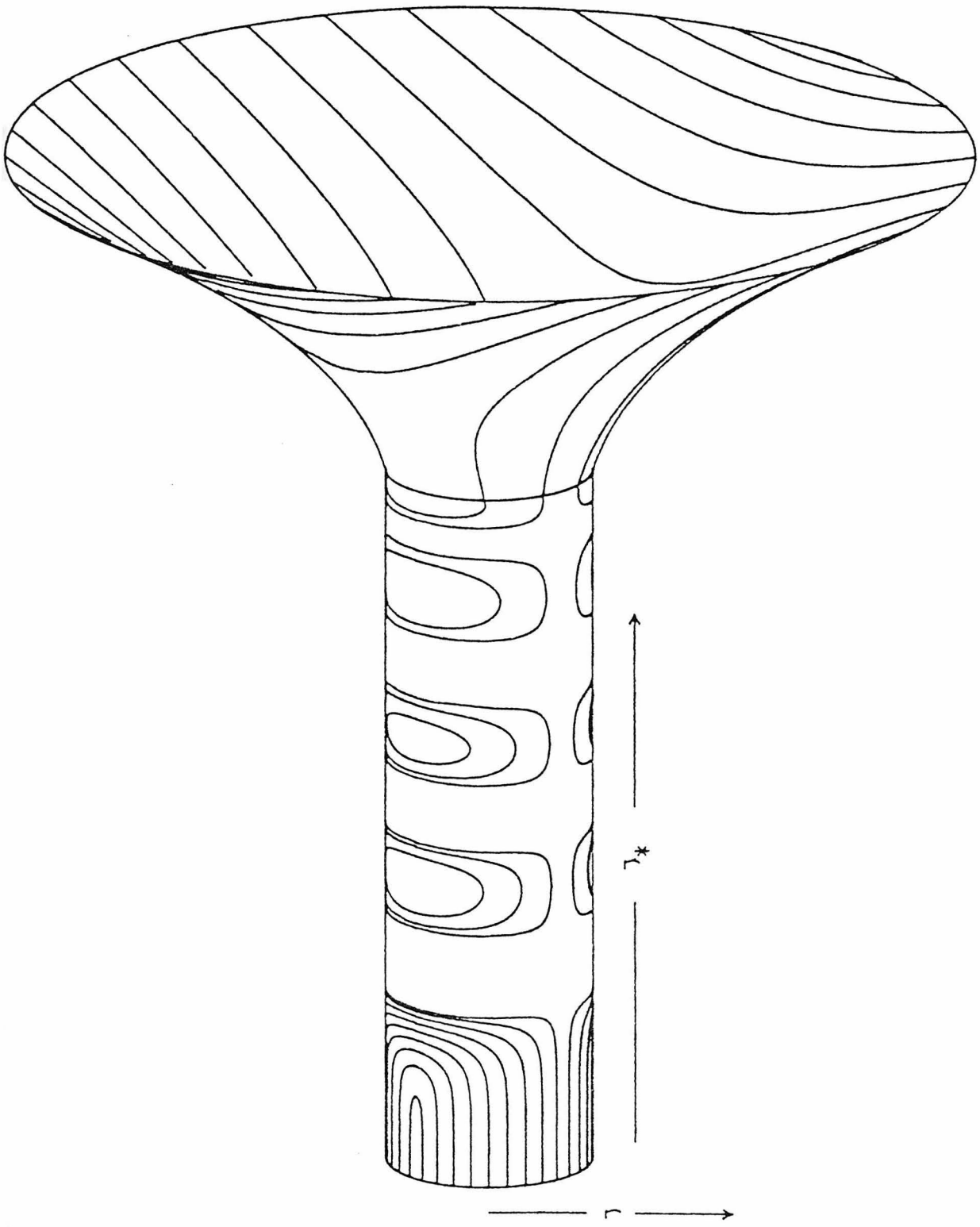

fig. 14

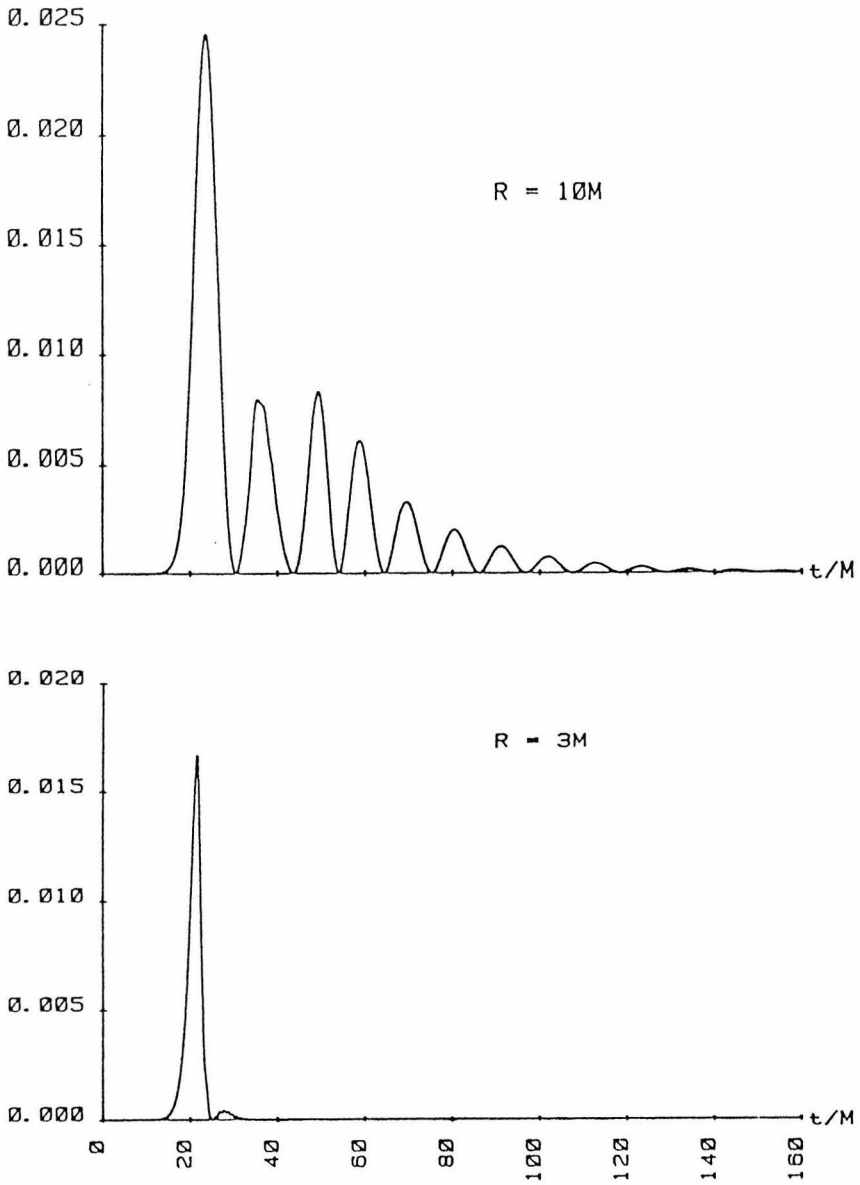
0.025
0.020
0.015
0.010
0.005
0.000
R = 10M
t/M
0.020
0.015
0.010
0.005
0.000
R = 3M
t/M
0
20
40
60
80
100
120
140
160

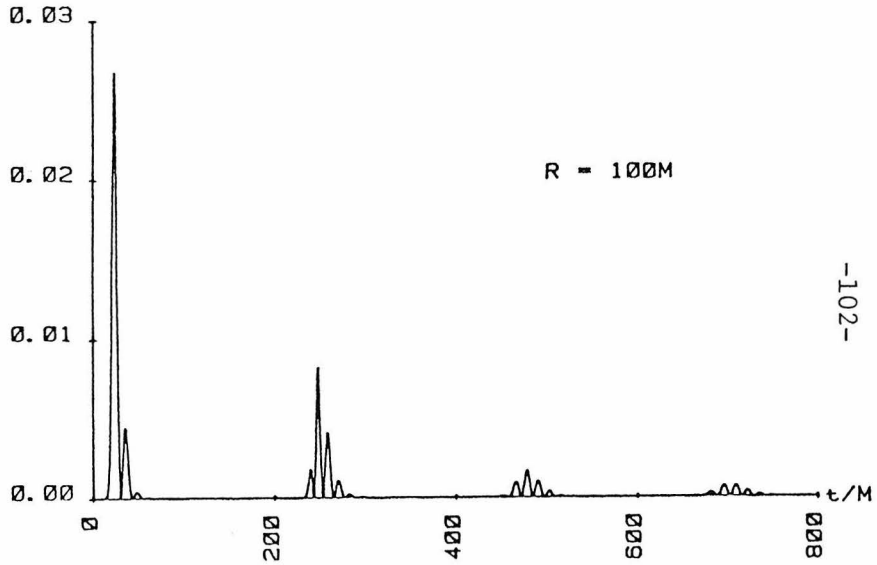
0.03
0.02
0.01
0.00
R = 100M
t/M
0
200
400
600
800

fig. 15

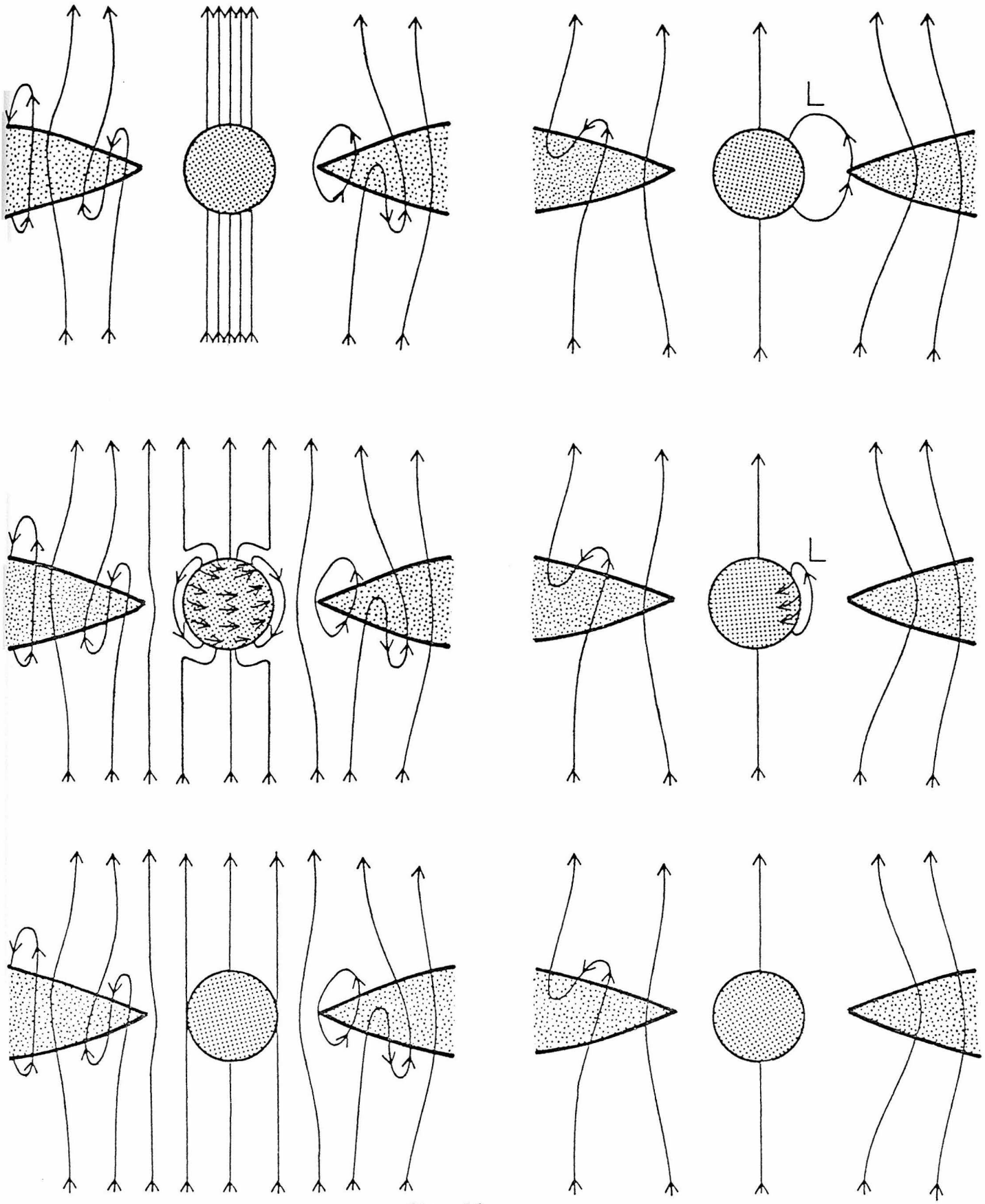

fig. 16

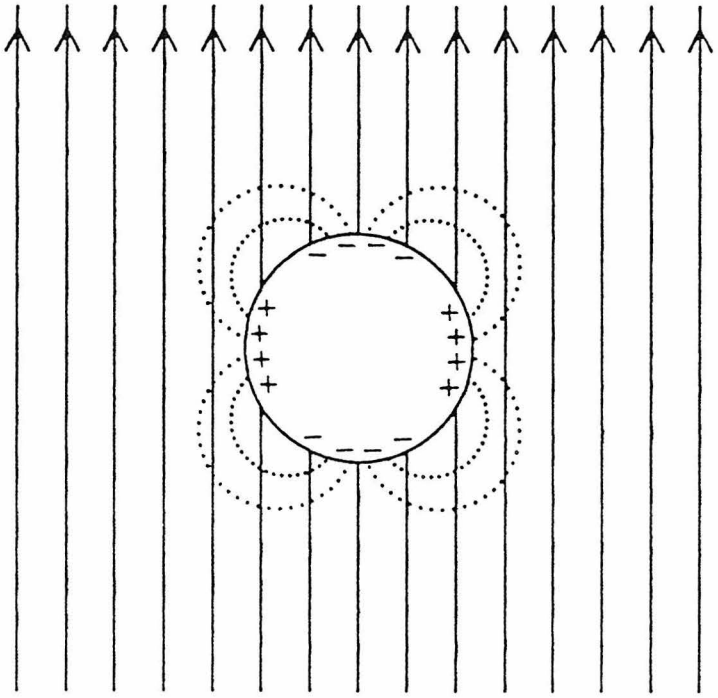

(a)

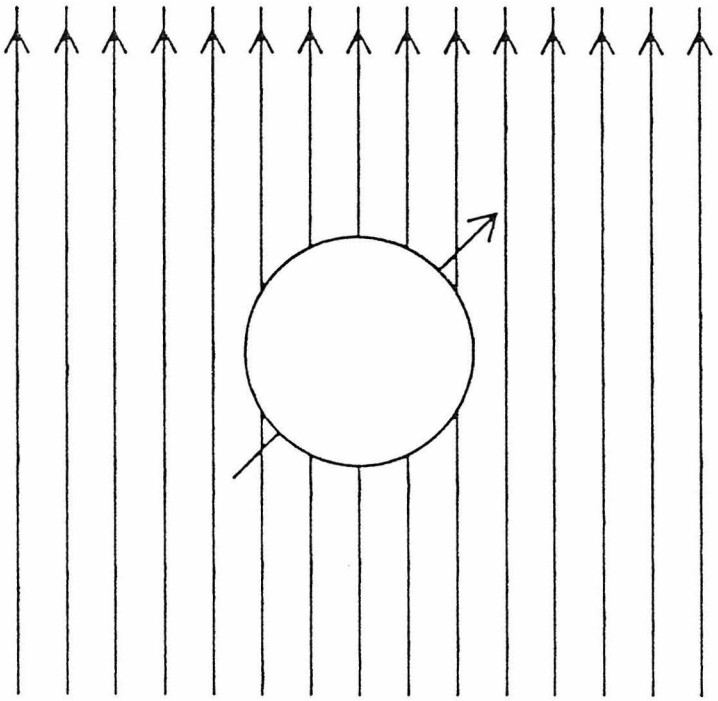

(b)

fig. 17

CHAPTER III

Multipole moments for stationary, non-asymptotically-flat systems in general relativity

Wai-Mo Suen

Theoretical Astrophysics 130-33, California Institute of Technology, Pasadena, CA 91125
(Received XX May 1985)

ABSTRACT

A formulation of multipole moments generalizing that of Thorne is proposed for the stationary, vacuum region of spacetime surrounding a source of gravity, without assuming asymptotic flatness. In this formalism, such a region of spacetime is characterized by four sets of moments, the internal mass and current moments (those of the internal source) and the external mass and current moments (those of the external universe), which are read out from a deDonder coordinate expansion of the metric density. These moments uniquely determine the vacuum region of spacetime and exhibit many desirable properties.

The interactions between a gravitating body and an external gravitational field can be described in terms of these moments, in close analogy with Newtonian theory. A derivation is given of the laws of force and torque for an isolated body acted on by an external field, generalizing the results of Thorne and Hartle and of Zhang.

As a model problem, the metric of a Schwarzschild black hole in an external quadrupolar gravitational field is studied. Among other results, we find that the black hole develops an induced quadrupole moment, which in turn generates a tidal field opposing the applied field. This effect, plus the fact that the horizon cannot expand when a quasistatic tidal force is applied, can be described in terms of effective 2-dimensional elastic moduli for the black hole horizon. The bulk modulus is $\tilde{\kappa}=\infty$, and the shear modulus is $\tilde{\mu}=-63/(20\pi M)$, where M is the hole's mass.

I. INTRODUCTION

The concept of multipole moments for curved spacetime is significant in many ways: Through analogy with Newtonian systems, multipole moments can provide important physical insights into solutions of the Einstein equations. Also, they provide a way to extract the information carried in a metric. Indeed, in the stationary spacetimes we are studying, we will show that the multipole moments contain all the information about the vacuum region of spacetime; the entire metric can be constructed from the multipole moments; in the words of Beig,[1] the multipole moments act as a "complete set of variables for the state space." In view of the success of solution-generating methods for the stationary axisymmetric vacuum Einstein equations,[2] a scheme using the multipole moments to classify and understand these solutions is clearly desirable. Besides their use in analyzing given metrics, multipole moments are also useful in constructing model spacetimes; we will give explicit examples of this in this paper. Multipole moments are also valuable in studying the structure of spatial infinity; indeed, the Geroch-Hansen definition of multipole moments for stationary asymptotically-flat spacetimes is intimately tied to the structure of spatial infinity.

Many efforts have been made to define the multipole moments of stationary asymptotically-flat spacetimes.[3-9] The recent works essentially concentrate on two approaches. The first approach works in the conformal completion of the 3-manifold of time-like Killing trajectories and defines the multipole moments as symmetric trace-free tensors at the point corresponding to spatial infinity. This approach was initiated by Geroch and Hansen[4] and continued by many others.[5,6] The beauty of the resulting definition is that it is completely geometric. The only possible arbitrariness

in determining the moments comes from the choice of the conformal factor. But Geroch[4] (see also Beig[1]) has shown that by introducing into the definition terms involving the Ricci tensor of the conformal space, an arbitrary change of the conformal factor affects the multipole moments in exactly the same way as translation affects the Newtonian moments. More importantly, it has been shown that the moments so defined have many of the properties which we would like multipole moments to have.[6]

By contrast, the second approach defines multipole moments as the coefficients of certain coordinate expansions of certain metric functions in physical spacetime using specially chosen coordinates;[7,8] this generalizes the usual procedure of reading the mass and angular momentum from the metric. Thorne's formalism[7] expands the metric in asymptotically Cartesian and mass centered (ACMC) coordinates, whereas Beig and Simon[8] expand the Hansen potentials[4] in similar coordinates. At first sight it appears that these formalisms have the unpleasant feature of depending crucially on the choice of coordinates. Both the Thorne formalism and the Beig-Simon formalism have solved this problem by showing that the moments so defined are independent of the coordinate system so long as one stays within the chosen class of coordinates, that they have a number of desirable properties, and that, in fact, they coincide with the geometrically defined Geroch-Hansen moments.[8,9] Compared with the Geroch-Hansen approach, these formalisms are closely tied to physical spacetime, in the sense that (1) one can read the moments directly from the metric of physical spacetime as the coefficients of a coordinate expansion, and (2) the formalisms are fortified with algorithms which in a straightforward manner reconstruct the metric from the multipole moments in terms of a series expansion. Hence they are rather convenient for application to physical

problems. Thorne's formalism is also tied to gravitational wave generation, and has been used in a number of astrophysical studies.[10] On the other hand, the development of the metric into series expansions creates problems: (1) Given a metric that is a solution to the Einstein equation, is the expansion in those specially chosen coordinates always convergent? (2) Given a set of multipoles, under what conditions will the expansions of the constructed metric converge? These questions have not been thoroughly investigated in either the Thorne formalism or the Beig-Simon formalism.

All of the formalisms discussed above deal only with bodies in asymptotically flat spacetime. Can one also analyze a system consisting of an isolated body in an externally imposed gravitational field in terms of multipole moments? This is the question that we want to answer in this paper. Surely in Newtonian gravitation such a system is well described in terms of multipole moments: from the expansion of the potential Φ ($\nabla^2\Phi=0$) in positive and negative powers of the radial coordinate r, one can read off a set of internal multipole moments characterizing the structure of the central body (and its gravitational field) and a set of external multipole moments characterizing the imposed external field (and its sources). Then the gravitational interaction can be described as follows: (i) The external l-pole field will distort the central body, and hence induce a change in the internal l-moment. (ii) The external l-pole field will couple to the internal l-moment (both intrinsic and induced) to produce a torque on the body, if their principal axes are not aligned. (iii) The external $(l+1)$-pole field coupled to the internal l-moment will produce an acceleration of the body.

What we wish to show in this paper is that the external and internal multipole moments of a stationary vacuum spacetime can be defined by a natural extension of Thorne's formalism, and that the gravitational

interaction of an isolated body with an external universe can be put in exactly the same language in general relativity as in Newtonian theory. In the case of an asymptotically-flat, empty external universe (vanishing external moments), the internal moments of the analysis reduce to those of Thorne;[7] and in the case of no internal body (vanishing internal moments), the external moments reduce to those of Zhang.[11]

The spirit of our analysis is rather different from that of the recent work by Thorne and Hartle[12] and Zhang[13] on the gravitational fields of isolated bodies interacting with an external universe. Briefly, they permit the gravitational field to be slowly varying with time, whereas we insist that it be stationary (except in Sec. V and Appendix B below where we generalize to slow time variations); they restrict attention to the lowest few multipole moments, whereas we consider all moments; and they regard the moments as defined only up to an uncertainty determined by the effects of coupling of the body to the external universe, whereas our moments are defined precisely. We will discuss these issues at greater length in the body of this paper.

In Sec. 2 we make precise the kind of system that we want to study and propose a definition of the multipole moments for such systems; and we describe an algorithm which enables us to construct the metric from a given set of multipole moments (basically a repetition of Thorne's algorithm for the asymptotically flat case). In Secs. 3 and 4 we explore some of the properties of the moments as defined in Sec. 2. In Sec. 5 we relax the exact stationary condition, and obtain the force and torque laws for the central body in terms of the multipole moments. In Sec. 6, as a model problem we employ our multipole moments to study the distortion of a Schwarzschild black hole under the influence of an external quadrupolar gravitational field;

and in Sec. 7 we summarize and discuss our results.

II. MULTIPOLE MOMENTS FOR STATIONARY SYSTEMS

We begin with a brief discussion of the systems to which our formalism applies and the situation where this formalism is most useful. We consider a stationary system with a gravitating body located in an external universe. Surrounding the world tube of the body (the region of spacetime which either has $T_{\mu\nu}\neq 0$ or is inside a horizon) there is a region of spacetime satisfying the vacuum Einstein equations. Call this region D. We shall define our multipole moments in terms of coordinate expansions of the metric density, which is a solution of the vacuum equations in D. It does not matter whether D extends to spatial infinity or not; in particular, no asymptotic flatness is assumed. Indeed, if we assume the spacetime to be asymptotically flat, then our external multipole moments will vanish, and our internal moments will trivially reduce to those of Thorne.[7] Where there are gravitational fields generated by external sources, we will have an additional set of moments, the external moments, to characterize the structure of the vacuum spacetime. Also, we need not make explicitly the assumption that the gravitational field is weak in D. However, in general the concept of a multipole expansion of a field is useful only when the field is smooth enough that it can be characterized by the first few terms of the expansion and the higher multipole moments can be neglected. In the same sense, the multipole expansion that we shall construct will be useful mainly for an "isolated" body in an external universe, for which the multipole expansion converges rapidly. We use the word "isolated" in the sense of Thorne and Hartle[12]: the external material is distant enough that it generates a Riemann curvature tensor near the central body having length scales $R,\mathcal{L} \gg L,M$

where

$\mathcal{R}$ = radius of curvature of external Riemann tensor,

$\mathcal{L}$ = inhomogeneity scale of external Riemann tensor,

M = mass of the central body

L = length scale (size) of the central body .

[The separation into external and internal quantities will be made precise in Sec. 3B. For the discussion here precise separation is not necessary.] For such a body there exists a "buffer" zone in the vacuum region D, at a typical radius r with $(M,L) \ll r \ll (\mathcal{L},\mathcal{R})$. In this buffer region, the multipole expansion typically is dominated by the first few moments, and the multipole formalism is most useful here.

A. The construction of the stationary vacuum metric in terms of multipole moments

Following Thorne,[7] our formalism is built on a deDonder coordinate system. We assume that there is a single coordinate system which satisfies the deDonder gauge condition in the vacuum D (though the origin of the coordinate may lies outside D). The structure of the spacetime in this vacuum region is given by a tensor field $\bar{h}^{\mu\nu}$, which is related to the metric density by

$$\tilde{g}^{\alpha\beta} = \sqrt{-g}\ g^{\alpha\beta} = \eta^{\alpha\beta} - \bar{h}^{\alpha\beta}\ ,\quad \eta^{\alpha\beta} = \mathrm{diag}(-1,1,1,1)\ ,\quad g = \det(g_{\mu\nu})\ . \tag{2.1}$$

From $g_{\mu\nu}$ it is straightforward to determine $\bar{h}^{\mu\nu}$, and vice versa, provided the metric is nondegenerate. We assume that the metric satisfies this requirement throughout the paper. In the following discussion we sometimes make no differentiation between $g_{\mu\nu}$ and $\bar{h}^{\mu\nu}$ and refer to both of them loosely as

the metric. The Einstein equation in deDonder coordinates reads:

$$\Box\bar{h}_{\alpha\beta} \equiv -\bar{h}_{\alpha\beta,00} + \bar{h}_{\alpha\beta,jj} = -16\pi W_{\alpha\beta} , \tag{2.2}$$

and the deDonder coordinate condition is

$$\bar{h}_{00,0} = \bar{h}_{0j,j} , \quad \bar{h}_{j0,0} = \bar{h}_{jk,k} . \tag{2.3}$$

Here $\alpha,\beta = 0,1,2,3$; $i,j = 1,2,3$; commas denote partial derivatives; and indices on all quantities except $g^{\mu\nu}$ and $g_{\mu\nu}$ are raised and lowered with the flat metric $\eta_{\alpha\beta}$ (which permits us to interchange upper and lower spatial indices according to convenience). The summation convention is used not only when one index is up and the other down, but also for Latin (spatial) indices when both are down. The $W_{\alpha\beta}$ in (2.2) is given by

$$W_{\alpha\beta} = (-g)t_{\alpha\beta}^{\text{L-L}} + \frac{1}{16\pi}(\bar{h}_{\alpha\mu,\nu}\bar{h}_{\beta}{}^{\nu,\mu} - \bar{h}_{\alpha\beta,\mu\nu}\bar{h}^{\mu\nu}) . \tag{2.4}$$

Here $t_{\alpha\beta}^{\text{L-L}}$ is the Landau-Lifshitz pseudotensor.

$$\begin{aligned} 16\pi(-g)t^{\alpha\beta}{}_{\text{L-L}} = {} & \tilde{g}^{\alpha\beta}{}_{,\lambda}\tilde{g}^{\lambda\mu}{}_{,\mu} - \tilde{g}^{\alpha\lambda}{}_{,\lambda}\tilde{g}^{\beta\mu}{}_{,\mu} + \tfrac{1}{2}g^{\alpha\beta}g_{\lambda\mu}\tilde{g}^{\lambda\nu}{}_{,\rho}\tilde{g}^{\rho\mu}{}_{,\nu} \\ & - (g^{\alpha\lambda}g_{\mu\nu}\tilde{g}^{\beta\nu}{}_{,\rho}\tilde{g}^{\mu\rho}{}_{,\lambda} + g^{\beta\lambda}g_{\mu\nu}\tilde{g}^{\alpha\nu}{}_{,\rho}\tilde{g}^{\mu\rho}{}_{,\lambda}) + g_{\lambda\mu}g^{\nu\rho}\tilde{g}^{\alpha\lambda}{}_{,\nu}\tilde{g}^{\beta\mu}{}_{,\rho} \\ & + \frac{1}{8}(2g^{\alpha\lambda}g^{\beta\mu} - g^{\alpha\beta}g^{\lambda\mu})(2g_{\nu\rho}g_{\sigma\tau} - g_{\rho\sigma}g_{\nu\tau})\tilde{g}^{\nu\tau}{}_{,\lambda}\tilde{g}^{\rho\sigma}{}_{,\mu} . \end{aligned} \tag{2.5}$$

The integrability condition for Eqs. (2.2) and (2.3) will be particularly important in later discussion; it is the Bianchi identity, which in deDonder coordinates reads:

$$W^{\alpha\beta}{}_{,\alpha} = 0 . \tag{2.6}$$

We shall now describe a systematic way of constructing the solution $\bar{h}_{\mu\nu}$

of the Einstein and gauge equations (2.2) and (2.3), in terms of expansions. This is essentially a repetition of the analysis in Ref.7, except for the contributions coming from the "external field." We present this construction in detail here since the formulas will be referred to frequently in later sections.

We start by writing

$$\bar{h}_{\alpha\beta} = \sum_{p=1}^{\infty} G^p \gamma^p_{\alpha\beta} , \tag{2.7}$$

where G is a "nonlinearity" book-keeping parameter, whose numerical value can be set to one. Then for each order in p, we have from Eqs. (2.2) and (2.3)

$$\gamma^p_{0j,0} = \gamma^p_{0j,j} , \quad \gamma^p_{jk,0} = \gamma^p_{jk,k} , \tag{2.8}$$

$$\Box \gamma^p_{\alpha\beta} = -16\pi W^p_{\alpha\beta}(\gamma^q_{\mu\nu} ; q < p) , \tag{2.9}$$

where $W^p_{\alpha\beta}$ is a polynomial in $\gamma^q_{\mu\nu}$ $(q < p)$ and its first two derivatives. These can be regarded as the defining equations for $\gamma^p_{\mu\nu}$. Throughout this paper we consider only the solutions of the Einstein equation which admit such "post-Minkowskian" expansions.[7,14] This assumption amounts to requiring the metric to be obtainable to arbitrary accuracy by iterating the linearized solution. It is physically reasonable to expect that in the weak field buffer region, all solutions admit such an expansion.

Next we specialize to the stationary situation. It is clear that we can always choose deDonder coordinates such that

$$\frac{\partial}{\partial x^0} = \frac{\partial}{\partial t} = \text{time-like Killing vector} . \tag{2.10}$$

Hence all $\partial / \partial t$ give zero. For $p = 1$ we have from (2.8), (2.9)

$$\gamma^1_{\alpha\beta,kk} = 0\,, \tag{2.11}$$

$$\gamma^1_{\mu j,j} = 0\,. \tag{2.12}$$

The general solution to Eq. (2.11) is, in symmetric trace-free ("STF") tensor form,

$$U_{00} = \sum_{l=0}^{\infty} A_{A_l}\partial_{A_l}\left(\frac{1}{r}\right) + \sum_{l=0}^{\infty} A'_{A_l}X_{A_l}\,, \tag{2.13}$$

$$\begin{aligned} U_{0j} = {} & \sum_{l=1}^{\infty}\left[\varepsilon_{jpq}B_{pA_{l-1}}\partial_{qA_{l-1}}\left(\frac{1}{r}\right) + \varepsilon_{jpq}B'_{pA_{l-1}}\hat{X}_{qA_{l-1}}\right], \\ & + \sum_{l=1}^{\infty}\left[C_{jA_{l-1}}\partial_{A_{l-1}}\left(\frac{1}{r}\right) + C'_{jA_{l-1}}X_{A_{l-1}}\right] + \sum_{l=0}^{\infty}\left[D_{A_l}\partial_{jA_l}\left(\frac{1}{r}\right) + D'_{A_l}X_{\langle jA_l\rangle}\right], \end{aligned} \tag{2.14}$$

$$\begin{aligned} U_{ij} = {} & \sum_{l=0}^{\infty}\left[\delta_{ij}E_{A_l}\partial_{A_l}\left(\frac{1}{r}\right) + \delta_{ij}E'_{A_l}X_{A_l}\right] + \sum_{l=2}^{\infty}\left[F_{ijA_{l-2}}\partial_{A_{l-2}}\left(\frac{1}{r}\right) + F'_{ijA_{l-2}}X_{A_{l-2}}\right] \\ & + \sum_{l=2}^{\infty}\left[\varepsilon_{pq\langle j}G_{i\rangle pA_{l-2}}\partial_{qA_{l-2}}\left(\frac{1}{r}\right) + \varepsilon_{pq\langle j}G'_{i\rangle pA_{l-2}}\hat{X}_{qA_{l-2}}\right] \\ & + \sum_{l=1}^{\infty}\left[H_{A_{l-1}\langle i}\partial_{j\rangle A_{l-1}}\left(\frac{1}{r}\right) + H'_{A_{l-1}\langle i}\hat{X}_{j\rangle A_{l-1}}\right] \\ & + \sum_{l=1}^{\infty}\left[J_{pA_{l-1}}\varepsilon_{pq\langle i}\partial_{j\rangle qA_{l-1}}\left(\frac{1}{r}\right) + J'_{pA_{l-1}}\varepsilon_{pq\langle i}\hat{X}_{j\rangle qA_{l-1}}\right] \\ & + \sum_{l=0}^{\infty}\left[K_{A_l}\partial_{ijA_l}\left(\frac{1}{r}\right) + K'_{A_l}\hat{X}_{ijA_l}\right]. \end{aligned} \tag{2.15}$$

We here adopt the conventions of Refs. 14, 15 that: (i) all indices between $\langle\ \rangle$ are to be symmetrized and made trace-free, and (ii) a $\hat{}$ over a tensor indicates that all its indices are to be symmetrized and made trace-free. All other conventions follow Thorne,[7] namely: (iii) a sequence of l indices is denoted by $S_{A_l} \equiv S_{a_1a_2a_3\cdots a_l}$,

(iv) $r \equiv (x_i x_i)^{1/2}$, $n_i \equiv x_i / r$, $X_{A_l} \equiv r^l N_{A_l} \equiv x_{a_1} x_{a_2} \cdots x_{a_l}$, (v) capital script letters denote symmetric trace-free tensors: $\mathcal{B}_{A_l} \equiv \hat{\mathcal{B}}_{A_l} \equiv \mathcal{B}_{\langle a_1 a_2 \cdots a_l \rangle}$, and (vi) ε_{ijk} is the alternating (flat-space Levi-Civita) symbol. One can easily see that the U's given in the form of Eqs. (2.13)–(2.15) satisfy the Laplace equation. [A thorough discussion of the properties of the $1/r^l$ part of these solutions and their relationship to various kinds of spherical harmonics is given in Ref. 7, part 1; the r^l part follows trivially. See also Pirani [16] for STF tensors.] Note that $\partial_{A_l}(1/r) = \hat{\partial}_{A_l}(1/r)$, and that there is no need to put a $\hat{}$ on those X_{A_l} that are contracted into an STF tensor. The structure of the terms in Eqs. (2.13)–(2.15) should be clear.

To obtain $\gamma^1_{\mu\nu}$, we substitute the U's into the stationary deDonder gauge condition (2.12) and arrive at

$$\gamma^1_{00} = \sum_{l=0}^{\infty} \left[\mathcal{A}_{A_l} \left(\frac{1}{r} \right)_{,A_l} + \mathcal{A}'_{A_l} X_{A_l} \right], \tag{2.16}$$

$$\gamma^1_{0j} = \sum_{l=1}^{\infty} \left[\varepsilon_{jpq} \mathcal{B}_{pA_{l-1}} \left(\frac{1}{r} \right)_{,qA_{l-1}} + \varepsilon_{jpq} \mathcal{B}'_{pA_{l-1}} \hat{X}_{qA_{l-1}} \right]$$

$$+ \sum_{l=1}^{\infty} \left[\mathcal{C}'_{jA_{l-1}} X_{A_{l-1}} \right] + \sum_{l=0}^{\infty} \left[\mathcal{D}_{A_l} \left(\frac{1}{r} \right)_{,ijA_l} \right], \tag{2.17}$$

$$\gamma^1_{ij} = \sum_{l=2}^{\infty} \left[\mathcal{F}'_{ijA_{l-2}} X_{A_{l-2}} \right] + \sum_{l=2} \left[\varepsilon_{pq\langle i} \mathcal{G}'_{j\rangle qA_{l-2}} \hat{X}_{pA_{l-2}} \right] + \sum_{l=1}^{\infty} \left[\mathcal{J}_{qA_{l-1}} \varepsilon_{pq\langle i} \partial_{j\rangle pA_{l-1}} \left(\frac{1}{r} \right) \right]$$

$$+ \sum_{l=0} \left[\mathcal{K}_{A_l} \partial_{ijA_l} \left(\frac{1}{r} \right) \right] + \sum_{l=1}^{\infty} \left[-\frac{1}{6} \mathcal{H}_{A_l} \delta_{ij} \partial_{A_l} \left(\frac{1}{r} \right) + \mathcal{H}_{A_{l-1}\langle i} \partial_{j\rangle A_{l-1}} \left(\frac{1}{r} \right) \right]$$

$$+ \sum_{l=1}^{\infty} \left[-\frac{1}{6} \frac{(2l^2+5l+3)}{l(2l-1)} \mathcal{H}'_{A_l} \delta_{ij} X_{A_l} + \mathcal{H}'_{A_{l-1}\langle i} \hat{X}_{j\rangle A_{l-1}} \right]. \tag{2.18}$$

The forms of these terms will be important both in building the metric from

multipole moments and in identifying multipole moments from a given metric, as we shall see.

Next we make use of the "residual" gauge freedom to make what is remaining in $\gamma^1_{\mu\nu}$ assume a form close to that of the Newtonian potential. Under a gauge transformation, $\gamma^1_{\mu\nu}$ transforms as:

$$\gamma^{1\,\mathrm{new}}_{\mu\nu} = \gamma^1_{\mu\nu} + \xi_{\mu,\nu} + \xi_{\nu,\mu} - \eta_{\mu\nu}\xi^{\alpha}{}_{,\alpha} \,. \tag{2.19}$$

With a ξ_μ satisfying

$$\Box\xi_\mu = 0, \tag{2.20}$$

i.e., without leaving deDonder coordinates, we can gauge $\gamma^1_{\mu\nu}$ into the form (the superscript "new" has been dropped and we have renamed the coefficients):

$$\gamma^1_{00} = \sum_{l=0}^{\infty} (-1)^l \frac{4}{l!} I_{A_l} \left(\frac{1}{r}\right)_{,A_l} + \sum_{l=1}^{\infty} \frac{4(2l-1)!!}{l!} Q_{A_l} X_{A_l} \,. \tag{2.21}$$

$$\gamma^1_{0j} = -\sum_{l=1}^{\infty} (-1)^l \frac{4l}{(l+1)!} \varepsilon_{jpq} S_{pA_{l-1}} \left(\frac{1}{r}\right)_{,qA_{l-1}}$$

$$- \sum_{l=1}^{\infty} \frac{4l\,(2l-1)!!}{(l+1)!} \varepsilon_{jpq} \mathcal{C}_{pA_{l-1}} \hat{X}_{qA_{l-1}} \tag{2.22}$$

$$\gamma^1_{ij} = 0 \,. \tag{2.23}$$

We call I_{A_l} and S_{A_l} the internal mass and current l-pole moments, and Q_{A_l} and $\mathcal{C}_{A_l}$ the external mass and current l-pole moments. The choice of normalization factors will be obvious later. Note that we have put in a rescaling of the spacetime coordinates to remove the constant parts from γ_{00}, i.e., to make the coordinate-independent part of g_{00} equal -1; and, as a

result, the summation for the external moments begins at $l=1$.

For this definition of multipole moments to make sense, we want to make sure that there is no more gauge freedom left. This is guaranteed by the following theorem:

Theorem 1: For any stationary second rank tensorial solution of the flat-spacetime wave equation (i.e., $\Box\gamma_{\mu\nu} = 0$,$\partial_t\gamma_{\mu\nu} = 0$), if $\partial_j\gamma_{\mu j} = 0$, then there exists a unique $\gamma^{\text{new}}{}_{\mu\nu}$ with the form given by (2.21)–(2.23) which is related to $\gamma_{\mu\nu}$ by the gauge transformation (2.19) with $\partial_t\xi_\mu = 0$.

We consider only the case $\partial_t\xi_\mu = 0$ as we require both t and t^{new} (time coordinates before and after the gauge change) to be tied to the time-like Killing vector. The proof of the theorem is trivial. The existence can be shown straightforwardly by explicit construction of the required ξ_μ. To prove the uniqueness, we assume that $\gamma_{\mu\nu}$ is of the form given by Eqs. (2.21)–(2.23), and try to construct, by a gauge change ξ_μ, another $\gamma^{\text{new}}_{\mu\nu}$ with the same form but different coefficients. Then it is easy to see that the requirements of the theorem restrict ξ_μ to

$$\xi_0 = A' \ , \ \xi_j = \varepsilon_{jpq}B'_p x_q + D'_j \ .$$

But this freedom cannot affect $\gamma_{\mu\nu}$. Hence the uniqueness.

Eqs. (2.21)–(2.23) define the multipole moments to G^1 order. What about the general nonlinear situation where we include in $\bar{h}_{\mu\nu}$ the terms of order G^n, with $n > 1$? With the $\gamma^1_{\mu\nu}$ given by Eqs. (2.21)–(2.23), we can generate $\gamma^p_{\mu\nu}$ by the following algorithm:

Algorithm A: (i) From $\gamma^1_{\mu\nu}$ of Eqs. (2.21)–(2.23), calculate $W^2_{\mu\nu}$ as the $O(G^2)$ part of Eq. (2.4). (ii) Invert the $p=2$ case of Eq. (2.9) (with vanishing time derivatives) to obtain

$$\gamma^2_{\alpha\beta} = -16\pi\Delta^{-1}W^2_{\alpha\beta} + U^2_{\alpha\beta} \ , \tag{2.24}$$

where $\Delta^{-1}W^2_{\mu\nu}$ denotes a special solution and $U^2_{\mu\nu}$ satisfies $\nabla^2 U^2_{\mu\nu} = 0$. [See Appendix A for the construction of a special solution; however the algorithm does not depend on how the special solution is constructed.] (iii) Next make use of the freedom of $U^2_{\mu\nu}$ to require $\gamma^2_{\mu\nu}$ to satisfy the stationary gauge condition $\partial_j \gamma^2_{\mu j} = 0$, i.e.,

$$\partial_j U^2_{\mu j} - 16\pi\partial_j \Delta^{-1} W^2_{\mu j} = 0 \ . \tag{2.25}$$

[Sometimes this equation will have no solution. We will discuss this point in detail in Secs. 3 and 5.] This requirement determines $U_{\mu\nu}$ partially; the undetermined parts of $U_{\mu\nu}$ have the forms of (2.16)–(2.18). (iv) Now use the gauge freedom of Eq. (2.19) to guarantee that there be no such Laplace-free and divergence-free terms in γ^2_{ij}, and that the only such terms in γ^2_{0j} have the form given by Eq. (2.22). Then the freedom in $U_{\mu\nu}$ amounts to a free choice of the G^2-order multipole moments. That this can always be done is guaranteed by theorem 1. Therefore if we are given the G^2 order moments, the $\gamma^2_{\mu\nu}$ is uniquely determined. (v) In the same way, we can obtain $\bar{h}_{\mu\nu}$ to arbitrary order in G; and the structure at arbitrary order will be such that the mass and current moments to that order are given by the Laplace-free terms in $\bar{h}_{00}$ and $\bar{h}_{0j}$, i.e., by terms of the form of Eqs. (2.21) and (2.22). All terms having different structure, i.e., different combinations of N_{A_l} and r^m in $\bar{h}_{00}$, $\bar{h}_{0i}$, and $\bar{h}_{0j}$ come from the nonlinear coupling of these multipole moments.

The mathematical formulae needed in algorithm A are given in appendix A. Examples of the construction are given in appendix B.

B. The general structure of the metric generated

What kind of structure will the metric generated by the algorithm A have? We make the following observations:

(i) *Logarithmic terms:* It is well known that in deDonder coordinates the metric often contains logarithmic terms, cf. Refs. 7, 14. In algorithm A, a logarithm will be produced in inverting the Laplacian operator for a source with the structure (Laplacian-free function)$/r^2$. Further iterations of such a logarithmic term give logarithms raised to integer powers. In general the power of $\ln(r)$ can be p [cf. Eq. (2.9)] after p iterations. However, all the logarithmic terms in deDonder coordinates in previous studies,[7,14] are connected with dynamical effects, e.g., tail phenomena, phase shifts, propagation on wrong characteristics, etc.. This make us suspect that there may be no logarithmic terms generated in the present stationary case. Indeed, Blanchet and Damour[14] (see also Ref. 7) have shown that there will be no logarithmic terms generated in the case of a stationary vacuum spacetime which is asymptotic flat, i.e., without the external universe. On the other hand, when there is only the external universe and no internal body, it is also easy to see that there will also be no logarithmic terms: In the region of consideration (vacuum, stationary spacetime with non-degenerate metric), $\bar{h}_{\mu\nu}$ satisfies an elliptical equation. Rearranging Eq. (2.2) gives:

$$\tilde{g}^{ij}\partial_i\partial_j\bar{h}_{\mu\nu} = -16\pi(-g)t_{\mu\nu}^{\mathrm{L-L}} - \bar{h}_{\alpha\mu,\nu}\bar{h}_{\beta}^{\nu,\beta}\,. \tag{2.26}$$

On the left hand side $\tilde{g}^{ij}$ is positive definite. The right hand side is an analytic function of $\bar{h}_{\alpha\beta}$ and its derivatives. [We see this by rewriting $g^{\mu\nu}g_{\rho\sigma}$ in $t_{\alpha\beta}^{\mathrm{L-L}}$ as $\tilde{g}^{\mu\nu}(\tilde{g}^{\rho\sigma})^{-1}$, which is analytic in $\bar{h}_{\mu\nu}$ since $\det(\tilde{g}^{\mu\nu}) = \det(g_{\mu\nu}) \neq 0$.] Thus, by Morrey's theorem,[17] the solution of Eq. (2.26) is analytic in the coordinates. Hence $\bar{h}_{\mu\nu}$ is a real analytic function of the coordinates and

contains no logarithmic terms. Next we ask, in the case where there are both an internal body and an external universe, will the coupling of the internal moments and the external moments produce logarithmic terms? We have checked explicitly that in $W^2_{\mu\nu}$ (cf. Sec. 5) all dangerous terms of the form (Laplacian-free function)$/r^2$ cancel exactly with each other. Moreover, in all the G^3 to G^6 cases we have spot checked, we also find miraculous cancellation. Therefore we make the following conjecture:

Conjecture 1: Any metric generated as a post-Minkowskian expansion [cf. Eq. (2.7)] by algorithm A will contain no logarithmic terms.

The absence of logarithmic terms is not necessary for the algorithm to work, but it certainly makes the formulae cleaner and the formalism nicer to work with.

(ii) *General form of the metric:* The $\bar{h}_{\mu\nu}$ generated by algorithm A has the following form:

$$\bar{h}_{00} = [\sum_{l=0}^{\infty} (-1)^l \frac{4}{l!} I_{A_l} \left(\frac{1}{r}\right)_{,A_l} + \sum_{l=1}^{\infty} \frac{4(2l-1)!!}{l!} Q_{A_l} X_{A_l}]$$

$$+ \{\sum_m (\sum_l A_{A_l} \hat{N}_{A_l}) r^m\} , \tag{2.27}$$

$$\bar{h}_{0j} = [-\sum_{l=1}^{\infty} (-1)^l \frac{4l}{(l+1)!} \varepsilon_{jpq} S_{pA_{l-1}} \left(\frac{1}{r}\right)_{,qA_{l-1}} - \sum_{l=1}^{\infty} \frac{4l(2l-1)!!}{(l+1)!} \varepsilon_{jpq} C_{pA_{l-1}} \hat{X}_{QA_{l-1}}]$$

$$+ \{\sum_m (\sum_l \varepsilon_{ijk} B_{jA_l} \hat{N}_{kA_l}) r^m\} , \tag{2.28}$$

$$\bar{h}_{ij} = \{\sum_m \sum_l (D_{ijA_l} N_{A_l} + E_{A_l\langle i} N_{j\rangle A_l} + F_{A_l} \hat{N}_{ijA_l} + G_{A_l} N_{A_l} \delta_{ij}) r^m\} . \tag{2.29}$$

The terms in square brackets are the multipole-moment terms ("multipole terms") which we use to generate the metric, whereas the terms in curly

brackets are those generated from the coupling of the moments ("coupling terms"). [In this paper we will always break any functions of the coordinates into sums of the form constant $\times \hat{N}_{A_l} r^m$ or constant $\times \hat{N}_{A_l} r^m \times$(Polynomial in $\ln(r)$) if there is any $\ln(r)$]. By "Laplacian-free term", we shall mean terms having the structure $\hat{N}_{A_l} r^l$ or $\hat{N}_{A_l} / r^{(l+1)}$. Note that the "multipole terms" are "Laplacian-free". In the coupling terms, $\mathcal{A}_{A_l}$, $\mathcal{B}_{A_l}$, $\mathcal{D}_{A_l}$, $\mathcal{E}_{A_l}$, $\mathcal{F}_{A_l}$, $\mathcal{G}_{A_l}$, are either STF constant tensors or STF constant tensors times a polynomial in $\ln(r)$. In the coupling terms the summations on m and l run over all integers which do not produce a term that is both Laplacian-free and divergence-free; i.e., the coupling-term sums contain no terms with the forms (2.16) and (2.17). [We have gauged the Laplacian-free and divergence-free terms away in step (iv) (and its higher order counter part) of algorithm A, except for terms of the form (2.22), which are multipole terms rather than coupling terms.] Next we note that in (2.27)–(2.29) the occurrences of ε_{ijk} in $\bar{h}_{\mu\nu}$ are determined by time reversal symmetry —i.e., $\partial / \partial t \to -(\partial / \partial t)$, $\bar{h}_{00} \to \bar{h}_{00}$, $\bar{h}_{0i} \to -\bar{h}_{0i}$, and $\bar{h}_{ij} \to \bar{h}_{ij}$ —which implies

$$\mathcal{V}_{A_l} \to \mathcal{V}_{A_l} , \quad \mathcal{Q}_{A_l} \to \mathcal{Q}_{A_l} ,$$

$$\mathcal{S}_{A_l} \to -\mathcal{S}_{A_l} , \quad \mathcal{C}_{A_l} \to -\mathcal{C}_{A_l} ,$$

$$\text{and} \quad \mathcal{W}_{00} \to \mathcal{W}_{00} , \quad \mathcal{W}_{0j} \to -\mathcal{W}_{0j} , \quad \mathcal{W}_{ij} \to \mathcal{W}_{ij} .$$

Note that there are no time-symmetry changing operations in forming $\mathcal{W}_{\mu\nu}$ from $\bar{h}_{\mu\nu}$ [cf. Eq. (2.4)]. We let n = (the number of $\bar{h}_{0j}$ or its derivatives in a term in $\mathcal{W}_{\mu\nu}$) = (the number of S_{A_l}) × (the number of C_{B_m}). Then clearly n is even in $\mathcal{W}_{00}$ and $\mathcal{W}_{ij}$, and odd in $\mathcal{W}_{0j}$. Since there is an ε_{ijk} associated with each current moment and since the product of two ε_{ijk} can be reduced to a set of Kronecker deltas, we conclude that there is exactly one ε_{ijk} in $\mathcal{W}_{0j}$ and

hence in $\bar{h}_{0j}$, and no ε_{ijk} in W_{00} and W_{ij} and hence in $\bar{h}_{00}$ and $\bar{h}_{ij}$.

(iii) *The choice of G:* Here we note that the choice of the expansion parameter G in Eq. (2.7) is of no significance for our definition of multipole moments. G can have any numerical value and the metric generated by algorithm A will still satisfy the Einstein equation. Besides the requirement that to G^0 order the metric should be Minkowskian, we are free to choose G to be any small parameter arising in the specific problem we are dealing with. In most cases a convenient choice for our multipole study is to choose all multipole terms to be of order G. This makes all higher order terms in G come only from the nonlinear coupling of the multipoles (coupling terms). We will make this choice throughout the rest of this paper unless we specify otherwise.

(iv) *The reading out of moments from a given metric:* From the general form given by Eqs. (2.27)–(2.29) we can read out the multipole moments for a given metric without first going through the generation process. Assume that a suitable metric (stationary, vacuum, admitting "post-Minkowskian expansion") has been given in arbitrary coordinates. Pick a deDonder coordinate system, and transform the given metric to this system. [In general it is a very hard task to transform a metric into a deDonder coordinate system exactly. However, in most cases we need only the first few moments and do not need an exact transformation. See the example in Sec. 6.] In general the $\bar{h}_{\mu\nu}$ thereby obtained will contain Laplacian-free and divergence-free terms in the "wrong" places. In this case, use the remaining gauge freedoms to get rid of the offending terms and bring the metric into the canonical deDonder form Eqs. (2.27)–(2.29); and from this metric read out the multipole moments. In the next subsection we will show that the multipole moments so obtained are unique (i.e., independent of the chosen deDonder

coordinate system), up to Newtonian-like transformations among themselves induced by Euclidean-like translations and rotations of the coordinates.

C. The residual coordinate freedom

It is obvious that with the requirement that the $\bar{h}_{\mu\nu}$ takes the form (2.27)–(2.29), our coordinate system is much more restricted than simply being stationary and deDonder [Eq. (2.3)]. Indeed we can easily show that the coordinate freedom has been restricted to Euclidean motions, i.e., to the freedom of choosing the origin of the coordinates and the orientation of the axes:

Suppose we have two metric densities $\tilde{g}'^{\mu\nu}(x') = \eta^{\mu\nu} - \bar{h}'^{\mu\nu}(x')$ and $\tilde{g}^{\mu\nu}(x) = \eta^{\mu\nu} - \bar{h}^{\mu\nu}(x)$. Both $\bar{h}'^{\mu\nu}(x')$ and $\bar{h}^{\mu\nu}(x)$ are in the required form of expansions Eqs. (2.27)–(2.29). We choose, for convenience, the parameter G in such a way that all the multipole terms in $\tilde{g}^{\mu\nu}$ are linear in G and all non-linear terms are coupling terms [see the discussion in point (iii) of Sec. 2B].

Suppose the coordinates are related by

$$x'^{\mu} = x^{\mu} + \lambda f^{\mu}(x^{i}) \,. \tag{2.30}$$

[We only have to consider infinitesimal transformations, i.e., keep the calculation to λ^1 order and drop all terms with λ^n $(n \geq 2)$ since finite transformations can be built by e-folding infinitesimal ones. Since both t' and t are tied to the Killing vector, we have f^{μ} independent of t.] Next we expand $f^{\mu}(x^{i})$ in G, and obtain

$$f^{\mu} = f^{\mu}_{0} + G f^{\mu}_{1} + G^{2} f^{\mu}_{2} + \cdots \,. \tag{2.31}$$

The metric densities are related to each other by

$$[\eta^{\mu\nu} - \bar{h}'^{\mu\nu}(x'^{i})] = \frac{1}{L} L^{\mu}{}_{\alpha} L^{\nu}{}_{\beta} [\eta^{\alpha\beta} - \bar{h}^{\alpha\beta}(x^{i})] \,. \tag{2.32}$$

where $L^{\mu}{}_{\alpha} = (\partial x'^{\mu})/(\partial x^{\alpha})$ and $L = |\det(L^{\mu}{}_{\alpha})|$. From (2.30)–(2.32) we obtain to G^0 order

$$f_0{}^{\mu,\nu} + f_0{}^{\nu,\mu} - \eta^{\mu\nu} f_0{}^{k}{}_{,k} = 0 \; ; \tag{2.33}$$

and to G^1 order

$$\bar{h}'^{\mu\nu}(x) = \bar{h}^{\mu\nu}(x) + \lambda \bar{h}^{\alpha\beta}(f_0{}^{\mu}{}_{,\alpha}\delta^{\nu}{}_{\beta} + f_0{}^{\nu}{}_{,\beta}\delta^{\mu}{}_{\alpha} - \delta^{\mu}{}_{\alpha}\delta^{\nu}{}_{\beta} f_0{}^{k}{}_{,k})$$

$$+ G\lambda(f_1{}^{\nu,\mu} + f_1{}^{\mu,\nu} - \eta^{\mu\nu} f_1{}^{k}{}_{,k}) \; ; \tag{2.34}$$

and likewise to higher order in G. From Eq. (2.33) we immediately know that

$f_0{}^0$ = constant ,

$f_0{}^i$ = Killing vector fields of Euclidean 3-space

$$= \varepsilon^i{}_{jk}\omega^j x^k + a^i \; , \tag{2.35}$$

where ω^j and a^i are constant vectors. Next we look at the case of G^1 order. Having already studied and understand the G^0 order freedom, we set $f_0{}^{\mu} = 0$. Then (2.34) just represents a gauge transformation. However theorem 1 tells us that our choice of the forms of $\gamma^{\mu\nu}$ and $\gamma'^{\mu\nu}$ leaves no gauge freedom and hence we have:

$$f_1{}^{\mu,\nu} + f_1{}^{\nu,\mu} - \eta^{\mu\nu} f_1{}^{k}{}_{,k} = 0 \; ; \tag{2.36}$$

which gives again the Euclidean motion as in (2.35). Using this argument repeatedly, we see that to arbitrary order in G, the freedom is no more than choosing the origin of the coordinates and the orientation of the axes. Hence the following theorem:

Theorem 2: If $\bar{h}_{\mu\nu}$ is in the form (2.27)–(2.29), the most general coordinate freedoms are Euclidean motions (2.35).

We well know from Newtonian theory that under a Euclidean motion the multipole moments of a body mix among themselves (e.g., a displacement ξ_j couples to the mass M to produce a change in the mass dipole moment $\delta M_j = M\xi_j$). In an analogous manner the Euclidean motions described above will cause a mixing of our multipole moments among themselves. Aside from this mixing, our moments are uniquely determined for any given vacuum stationary region of spacetime D.

Now, with the multipole moments defined, we must ask why we should choose such a definition. What is the physical significance of these multipole moments? The next two sections will be devoted to this question.

III. SOME PROPERTIES OF THE MULTIPOLE MOMENTS

A. Relationship of the multipole moments to their sources

Any definition that we might adopt to extend the concept of multipole moments for fields in flat space to fields in curved space, or to the curved spacetime itself, can only be justified by the properties of the resulting multipole moments. Here we try to show that the multipole moments defined in Sec. 2 have many properties that we would expect multipole moments to have.

In Newtonian theory the multipole moments read off from Φ are related intimately to the internal structures of their sources. But in general relativity integration over the source may not always be meaningful (e.g., for a black hole). In the case of our present analysis, our deDonder coordinates might not always be extendible into the interior of the source (even if there is no spacetime singularity), unless the material source is gravitating weakly enough. Therefore, we do not in general have something which corresponds

to a Newtonian integral over the source. However, if gravity is weak enough that we can use linearized theory (approximation of order G^1), we easily obtain [by including the material stress-energy tensor in Eq. (2.4)]

$$I_{A_l} = \int T^{\text{in}}_{00} r^l N_{\langle A_l \rangle} d^3x \ , \tag{3.1}$$

$$\mathcal{S}_{jA_l} = \int \varepsilon_{pq\langle j} X_{A_l\rangle} x_p (-T^{\text{in}}_{0q}) d^3x \ , \tag{3.2}$$

$$\mathcal{Q}_{A_l} = \int T^{\text{ext}}_{00} \frac{N_{\langle A_l \rangle}}{r^{l+1}} d^3x \ , \tag{3.3}$$

$$\mathcal{C}_{jA_l} = \int \varepsilon_{pq\langle j} N_{A_l\rangle} n_p (-T^{\text{ext}}_{0q}) \frac{1}{r^{l+1}} d^3x \ , \tag{3.4}$$

where $T^{\text{in}}_{\mu\nu}$ and $T^{\text{ext}}_{\mu\nu}$ are the material stress energy tensor for the interior body and the external universe respectively. Notice that we have chosen the normalization factor in Eqs. (2.21), (2.22) or Eqs. (2.27), (2.28), so that Eqs. (3.1)–(3.4) have the "expected" form. The physical meaning of the multipoles is clear in these formulas.

These desirable relations between the multipole moments and their sources are exact only for the linearized theory, i.e., when nonlinear interaction of the gravitational field is negligible. However, in view of these relations we would like to define exactly an "internal spacetime" and an "external spacetime" corresponding to a given physical spacetime with a given set of internal and external moments. Suppose that from the stationary vacuum metric of a given physical spacetime we have read out the moments (Sec. 2B). We then pick out the external moments and use algorithm A to construct from them a stationary metric. This we call the "external spacetime" or "external universe". Likewise we define the "internal universe" corresponding to the physical spacetime; and we can then use our formalism to discuss in an exact fashion the gravitational interactions

between the internal and external spacetimes. This exact procedure is analogous to the approximate procedure that Thorne and Hartle[12] used to separate out the internal body metric and external universe metric in their study of a body interacting with an external universal. Carried out in terms of asymptotic expansions, their separation and subsequent analysis is exact only in the limiting case of vanishing internal body or external universe. We will discuss this point further in Sec. 5.

B. Relationship of multipole moments to curvature

It is easy to work out the Riemann curvature tensor in terms of the multipole moments to order G^1:

$$R_{0i0j} = -\sum_{l=0}^{\infty} \frac{(-1)^l}{l!} I_{A_l} \left(\frac{1}{r}\right)_{,ijA_l} - \sum_{l=2}^{\infty} \frac{(2l-1)!!}{(l-2)!} \mathcal{Q}_{ijA_{l-2}} X_{A_{l-2}} , \tag{3.5}$$

$$R_{0ijk} = -\sum_{l=1}^{\infty} (-1)^l \frac{2l}{(l+1)!} \varepsilon_{jkq} \mathcal{S}_{mA_{l-1}} \left(\frac{1}{r}\right)_{,iqmA_{l-1}}$$

$$- \sum_{l=2}^{\infty} \frac{2(2l-1)!!}{(l-2)!} \varepsilon_{jkq} \mathcal{Q}_{qiA_{l-2}} X_{A_{l-2}} , \tag{3.6}$$

$$R_{ipjq} = -\{\delta_{ij}\delta_{pm}\delta_{qn} + \delta_{pq}\delta_{im}\delta_{jn} - \delta_{iq}\delta_{pm}\delta_{jn} - \delta_{jp}\delta_{im}\delta_{qn}\}$$

$$\times \{\sum_{l=0}^{\infty} \frac{(-1)^l}{l!} I_{A_l} \left(\frac{1}{r}\right)_{,mnA_l} + \sum_{l=2}^{\infty} \frac{(2l-1)!!}{(l-2)!} \mathcal{Q}_{mnA_{l-2}} X_{A_{l-2}}\} . \tag{3.7}$$

The structure of the curvature tensor in terms of the multipole moments is clear in these formulas. To order G^1 the "electric part" [12,18] R_{0i0j} of the curvature is determined by the mass moments, whereas the "magnetic part" R_{ijk0} is determined by current moments. In any vacuum spacetime these electric and magnetic parts contain all the information in the curvature tensor. To higher order of coupling, using the time reversal

symmetry considerations of Sec.2B, we know that there is an even number of current moments in each term of R_{0i0j} (and R_{ipjq}), whereas there is an odd number of current moments in each term of R_{0ijk}. An immediate consequence of this is that if a stationary spacetime has no current moments, the "magnetic part" of its Riemann curvature will vanish to all orders in G. [In Sec. 4 we will show that such a stationary spacetime is in fact static.]

C. Constraints on the multipole moments for a stationary spacetime

Here we ask the question: if we specify a set of moments, does it always generate a stationary spacetime? It is easy to see that there are two problems that may arise. The first problem is that the expansion of $\bar{h}^{\mu\nu}$ generated by algorithm A may not converge. In general relativity, this problem is much more serious than in the corresponding Newtonian expansion due to the non-linear coupling. We will not try to solve the question of what the requirement is on the multipole moments such that the algorithm gives a convergent series, but will merely restrict attention to sets of multipole moments which do so.

The second problem is also well known. Given a set of moments, the algorithm can generate a solution to Eqs. (2.2). However, this solution may or may not satisfy the time-independent gauge condition [Eq. (2.3) plus Eq. (2.10)], so that it may or may not be a solution of the stationary Einstein equations. We will now examine this question.

We look at step (iii) of the algorithm for the generation of $\bar{h}^{\mu\nu}$. The question is: what are the constraints, if any, on the multipole moments such that we can find a homogeneous solution $U_{\mu\nu}$ to Eq. (2.25), thereby making $\bar{h}_{\mu\nu}$ satisfy the gauge condition? Suppose we have generated $\bar{h}_{\mu\nu}$ to order

$p-1$ and are now trying to carry the algorithm to order p. Since $\bar{h}_{\mu\nu}$ is to all orders explicitly time-independent, we have to find U^p_{0j} and U^p_{ij} such that [Eq. (2.25)]

$$\partial_j U^p_{0j} + 4\pi\partial_j \int_D \frac{W^p_{0j}}{|x-x'|} d^3x = 0 , \tag{3.8}$$

$$\partial_j U^p_{ij} + 4\pi\partial_j \int_D \frac{W^p_{ij}}{|x-x'|} d^3x = 0 , \tag{3.9}$$

with

$$\nabla^2 U^p_{0j} \equiv U^p_{0j,kk} = 0 ; \quad \nabla^2 U^p_{ij} \equiv U^p_{ij,kk} = 0 , \tag{3.10}$$

where $\bar{D}$ is a $t =$ constant hypersurface in D, the vacuum spacetime sandwiched between the internal and external sources. First we notice that the second terms of Eqs. (3.8) and (3.9) are ∇^2 free, i.e., they are scalar and vector harmonics respectively, as guaranteed by the integrability condition [Eq. (2.6)]. Therefore they can always be expanded as in Eqs. (2.13) and (2.14). It is easy to show that all terms of the form (2.13) can be obtained from the divergence of the vector harmonic U_{0j} except for a term of the form (i) A/r. Likewise any term of the form (2.14) can be obtained from the divergence of the tensor harmonic U_{ij}, except for terms having the form (ii) C_i/r and (iii) $\varepsilon_{ipq} B_p (1/r)_{,q}$. Therefore, for possible failure of the construction of $\gamma^p_{\mu\nu}$ (the p^{th} order part of $\bar{h}_{\mu\nu}$), we have only to search for terms with these forms (i)–(iii) in the differentiated integrals of Eqs. (3.8) and (3.9).

Consider, first, dangerous A/r terms in the differentiated integral of (3.8), which can be written as:

$$\partial_j \int_D \frac{W^p_{0j}(x')}{|x-x'|} d^3x' = - \oint_{\partial D} \frac{W^p_{0j}(x')}{|x-x'|} d^2_j x'$$

$$= - \oint_{\partial D} W^{\mathcal{P}}_{0j}(x') \left[\sum_{lm} \frac{4\pi}{2l+1} \frac{r_<^l}{r_>^{l+1}} Y^{lm}_{J_l} Y^{*lm}_{K_l} N_{J_l} N'_{K_l} \right] d^2_j x' \,. \tag{3.11}$$

Here we have expanded $1/|x-x'|$ in terms of symmetric trace-free tensors. (The $Y^{lm}_{J_l}$ are defined in Thorne[7]; see also appendix A). Immediately we notice an interesting feature: if there is only an external universe and no internal body, then $r_>$ is always r' and no $1/r$ term can appear [i.e., there are no dangerous terms of types (i) above]. It is also easy to see that if there is no external universe (i.e., all external moments are zero), the integral is also zero. We hence look at the case where both a central body and an external universe exist. The coefficient of the $1/r$ term is given by the following integral over the "inner" surface $\partial_i \bar{D}$ of $\bar{D}$ (the intersection of a t=constant surface and a 2-surface bounding the central body's world tube):

$$\int_{\partial_i \bar{D}} (-W^{\mathcal{P}}_{0j}) d^2_j x' = \int_{\partial_i \bar{D}} (-W^{\mathcal{P}}_{0j}) n'_j r'^2 d\Omega' \,. \tag{3.12}$$

Notice that despite the appearance of r'^2, the integral is independent of r', as guaranteed by $\partial_j W^{\mathcal{P}}_{0j} = 0$. Next we notice that the vector field $W^{\mathcal{P}}_{0j}$ can always be expanded as

$$W^{\mathcal{P}}_{0j} = \sum_l [E_{jA_{l-1}}(r) N_{a_{l-1}}]^T + n_j R_{A_l}(r) N_{A_l} + \{\varepsilon_{jpq} n_p B_{qA_{l-1}}(r) N_{A_{l-1}}\} \,, \tag{3.13}$$

where E_{A_l}, B_{A_l}, and R_{A_l} are STF tensors depending only on the radius r. T indicates taking the transverse part [cf. Ref. 7, Eq. (2.25b)]. But on the other hand, from the time-reversal symmetry considerations of Sec. 2B, we know that W_{0j} has exactly one ε_{abc} in each of its terms. Therefore in Eq. (3.13) only the last terms inside the curly brackets { } are non-zero. Inserting this result into Eq. (3.12) gives zero. Hence we have no constraints arising from $\partial_j \gamma^{\mathcal{P}}_{0j} = 0$.

The search for dangerous C_i/r and $\varepsilon_{ipq}B_p(1/r)_{,q}$ terms in (3.9) proceeds similarly. Again, if there is either no internal body or no external universe, there is no constraint. Otherwise the constraint requires

$$\int_{\partial_i \mathcal{D}} (-W^p_{ij}) n'_j r'^2 d\Omega' = 0 , \tag{3.14}$$

and

$$\int_{\partial_i \mathcal{D}} \varepsilon_{iml} (-W^p_{lj}) n'_m n'_j r'^3 d\Omega' = 0 . \tag{3.15}$$

This time we can find no symmetry requirement to force the surface integrals to vanish. Indeed, it is straightforward to show that to the first nonlinear coupling of the multipole moments, i.e., $p=2$ the integrals (3.14) and (3.15) are given respectively by

$$\sum_{l=1}^{\infty} \left[\frac{(2l-1)!!}{(l-1)!} I_{A_{l-1}} \mathcal{Q}_{iA_{l-1}} - \frac{4(2l-1)!!}{l(l-2)!} \mathcal{C}_{iB_{l-1}} \mathcal{S}_{B_{l-1}} \right] , \tag{3.16}$$

$$- \sum_{l=1}^{\infty} \left[\frac{(2l-1)!!}{(l-1)!} \varepsilon_{iab} \mathcal{Q}_{aA_{l-1}} I_{bA_{l-1}} - \frac{4l^2(2l-1)!!}{(l+1)!} \varepsilon_{iab} \mathcal{C}_{aA_{l-1}} \mathcal{S}_{bA_{l-1}} \right] . \tag{3.17}$$

That is, if we let our multipole moments be of order G, then to order G^2 no choice of the homogeneous part U^2_{ij} can make γ^2_{ij} satisfy the gauge condition [Eq. (2.3)] with vanishing time derivations, unless expressions (3.16) and (3.17) both vanish. If these constraints are violated, the internal and external moments must couple with each other in such a way as to prevent us from generating a metric which satisfies the stationary vacuum Einstein equations. It is easy to convince oneself that this is not an artifact of the algorithm. Indeed, in the Newtonian theory it is precisely a coupling of the form (3.16) that creates the gravitational force exerted on the internal body by the external universe, and it is (3.17) which gives the torque. We will

discuss these points further in Sec. 5.

It is clear that once the stationary gauge conditions [(2.8) plus (2.10)] are satisfied there will be no further complication in the construction of the metric from the multipole moments, so we conclude this section with the following theorem:

Theorem 3: Given any set of multipole moments, assuming that algorithm A generates a convergent series, the metric generated as a post-Minkowskian expansion (2.7) will satisfy the stationary vacuum Einstein equations (2.8), (2.9) and (2.10) to order p in the region D if and only if Eqs. (3.14) and (3.15) are satisfied up to that order. [These correspond, at leading order in the coupling, to the vanishing of expressions (3.16) and (3.17)].

IV. FURTHER PROPERTIES OF THE MULTIPOLE MOMENTS

In this section we go on to investigate some other properties of the multipole moments.

Two essential properties that we would like our multipole moments to have are captured in the "Geroch conjectures." These conjectures were originally posed for the Geroch-Hansen multipoles[3] of a stationary asymptotically-flat spacetime, and were proved in that context in Ref. 6. They are, as stated by Beig and Simon[8],

(1) Geroch's first requirement: A given (stationary) spacetime is uniquely characterized by its moments.

(2) Geroch's second requirement: Given a set of moments, there always exists, modulo convergence problems, a spacetime corresponding to the moments.

These can be regarded as two important requirements for any definition

of multipole moments, including our own.

We have studied the second requirement in Sec. 3C. One can see that our moments do not quite meet this requirement, as theorem 3 shows. However, as Newtonian theory would suggest, additional constraints on the moments for a stationary spacetime are expected when both internal and external material are present. The problem is, do the constraints implied by theorem 3 have the correct physical origin? We give a positive answer to this question in the next section.

Next we look at the first requirement. As in other parts of the paper, we will consider only metrics in a region D of stationary vacuum spacetime that can be covered by a single deDonder coordinate system and that admit a Post-Minkowskian expansion. As discussed in Sec. 2, we identify a unique set of moments, up to Euclidean motions of the coordinates, from the expansion of $\bar{h}_{\mu\nu}$. From these moments and the algorithm A for generating the non-linear coupling terms, all other parts of $\bar{h}_{\mu\nu}$ are determined. Hence we have:

Theorem 4: The moments that we have defined satisfy Geroch's first requirement.

Next we go on to some other properties which are also exhibited by the Geroch-Hansen multipoles (or the Thorne multipoles) in a stationary asymptotically-flat spacetime.[6,9]

Theorem 5: A stationary spacetime is static if and only if all its current moments vanish.[6]

Proof: If the current moments vanish, then clearly algorithm A gives $\bar{h}_{0i} = 0$. Therefore $g_{0i} = 0$. Together with $(\partial/\partial t)g_{\mu\nu} = 0$, this implies that the spacetime is static. On the other hand, if the spacetime is static, it is always possible to find a deDonder coordinate system in which (i) $\partial/\partial t$ is

the time-like Killing vector and (ii) $\partial/\partial t$ is orthogonal to the t = constant hypersurface.[19] Hence we have $\bar{h}_{0i} = 0$ in the required form (2.31)–(2.33). The current moments in this coordinate system are therefore zero. That coordinate changes cannot affect this result is guaranteed by theorem 2, as Euclidean motions cannot affect (i),(ii).

Theorem 6 : A static spacetime is flat if and only if all its mass moments vanish.[6]

Proof: Since we are considering static spacetimes, the current moments vanish (theorem 5). Now if the mass moments vanish, we immediately have, from the algorithm, $\bar{h}_{\mu\nu} = 0$. Hence $g_{\mu\nu} = \eta_{\mu\nu}$ and the spacetime is flat. On the other hand, if spacetime is flat then there are coordinates with $g_{\mu\nu} = \eta_{\mu\nu}$ ($\bar{h}_{\mu\nu} = 0$). These coordinates trivially satisfy our coordinate requirements and the moments are read out to be zero. Again coordinate changes cannot affect the result.

Theorem 7: Spacetime is axisymmetric if and only if the multipole moments, in coordinate systems tied to the rotational Killing vector, are axisymmetric.[9]

[In an axisymmetric situation it is more convenient to use spherical coordinates (r,θ,φ) and spherical harmonics than Cartesian coordinates and STF tensors. For relations between STF tensor notation and spherical harmonic notation see Ref. 7. Here by "a coordinate system tied to an axisymmetric spacetime" we mean that $\partial/\partial\varphi$ is the rotational Killing vector, and by "axisymmetric multipole moments" we mean that the multipole moments in spherical harmonic form are proportional to δ_0^m with m being the azimuthal quantum number.]

Proof: If the multipole moments in spherical harmonic form have components with $m \neq 0$ then the metric will not be φ independent, since

contributions from different moments cannot cancel with each other. On the other hand, if the moments are axisymmetric, then since the construction of $W_{\mu\nu}$ from $\bar{h}_{\mu\nu}$ and the inversion of the Laplacian-operator preserve this symmetry, the metric generated by algorithm A is axisymmetric.

There are two points worth noting from the above discussions: the first is that essentially all the desirable properties of the Geroch-Hansen moments and Thorne moments for a stationary asymptotically-flat spacetime are preserved in our present definition. This strongly suggests that we have a reasonable choice for extending the definition of the moments into an arbitrary stationary spacetime.

The second point is that with our explicit algorithm for generating the full metric from the multipole moments, all the above theorems are proved trivially. This gives us confidence in believing that this entire construction is a powerful way both to describe and to investigate the structure of a stationary, vacuum region of spacetime.

V. THE LAWS OF FORCE AND TORQUE

In Sec. 3, we showed that the multipole moments must satisfy the constraints (3.14) and (3.15) before they can generate a stationary vacuum spacetime. The question that we want to study in detail in this section is what would happen if the constraints [Eqs. (3.14) and (3.15)] were not observed. Indeed, we would expect these violations of the gauge condition to produce a time-evolving momentum and angular momentum, i.e., to generate laws of motion and precession (force and torque laws) for the central body.

Let us consider the case where we are given a certain set of moments, $\mathcal{I}_{A_l}$, $\mathcal{Q}_{A_l}$, $\mathcal{S}_{A_l}$, and $\mathcal{C}_{A_l}$, each of order G. Let G be small, so that we will keep

terms only up to G^2. To construct a metric satisfying the Einstein equations to order G^2, we proceed according to algorithm A. To order G^2, $W_{\mu\nu}$ is given by

$$-16\pi W^2_{00} = -\frac{3}{2}\gamma^1_{0j,k}\gamma^1_{0k,j} - \frac{1}{2}\gamma^1_{0j,k}\gamma^1_{0j,k} + \frac{7}{8}\gamma^1_{00,k}\gamma^1_{00,k} , \tag{5.1}$$

$$-16\pi W^2_{0i} = \gamma^1_{00,k}\gamma^1_{i0,k} - \gamma^1_{00,k}\gamma^1_{0k,i} , \tag{5.2}$$

$$-16\pi W^2_{ij} = -\frac{1}{4}[\gamma^1_{00,i}\gamma^1_{00,j} - \frac{1}{2}\delta_{ij}\gamma^1_{00,l}\gamma^1_{00,l}] + [\gamma^1_{0m,i}\gamma^1_{0m,j} - \frac{1}{2}\delta_{ij}\gamma^1_{0m,l}\gamma^1_{0m,l}]$$

$$+ [\gamma^1_{0i,k}\gamma^1_{0j,k} - \gamma^1_{0i,k}\gamma^1_{0k,j}] - [\gamma^1_{0j,k}\gamma^1_{0k,i} - \frac{1}{2}\delta_{ij}\gamma^1_{0l,k}\gamma^1_{0k,l}] . \tag{5.3}$$

After inserting $\gamma^1_{\mu\nu}$ of (2.21)–(2.23) into Eqs. (5.1)–(5.3), we can carry out the Poisson integral and determine the homogeneous term U_{ij} that makes $\gamma_{ij,j}$ zero, as described in the algorithm A. [In appendix B we carry out this process explicitly.] Then, as discussed in Sec. 3, when we come to terms of the form $\mathcal{C}_i/r$ and $\varepsilon_{ipq}\mathcal{B}_p(1/r)_{,q}$, we are stuck. We have

$$\gamma^2_{ij,j} = -\frac{4}{r}\dot{\mathcal{P}}_i - 2\varepsilon_{ijk}\dot{\mathcal{S}}_j\frac{n_k}{r^2} ,$$

with

$$\dot{\mathcal{P}}_i = \text{(formula 3.16)} , \tag{5.4}$$

$$\dot{\mathcal{S}}_j = \text{(formula 3.17)} . \tag{5.5}$$

[The reason for this notation will be clear shortly.] No choice of time-independent homogeneous term can annul this. Therefore to satisfy the gauge conditions Eqs. (2.3) we are forced to include terms in γ_{00} and γ_{0j} which are explicitly dependent on time, and the resulting $\bar{h}_{\mu\nu}$ read, up to order G^2:

$$\bar{h}_{00} = 4\frac{V}{r} + 4\left(V_a + \dot{P}_a\frac{t^2}{2}\right)\frac{n_q}{r^2} + \sum_{l=2}^{\infty}(-1)^l\frac{4}{l!}V_{A_l}\left(\frac{1}{r}\right)_{,A_l} + \sum_{l=1}^{\infty}\frac{4(2l-1)!!}{l!}\mathcal{Q}_{A_l}X_{A_l}$$

$$+ \text{coupling terms}, \tag{5.8}$$

$$\bar{h}_{0j} = -2\varepsilon_{jpq}[\mathcal{S}_p + \dot{\mathcal{S}}_p t]\frac{n_q}{r^2} - \frac{4}{r}\dot{P}_j t$$

$$-\sum_{l=2}^{\infty}(-1)^l\frac{4l}{(l+1)!}\varepsilon_{jpq}\mathcal{S}_{pA_{l-1}}\left(\frac{1}{r}\right)_{,qA_{l-1}} - \sum_{l=1}^{\infty}\frac{4l(2l-1)!!}{(l+1)!}\varepsilon_{jpq}\mathcal{Q}_{pA_{l-1}}\hat{X}_{qA_{l-1}}$$

$$+ \text{coupling terms}, \tag{5.9}$$

$$\bar{h}_{ij} = \text{coupling terms}. \tag{5.10}$$

[The coupling terms are time-independent terms of order G^2, contributed by the coupling of moments through $W^2_{\mu\nu}$ as discussed in algorithm A. In addition, in $\bar{h}_{00}$ there is an extra coupling term $-2n_a\dot{P}_a$ so that $\bar{h}_{00}$ will still satisfy Eq. (2.2) after the inclusion of the t^2 term. All these coupling terms have a combination of N_{A_l} and r^m different from the explicitly given "multipole terms." Their general structure is shown in Sec. 2B, and they are completely determined by the multipole terms. Thus, they carry no extra information and are not interesting in the present study.] The $\bar{h}_{\mu\nu}$ of Eqs. (5.8)–(5.10) gives us a metric satisfying the Einstein equations to order G^2. We note that this metric is accurate only for a finite duration of time; i.e., t can be at most be so large that $\dot{P}_a t^2$ or $\dot{\mathcal{S}}_p t$ become of order G^1; otherwise the higher-order iterations can no longer be considered small. From Eqs. (5.8) and (5.9), we clearly would identify the multipole moments of the internal body at time t to be

$$\text{Mass dipole} = V_a + \dot{P}_a\frac{t^2}{2},$$

$$\text{Current dipole} = \mathcal{S}_p + \dot{\mathcal{S}}_p t \ ,$$

where P_a and $\mathcal{S}_p$ are the "given" values of the moments at time $t = 0$. Or, in other words, since

(momentum) = (rate of change of mass dipole moment),

we have

(rate of change of momentum of the internal body)

$$= \frac{d^2}{dt^2}(\text{dipole moment})_i = \dot{P}_i \text{ [given by Eq. (5.4)]} \ ,$$

and

$$(\text{rate of change of current moment})_i = \dot{\mathcal{S}}_i \text{ [given by Eq. (5.5)]} \ .$$

This is why the symbols $\dot{P}_i$ and $\dot{\mathcal{S}}_i$, with the dot denoting the time derivative, are used. [For some relevant discussions, see Sec. 8 of Ref.7.]

Some comments on the laws of motion and precession as given by Eqs. (5.4) and (5.5) are in order now. Although the calculation of the G^2-order terms does not require the assumption of a weak field, Eqs. (5.4) and (5.5) are good approximations to the laws of force and torque only when the contributions of G^3(and higher)-order terms are negligible. That is, we require that there exist a weak-field region (buffer zone, cf. Ref. 12) in the spacetime under consideration, with typical radius r so that the G^1-order quantities I_{A_l}/r^{l+1}, $\mathcal{Q}_{A_l}r^l$, $\mathcal{S}_{A_l}/r^{l+1}$, and $\mathcal{C}_{A_l}r^l$ are small, and we imagine our calculation to be carried out there. Notice also that we have placed no constraints on the central body; i.e., it can have a strong field, or even be a black hole. As long as it is isolated enough, the force and torque laws are given accurately by Eqs. (5.4) and (5.5). Notice that this is exactly the same situation

as is treated by Thorne and Hartle[12] and Zhang.[13] Thorne and Hartle[12] have considered only the case $\mathcal{V}_a = \mathcal{Q}_a = \mathcal{C}_a = 0$ (i.e., mass-centered and inertial coordinates). They derive the leading term ($l = 2$) in Eqs. (5.4) and (5.5). Zhang derives the next corrections ($l = 3$), as well as terms that entail time derivatives of the multipole moments and thus vanish for our quasi-stationary situation. If we denote the timescale of variation of the moments by T, in our analysis we have thrown away contributions to the force and torque laws which are of order $(1/T)\times G$. [If the time rate of change of the multipole moments results solely from the gravitational interaction, $1/T$ is at most of order G^2 and the contribution to the Zhang's time-derivative laws to $\dot{\mathcal{P}}_i$ and $\dot{\mathcal{S}}_i$ will be at most of order G^3 which is beyond the accuracy of (5.4),(5.5)].

Equations (5.4), (5.5) determine the force and torque to first order in the moment-moment coupling for an arbitrary central body in an arbitrary external gravitational field; arbitrary in the sense that both the central body and the external gravitational field can have arbitrary multipole moments. With our present formulation, it is straightforward, though tedious, to carry the calculation to higher order in G (but zero order in $1/T$).

It has been argued by Thorne and Hartle that the force and torque laws for strongly relativistic bodies, in terms of multipole moments, should be the same as for a nearly Newtonian body with negligible self-gravity (cf. Ref. 12, Sec. IC). Indeed, when $\mathcal{S}_{A_l} = 0$ and $\mathcal{C}_{A_l} = 0$, Eqs. (5.4) and (5.5) reduce exactly to the formulae we would obtain from Newtonian theory:

$$\dot{\mathcal{P}}_i = -\int \rho \nabla_i \Phi d^3x \ . \tag{5.11}$$

$$\dot{\mathcal{S}}_i = -\int \varepsilon_{ijk} x_j \rho \nabla_k \Phi d^3x \ . \tag{5.12}$$

where Φ is the external universe's Newtonian potential ($g_{00} = -1-2\Phi+\cdots$).

The results of Thorne and Hartle[12] and Zhang[13] are expressed not in terms of the external multipole moments $\mathcal{Q}_{A_l}$ and $\mathcal{C}_{A_l}$, but in terms of the curvature produced by the "external universe," which they define in terms of an asymptotic expansion (cf. Ref. 12). In their way of separating out an external universe, there are uncertainties in the definitions of the mass, momentum, and angular momentum for the central body, which become precise only in the limit of vanishing external universe. In the present analysis, all the moments, including the mass as the monopole moment, the momentum as the time-derivative of the mass dipole and the angular momentum as the current dipole, are uniquely and unambiguously defined. Of course, one can always question whether this specific choice of definition is desirable. To this end the formulas (5.4) and (5.5) which agree exactly with the Newtonian expressions again support a positive answer.

We can easily write down the force and torque laws to order G^2 (i.e., to the leading order in moment-moment coupling) in a geometrical form in a way analogous to Eq. (1.11) of Ref.12. We refer to the coordinate system where $\bar{h}_{\mu\nu}$ takes the form (5.8)–(5.10) as the "instantaneous rest frame" of the central body at $t = 0$. As in Sec. 3, we can separate out from the exact spacetime metric at $t = 0$ a metric of the central body (built with I_{A_l} and $\mathcal{S}_{A_l}$) and a metric of the external universe (built with $\mathcal{Q}_{A_l}$ and $\mathcal{C}_{A_l}$). The force and torque laws will be written down in terms of a set of 4-vectors and 4-tensors, living at the origin of the external universe and defined as follows: (i) The 4-velocity of the central body is defined as the unit vector $\vec{U}$ in the direction of $\partial/\partial t$. (ii) $P^\mu = IU^\mu$ is the 4-momentum of the central body, I being the body's mass, i.e., its internal mass monopole moment. (iii) $I_{\Omega_l}, \mathcal{S}_{\Omega_l}, \mathcal{Q}_{\Omega_l}$ and $\mathcal{C}_{\Omega_l}$ are 4-tensors orthogonal to $\partial/\partial t$ and with nonzero

components in the body's instantaneous rest frame given by $I_{A_l}, \mathcal{I}_{A_l}, \mathcal{Q}_{A_l}, \mathcal{C}_{A_l}$ where $a_i = 1,2,3$; $\omega_l = 0,1,2,3$. Then to order G^2, we have:

$$P_{\alpha;\beta}U^\beta = \sum_{l=1}^{\infty}\left\{\frac{(2l-1)!!}{(l-1)!}\mathcal{Q}_{\alpha\Omega_{l-1}}I^{\Omega_{l-1}} - \frac{4(2l-1)!!}{l(l-2)!}\mathcal{C}_{\alpha\Omega_{l-1}}\mathcal{I}^{\Omega_{l-1}}\right\}, \tag{5.16}$$

$$\mathcal{I}_{\alpha;\beta}U^\beta = -\sum_{l=1}^{\infty}\left\{\frac{(2l-1)!!}{(l-1)!}\varepsilon_{\mu\alpha\beta\gamma}\mathcal{Q}^{\beta\Omega_{l-1}}I^{\gamma}{}_{\Omega_{l-1}}\right.$$

$$\left. - \frac{4l^2(2l-1)!!}{(l+1)!}\varepsilon_{\mu\alpha\beta\gamma}\mathcal{C}^{\beta\Omega_{l-1}}\mathcal{I}^{\gamma}{}_{\Omega_{l-1}}\right\} \tag{5.17}$$

where $\varepsilon_{\mu\alpha\beta\gamma}$ is the Levi-Civita tensor and semicolons ";" denote covariant derivatives, in the external universe.

To be able to integrate Eqs. (5.16) and (5.17), we have to provide information on how the moments change (except the monopole and dipole moments). This requires the specification of the equation of state of the material making up the body and the external universe, as in general they are distorting each other and changing each other's multipole moments through gravitational interaction. (For more discussion of this point see Ref. 12.)

The present formulation suggests a way to define a rigid body in general relativity. If the body evolving forward in time in a quasi-stationary external universe changes only its mass dipole moment and current dipole moment, and all the other moments have values that can be related to those at $t = 0$ by a rotation and translation, clearly we would like to say that the body is rigid. That is, a rigid body does not develop induced multipole moments. Note that the force and torque laws for such a rigid body can be obtained to arbitrary accuracy by the quasi-stationary calculation carried to higher order in G. It would be interesting to study how this notion of rigid body

relates to the usual definition of constant proper distance between adjacent matter elements.

Although the present derivations of the force and torque laws are presented in terms of the secular changes in γ_{00} and γ_{0j} which are forced into existence by the gauge condition, this actually amounts to a calculation of the integrals

$$\dot{P}_i = -\oint_{\partial_i D} W_{ij}\, d_j^2 x \ , \tag{5.18}$$

$$\dot{\mathcal{S}}_i = -\oint_{\partial_i D} \varepsilon_{ijk} x_j W_{kl}\, d_l^2 x \ , \tag{5.19}$$

as discussed in Sec. 3. Since we have identified $\dot{P}_i$ and $\dot{\mathcal{S}}_i$ as the change in momentum and angular momentum of the central body, W_{ij} clearly has the physical meaning of a stress 3-tensor. By $\partial_\mu W^{\mu\nu} = 0$, W^{0i} is the energy flux and W^{00} is the energy density of the gravitational field. Indeed, repeating the same line of argument as that which leads to (5.18) and (5.19), we arrive at

$$\dot{M} = -\oint_{\partial_i D} W^{0j}\, d_j^2 x \ , \tag{5.20}$$

where $\dot{M}$ is the time rate of change of mass $M = V$ of the central body. In our quasi-stationary approximation, (3.13) gives $\dot{M} = 0$. Therefore, our identification of multipole moments has led us also to the identification of $W^{\mu\nu}$ as given by Eq. (2.4) as the gravitational stress-energy tensor in our special deDonder coordinate system (deDonder coordinate condition plus certain choice for fixing the residual gauge freedom). Note that this $W^{\mu\nu}$ differs from the Landau-Lifshitz pseudotensor by two additional terms.

To summarize, our present treatment of a stationary or quasi-stationary spacetime produces a very Newtonian-like picture: the gravitational field is characterized by a scalar potential $\bar{h}_{00}$ and a vector potential $\bar{h}_{0j}$, determined by the mass moments and current moments respectively, evolving in a flat background with a nonlinear interaction between them; the gravitational interaction between gravitating bodies can be described in terms of the coupling of the multipole moments of $\bar{h}_{00}$ and $\bar{h}_{0j}$; and associated with this interaction there is a stress-energy tensor constructed from the gravitational field at quadratic order and higher.

Of course, we would not expect this picture to be useful in a highly dynamical situation, where no time-like Killing vector or nearly-Killing vector exists.

VI. AN EXAMPLE: A SCHWARZSCHILD BLACK HOLE IN AN EXTERNAL GRAVITATIONAL FIELD

In this section we study, by our multipole formalism, a Weyl solution which can be interpreted as a Schwarzschild black hole residing in an external universe. One purpose of this study is to illustrate the process of identifying the multipole moments of a spacetime as proposed in earlier sections. Another reason is for the interest of such a spacetime itself. We mentioned in the introduction that in Newtonian theory the gravitational interaction between bodies can be separated into three aspects in the language of multipole moments: the force (coupling of the form $Q_{iA_l}I_{A_l}$), the torque (coupling of the form $\varepsilon_{ijk}Q_{jA_l}I_{kA_l}$), and the distortion (changes of the multipole moments due to interaction). In general relativity the first two effects are governed by the field equations alone, and we have shown that they can be discussed in exactly the same manner as in Newtonian theory. For the

distortion effect, we generally require more information than just the field equations, namely the equation of state of the material making up the gravitating bodies. However, there is one exception: a black hole, which requires no additional equation of state to describe it fully. Therefore we should be able to determine the distortion of a black hole by an external gravitational field using only the Einstein equations. Indeed, in the recently introduced viewpoint of the horizon as a membrane (for review, see Thorne *et al.*[20]), we would expect a black hole under external gravitational perturbations to be deformed like an elastic sphere, and thereby acquire an "induced multipole moment." It is precisely this interesting possibility which originally induced the author to look into the present subject of studying the multipole structure of a stationary space which is not asymptotically flat.

There have been many studies of Schwarzschild black holes under the influence of static external gravitational fields.[21,22,23] Using the Weyl construction, it has been shown that such perturbations produce no drastic change in the hole. The existence of a horizon, and the topology of the external spacetime and the horizon remain unchanged.[21,22] Hence it is appropriate to regard the spacetime as consisting of a distorted Schwarzschild black hole residing in an external universe. Such a spacetime is described by:[24]

$$ds^2 = -e^{2U_s}e^{2U}dt^2 + e^{-2U_s-2U+2V_s+2V}(d\rho^2 + d\tilde{z}^2)+\rho^2 e^{-2U_s}e^{-2U}d\varphi^2 , \quad (6.1)$$

where U_s and V_s are the Schwarzschild solution[24] and the U and V are functions of ρ and $\tilde{z}$ satisfying

$$\nabla^2 U = \left[\frac{1}{\rho}\frac{\partial}{\partial\rho}\left(\rho\frac{\partial}{\partial\rho}\right) + \frac{1}{\rho^2}\frac{\partial^2}{\partial\varphi^2} + \frac{\partial^2}{\partial\tilde{z}^2}\right]U = 0 , \quad (6.2)$$

$$V_{,\rho} = \rho(U_{,\rho}^2 - U_{,\tilde{z}}^2) + 2\rho(U_{s,\rho}U_{,\rho} - U_{s,\tilde{z}}U_{,\tilde{z}}) , \quad (6.3)$$

$$V_{,\tilde{z}} = 2\rho(U_{,\rho}U_{,\tilde{z}}) + 2\rho(U_{s,\rho}U_{s,\tilde{z}} + U_{,\rho}U_{,\tilde{z}}) \,. \tag{6.4}$$

This metric is valid for the region of vacuum spacetime between the horizon and the external distribution of material, i.e., the region D.

Now as the simplest possible model problem, we consider a "quadrupolar-like" perturbation, i.e.,

$$U = \frac{A}{4}(2\tilde{z}^2 - \rho^2) \,. \tag{6.5}$$

Clearly this satisfies Eq. (6.2) and can be regarded as representing the gravitational field generated by a material ring on the equatorial plane ($\tilde{z} = 0$) at a large distance ($\rho \to \infty$). [A is essentially (mass of the ring) / (radius of the ring)^3.] We regard A as a small parameter and carry out our calculations only to order A^1. We then substitute Eq. (6.5) into Eqs. (6.3) and (6.4) to solve for V. The solution can be expressed in a particularly simple way in terms of the "Schwarzschild coordinates," (r_s, θ), which are related to ρ and $\tilde{z}$ by

$$\rho = \sqrt{r_s(r_s - 2m)}\sin\theta \,,$$

$$\tilde{z} = (r_s - m)\cos\theta \,.$$

In the coordinates r_s, θ, and φ, the line element for the perturbed spacetime to first order in A is given by

$$ds^2 = -\left[1 - \frac{2m}{r_s}\right](1+2U)dt^2 + (1-2U+2V)\left[\frac{dr_s^2}{1-2m/r_s} + r_s^2 d\theta^2\right]$$

$$+ (1-2U)r_s^2\sin^2\theta d\varphi^2 \,, \tag{6.6}$$

where

$$U = \frac{A}{4}[2\cos^2\theta(r_s - m)^2 - r_s(r_s - m)\sin^2\theta] , \tag{6.7}$$

$$V = -Am\sin^2\theta(r_s - m) . \tag{6.8}$$

Now the question is: What are the multipole moments for this spacetime according to our scheme? The only difficult step in answering this question is to rewrite the line element (6.6) in terms of deDonder coordinates. After this step, it will be straightforward to read out the multipole moments. In principle we can solve the second-order equation

$$\tilde{g}^{\mu\nu}\partial_\mu\partial_\nu x'^\lambda + (\partial_\mu\tilde{g}^{\mu\rho})\partial_\rho x'^\lambda = 0 . \tag{6.9}$$

to obtain a deDonder coordinate system x' in terms of the old coordinates. But in most cases this is an extraordinarily difficult task. As our present step-by-step method of working out the required coordinate change can be used for a wide class of problems in reading out multipole moments, we will describe it in detail here.

We first note that if $A = 0$ in Eq. (6.6), the transformation to deDonder coordinates is easy, as the metric is now spherical symmetric. A solution of (6.9) is given by

$$\begin{aligned} x_1 \equiv x &= (r_s - m)\sin\theta\cos\varphi , \\ x_2 \equiv y &= (r_s - m)\sin\theta\sin\varphi , \\ x_3 \equiv z &= (r_s - m)\cos\theta , \end{aligned} \tag{6.10}$$

with no change in the time coordinate. If we perform this transformation to Eq. (6.6) for this $A = 0$ case, we obtain the well known deDonder coordinate expression for the Schwarzschild metric [see e.g., Eq. (8.2.15) of Weinberg[25]].

Of course, for finite A, the coordinate transformation (6.10) will not bring us to deDonder coordinates. But nevertheless, we perform this transformation for the metric of Eq. (6.6) and write down the resulting metric density $\tilde{g}^{\mu\nu} \equiv \sqrt{-g}\, g^{\mu\nu}$ in terms of these coordinates. From these $\tilde{g}^{\mu\nu}$ we find

$$\tilde{g}^{x\mu}{}_{,\mu} = 2Am\frac{x}{r} + O\left(\frac{1}{r^4}\right), \tag{6.11}$$

$$\tilde{g}^{y\mu}{}_{,\mu} = 2Am\frac{y}{r} + O\left(\frac{1}{r^4}\right), \tag{6.12}$$

$$\tilde{g}^{z\mu}{}_{,\mu} = 0, \tag{6.13}$$

here $r \equiv (x^2 + y^2 + z^{2)1/2}$. We have dropped terms with $O(1/r^4)$ as we are interested only in the first few moments. [In fact, it is intuitively clear that there will only be an induced quadrupole moment (if there are any induced moments at all) generated by the external quadrupolar field. As internal quadrupole moments arise at $1/r^3$, we can drop all $1/r^4$ terms and still expect to have lost no information. We will discuss this point in more detail later.]

Again we put these $\tilde{g}^{i\mu}{}_{,\mu}$ into Eq. (6.9) and solve for new coordinates:

$$x'^i = x^i - AH^i \; ; \quad t' = t \, , \tag{6.14}$$

with H^i satisfying

$$H^x{}_{,kk} - m^2\frac{x_i x_j}{r^4}H^x{}_{,ij} - 2m\frac{x}{r} = O\left(\frac{1}{r^5}\right), \tag{6.15}$$

$$H^y{}_{,kk} - m^2\frac{x_i x_j}{r^4}H^y{}_{,ij} - 2m\frac{y}{r} = O\left(\frac{1}{r^5}\right),$$

$$H^z = 0 \,. \tag{6.16}$$

Now it again is easy to solve this set of equations and obtain the deDonder coordinates to A^1 order:

$$x' = x\left(1 - \frac{Amr^3}{2(m^2+r^2)}\right), \tag{6.17}$$

$$y' = y\left(1 - \frac{Amr^3}{2(m^2+r^2)}\right), \tag{6.18}$$

$$z' = z \,. \tag{6.19}$$

It is now straightforward to transform the metric density into the new coordinates, and perform the required gauge change to cast it into the required form [Eqs. (2.27)–(2.29)]. The resulting expression for $\bar{h}^{\mu\nu}(= \eta^{\mu\nu} - \tilde{g}^{\mu\nu})$ is (with the primes on x, y, z and r dropped):

$$\begin{aligned}\bar{h}_{tt} = {} & 4\frac{I}{r} + 7\frac{I^2}{r^2} + 8\frac{I^3}{r^3} \\ & + 6Q_{ab}N_{ab}r^2 + (21Ir + 24I^2 + 6\frac{I^3}{r} - 6\frac{I^4}{r^2})Q_{ab}N_{ab} \\ & + I_{ab}\frac{N_{ab}}{r^3} + O(\frac{1}{r^4}) \,,\end{aligned} \tag{6.20}$$

$$\begin{aligned}\bar{h}_{ij} = {} & I^2\frac{n_i n_j}{r^2} + Ir(\delta_{ij}Q_{ab}N_{ab} - 6Q_{a\langle i}\hat{N}_{j\rangle a} + 4Q_{ij}) \\ & + \frac{I^3}{r}(-3Q_{ab}\hat{N}_{ijab} - \frac{12}{7}Q_{a\langle i}\hat{N}_{j\rangle a} - 2Q_{ab}N_{ab}\delta_{ij} - \frac{64}{35}Q_{ij}) \\ & + \frac{I^4}{r^3}(\frac{8}{7}\delta_{ij}Q_{ab}N_{ab} + 5Q_{ab}\hat{N}_{ijab}) + O(\frac{1}{r^4}) \,,\end{aligned} \tag{6.21}$$

where

$$Q_{ij} = \frac{1}{6}A\begin{pmatrix}1 & 0 & 0\\ 0 & 1 & 0\\ 0 & 0 & -2\end{pmatrix}, \tag{6.22}$$

$$M = m\left(1 - \frac{1}{2}Am^2\right), \tag{6.23}$$

$$M_{ij} = -\frac{4}{7}Q_{ij}m^5 = -\frac{2}{21}Am^5\begin{pmatrix}1 & 0 & 0\\ 0 & 1 & 0\\ 0 & 0 & -2\end{pmatrix}. \tag{6.24}$$

Now $\bar{h}_{\mu\nu}$ is in the required form of (2.27)–(2.29) and it is easy to read out the multipole moments from the Laplacian-free terms of $\bar{h}_{tt}$. They are the mass monopole M, external quadrupole Q_{ij} and internal quadrupole M_{ij} given by (2.22)–(2.24) and there are no other multipole moments. It is clear that there cannot be any higher-polar-induced moment as there is no way to construct a STF tensor with more than two indices with Q_{ij} and δ_{ij}. Therefore terms with order in $1/r$ higher than 4 will contain only "the coupling terms" solely determined by the coupling of the moments M, Q_{ij} and M_{ij}.

Next we discuss the meaning of the identified moments.

(i) The quadrupole-like term in the perturbation (6.5) generates an external quadrupole moment Q_{ij} as expected.

(ii) We can understand the value of the hole's monopole moment M in the following way: As Geroch and Hartle[22] have shown, the horizon 2-geometry is determined by the line element:

$$dS_H^2 = 4m^2\exp(-2U|_{\substack{\rho=0\\ \tilde{z}=m}})\times$$

$$\left[\exp(2U|_{\rho=0} - 2U|_{\substack{\rho=0\\ \tilde{z}=m}})d\theta^2 + \exp(2U|_{\substack{\rho=0\\ \tilde{z}=m}} - 2U|_{\rho=0})\sin^2\theta d\varphi^2\right], \tag{6.25}$$

where ρ and $\tilde{z}$ are the Weyl coordinates as in Eq. (6.1). $U|_{\rho=0}$ becomes a function of θ by writing $z = m\cos\theta$. From this and the present choice of U

[Eq. (6.5)], the horizon area is given by

$$\text{Horizon area} = \int 4m^2 e^{-Am^2} d\theta d\varphi = 16\pi m^2(1 - Am^2)$$

to first order in A. But this is just $16\pi I^2$! That is, the monopole moment we defined through our scheme turns out to be the same as the irreducible mass of the black hole. In other words, if we let the mass of a hole in an asymptotically-flat spacetime defined in the usual way be M, and then bring the hole into the external field in a quasi-stationary way (i.e., adiabatically), we will have $I = M$.

Again we can make use of the argument of Thorne and Hartle[12] that as analyzed in the buffer zone where our moments are defined, a black hole is nothing special. This make us expect (but certainly not prove in any rigorous sense) that regardless of what the central body is, the mass I that we define for it has the same value as it would have if the body were brought into the external field in a quasi-stationary way. This is surely a support for our scheme of defining multipole moments. Starting from a somewhat arbitrary choice of coordinate conditions, we have ended up with a physically preferred definition of mass. Of course, the calculation presented is only correct to first order in the perturbation treatment and only for quadrupole perturbations. It would be interesting to show that we can attach the same physical meaning to I when the perturbation is "exponentiated."

(iii) Now we look at the internal quadrupole moment (6.25). Through Eq. (3.6) we see that the "applied" tidal field is weakened by the effect of the induced moment, as we might have expected from the analogy of a conducting sphere in an external electric field. The existence of such an induced quadrupole moment is very suggestive, and surely represents a not yet investigated property of black holes. In order to better understand this

induced quadrupole moment, we shall compare it with the induced quadrupole moment of an elastic spherical shell of matter.

Consider a spherical shell with radius r_0, uniform thickness $s \ll r_0$ and surface mass density $\sigma = M/4\pi r_0^2$. We put this shell in a quadrupolar gravitational field. The Newtonian gravitational force on the shell per unit area is

$$f^i = -\sigma R_{0i0j}x^j = 3\sigma Q_{ij}x^j \ . \tag{6.26}$$

For a thin shell, to first order in s, it can be shown that the 3-dimensional displacement of a matter element, $\xi^i = x^i_{\rm new} - x^i_{\rm old}$, is determined by: (i) Force balance:

$$f^i n_i = K_{\delta\varepsilon}\tau^{\delta\varepsilon} \ , \quad f^\delta = -\tau^{\delta\varepsilon}{}_{|\varepsilon} \ . \tag{6.27}$$

where $\tau^{\delta\varepsilon}$ is the shell's 2-dimensional stress tensor, $K_{\delta\varepsilon}$ is its extrinsic curvature (equals to $g_{\delta\varepsilon}/r_0$ for our spherical shell with 2-dimensional metric $g_{\delta\varepsilon}$ and radius r_0), n_i is its unit normal, and "|" is a 2-dimensional covariant derivative in the shell. (ii) Two-dimensional stress-strain relation:

$$\tau^{\delta\varepsilon} = 2\tilde{\mu}\Sigma^{\delta\varepsilon} + \tilde{\kappa}g^{\delta\varepsilon}\Theta \ , \tag{6.28}$$

where $\tilde{\mu}$ and $\tilde{\kappa}$ are the shell's 2-dimensional shear and bulk moduli, and $\Sigma^{\delta\varepsilon}$ and Θ are its 2-dimensional shear and expansion, which can be expressed in terms of the 3-dimensional displacement by

$$\Sigma_{\delta\varepsilon} = \frac{1}{2}(\xi_{\delta|\varepsilon} + 2K_{\delta\varepsilon}\xi_i n^i) - g_{\delta\varepsilon}\Theta \ , \tag{6.29}$$

$$\Theta = g^{\delta\varepsilon}(\xi_{\delta|\varepsilon} + K_{\delta\varepsilon}\xi_i n^i) \ , \tag{6.30}$$

It can be shown that the 2-dimensional shear and bulk moduli $\tilde{\mu}$ and $\tilde{\kappa}$ are related to the 3-dimensional moduli μ and κ and the shell's thickness s by

$\tilde{\mu}=\mu s$ and $\tilde{\kappa}=2\mu s\,(6\kappa+2\mu)/\,(3\kappa+4\mu)$.

This set of equations can be solved easily for a spherical shell. For the applied force of (6.26) with $\mathcal{Q}_{ij}$ given by (6.22), we find

$$\xi_\theta = \frac{3}{4}\frac{r_0^4\sigma A}{\tilde{\mu}}\cos\theta\sin\theta\ ,\ \xi_\varphi = 0. \tag{6.31}$$

$$\xi_r = \frac{1}{2}\frac{r_0^3\sigma A}{\tilde{\mu}}\left\{\frac{2\tilde{\mu}-3\tilde{\kappa}}{4(\tilde{\mu}-\tilde{\kappa})}\right\}(\sin^2\theta - 2\cos^2\theta)\ . \tag{6.32}$$

From this we obtain the induced quadrupole moment:

$$I_{ij} = \frac{8\pi}{5}\frac{r_0^6\sigma^2}{\tilde{\mu}}\left\{\frac{7\tilde{\mu}-9\tilde{\kappa}}{2(\tilde{\mu}-\tilde{\kappa})}\right\}\mathcal{Q}_{ij}\ . \tag{6.33}$$

From this formula and the relations between $\tilde{\mu},\tilde{\kappa}$ and μ,κ we immediately see that for ordinary material having positive elastic moduli (i.e., positive μ,κ), the induced moment has the same sign as that of the moment of the applied field. Hence the tidal field will be strengthened [cf. Eq.(3.5)] instead of weakened as in the case of a black hole. [Clearly, this will also be true for a solid body made of ordinary material.] This is surely a surprising result. The static response of a black hole to an external gravitational field is qualitatively different from that of an ordinary body.

Next we would like to compare the induced moment of (6.33) to that of the black hole [Eq. (6.24)] to determine the "effective" elastic moduli of the black hole horizon. Since a black hole under a quasi-stationary external field will not undergo expansion at any location on its horizon, it must have $\Theta=0$ everywhere. By comparison with Eq. (6.28) we see that the hole must have infinite 2-dimensional bulk modulus

$$\tilde{\kappa} = \infty\ , \tag{6.34}$$

[In terms of the 3-dimensional moduli, this correspond to $\kappa = -4\mu/3$, i.e., Poisson ratio equals to one. Of course a negative elastic modulus is impossible for a shell made up of ordinary material. But this need not trouble us as a black hole horizon is no ordinary material]. With this choice of $\tilde{\kappa}$ and the requirement $r_0=2M$, equating the K_{ij} of (6.24) and (6.33) gives

$$\tilde{\mu} = -\frac{63}{20\pi}\frac{1}{M}, \tag{6.35}$$

for the effective surface shear modulus of a Schwarzschild black hole. Surely a black hole is very different from ordinary material in that it has a negative shear modulus. It is also different from ordinary material in a related aspect: A shell of ordinary material with K_{ij} given by Eq. (6.24) is prolate; but our distorted horizon as given by Eq. (6.25) is actually oblate since its equatorial circumference is $4\pi m$, whereas its polar circumference is $4\pi m - 3\pi A m^3$. However, for a black hole there is no clear reason to expect that the shape of the horizon should bear the same relationship to the asymptotic field structure as for ordinary matter. (Nevertheless, a Kerr hole has an oblate horizon and an "oblate" asymptotic field structure.[26])

As given by Eq. (6.35), the shear modulus is inversely proportional to M, i.e., a smaller hole is stiffer, as we might have expected. Indeed, if the shear modulus is to be an intrinsic property of the black hole, by dimensional analysis it must be proportional to $1/M$ (and not, say, AM). But is it truly an intrinsic property of the black hole, in other words, independent of the kind of perturbation considered? This can be determined by considering perturbations of higher order l. Surely we would hope that the coefficients in front of $1/M$ in (6.35) would assume the same value under different perturbations. However it will still be very interesting even if it turns out that for an arbitrary l-pole perturbation the coefficient is not exactly constant

but is a smoothly increasing (or decreasing) function of l, in addition to the $1/M$ behavior, so that the ability of a black hole to oppose an applied l-pole tidal field can be nicely described. Such a calculation is currently being carried out.

VII. DISCUSSION AND CONCLUSION

In this section we will first summarize the results of the preceding sections and then discuss some of the remaining issues.

We have studied the structures of stationary vacuum spacetimes, without assuming asymptotic flatness, in terms of deDonder coordinate expansions in a way that can be regarded as a natural extension of Thorne's formalism.[7] We have succeeded in identifying some parts of the metric that carry all the information about the vacuum spacetime, namely, the multipole terms. Out of these we can read the multipole moments characterizing the spacetime. There are four sets of moments: internal mass multipoles I_{A_l}, internal current multipoles $\mathcal{J}_{A_l}$, external mass multipoles $\mathcal{Q}_{A_l}$, and external current multipoles $\mathcal{C}_{A_l}$ characterizing respectively the central body and the external universe. In particular, the mass, the momentum and the angular momentum of a body in an external universe are defined precisely in terms of the internal monopole and dipole moments. We have shown that these moments have the usual properties that one desires in a multipole (Secs. 3 and 4). We have constructed an algorithm so that all other parts of the metric can be determined in terms of the multipole moments (algorithm A). We have given explicit examples of this construction for the first few lowest moments (appendix B). We have discussed the general structure of the metric obtained from the algorithm and we have given a prescription to read out the multipole moments for given stationary vacuum spacetimes.

We have obtained the force and torque laws in terms of the multipole moments in quasi-stationary situations, thereby generalizing the results of Thorne and Hartle[12] and Zhang[13] to arbitrary l-poles. These laws are completely analogous to the Newtonian case even though the central body can be strongly gravitating. Related to these laws of motion and precession is an expression for the gravitational stress-energy tensor in our deDonder coordinate system.

We have shown that it is also possible to discuss the distortion of gravitating bodies under their mutual interaction in terms of the multipole moments. For a black hole this distortion is solely determined by the Einstein equations. We have shown explicitly that a Schwarzschild hole subjected to an external quadrupolar field will develop an induced quadrupole moment which in turn produces a tidal field opposing that of the applied field. This response is qualitatively different from that of a body made up of ordinary matter. This behavior can be described by effective surface elastic moduli (with a negative shear modulus inversely proportional to the mass of the black bole and an infinite bulk modulus). However, as the calculation is performed only for a quadrupolar external field, it is not yet clear how intrinsic the shear modulus is for black holes, i.e., how sensitive it is to different kinds of perturbation. Also in this model problem we have shown that our mass monopole has a good physical meaning; it is the body's remaining mass, if the external field is switched off quasi-stationarily.

Let us now turn to the remaining issues of the development. An important problem is to establish a criterion for the convergence of the series in our algorithm for building the metric from the coupling of the multipole moments. This is a generic problem common to all studies using series expansions.[7,8] However, it is also intuitively clear that in the buffer region (if

it exists, cf. Sec. 2) and for physically reasonable choices of the moments, the algorithm will generate convergent series. It is only of academic interest to prove it rigorously for the weak-field case.

Throughout the paper we have considered only metrics which are expandable in post-Minkowskian expansions in deDonder coordinates[7,14]. It is almost certain that there are stationary vacuum metrics which lie outside this class. It would be illuminating to find out explicitly what kind of solution is not expandable. However it is again intuitively clear that in a weak field buffer region, for which our formalism is intented, the linearized theory will produce the leading order result and the metric can be obtained to arbitrary accuracy by iterating the linearized solution.

We have seen miraculous cancellations of logarithmic terms in the iteration process of algorithm A. Although the algorithm does not depend on the vanishing of the logarithmic terms, the metric generated will have a cleaner structure without them. It would be interesting if the conjecture in Sec. 2B could be proved.

We have chosen some very specific coordinate conditions to study the geometric structure of the spacetime. How much of our study just reflects the choice of the coordinate conditions? How geometric are the multipole moments we have defined? This question will best be answered if we can find a coordinate-independent approach leading to the same set of moments. Indeed, when the spacetime is asymptotic flat, the external moments $(\mathcal{Q}_{A_l}, \mathcal{C}_{A_l})$ vanish and the internal moments $(I_{A_l}, \mathcal{S}_{A_l})$ reduce to those of Thorne[7], i.e., they are the same moments as defined by the Geroch-Hansen geometric approach. It would be desirable to have a study along the lines of Geroch and Hanson for spacetimes which are not asymptotic flat, i.e., spacetimes with both internal and external moments. Is it possible to invent

some treatment that "folds up" the buffer zone to one point Λ analogous to the "point-at-infinity" Λ in Geroch's approach?

Imagine that we are given a certain set of multipole moments and are asked whether the metric generated as a post-Minkowskian expansion from these moments is stationary or not. In Sec. 3, we have shown that for the metric to be exactly stationary to all orders of coupling, the given multipole moments have to satisfy the constraints (3.14), (3.15) for all p. For $p=2$, these constraints require the expressions (3.16), (3.17) to vanish. What will the higher-order constraints look like? How will they restrict the "state space" of the stationary spacetime? Through the analysis of Sec. 5, these higher-order couplings will give contributions to the laws of force and torque which are solely general relativistic in the sense that they do not have Newtonian analogs.

It is very inconvenient to use our formalism in its present form to read out the multipole moments for a metric given in arbitrary coordinates, since we must first transform it into a very specific coordinate system. The situation can possible be improved by relaxing the coordinate requirements for the read-out to something generalizing the "ACMC" requirement of the asymptotically flat case.[7] Of course it would be even better to get rid of all the coordinate requirements entirely and do the read-out by means of a geometric approach.

The last remark we wish to make is that in Sec. 5 we have relaxed the requirement of stationarity to allow for a little bit of time evolution. It would be interesting to investigate the possibility of developing this into a truly 3+1 algorithm (when augmented by the equation of state of the material) for integrating forward in time (for systems behaving not too violently), so that the physics in any time slice will be fully described by the

multipole moments at that time.

ACKNOWLEDGEMENTS

The many suggestions on the presentation made by Kip Thorne and Luc Blanchet were essential in preparing the manuscript. I would like to thank Luc Blanchet, Yekta Gürsel, Kip Thorne, Ulvi Yurtsever, and Xiaohe Zhang for fruitful discussions. I would like to acknowledge the use of MACSYMA in checking many of the equations in Sec. 6 and appendix B. This research was supported in part by the National Science Foundation [AST 82-14126].

APPENDIX A

In this appendix, we write down some useful formulas for symmetric trace-free ("STF") tensors which are required to carry out algorithm A. As in other parts of this paper, we adopt the notation of Ref. 7. We will not repeat any formula which has already appeared in that article. Blanchet[14] also gives a collection of useful formulas for STF tensors.

1. Expansion formulas

One useful expansion formula is

$$\frac{1}{|x-x'|} = \sum_{lm} \frac{r_<^l}{r_>^{l+1}} Y^{lm}_{J_l} Y^{*lm}_{K_l} N_{J_l} N'_{K_l} \ . \tag{A1}$$

Here $J_l = j_1 j_2 \cdots j_l$ and $N_{J_l} = n_{j_1} n_{j_2} \cdots n_{j_l}$. Repeated indices are to be summed unless otherwise stated. The $Y^{lm}_{J_l}$ with $-l \le m \le l$ form a basis for the $(2l+1)$ dimensional vector space of STF tensors; for their definition see Ref.7, Sec. II.C.

A useful formula for the contraction of STF tensors is:

$$\sum_m Q_{A_l} Y^{lm}_{A_l} P_{B_l} Y^{*lm}_{B_l} = \frac{1}{4\pi} \frac{(2l+1)!!}{l!} Q_{\langle A_l \rangle} P_{\langle A_l \rangle} \ . \tag{A2}$$

The proof is trivial.

For breaking up the STF combination of N_{A_l}, we use

$$N_{\langle iA_l \rangle} = n_i N_{\langle A_l \rangle} - \frac{1}{2l+1} \sum_{s=1}^{l} \delta_{ia_s} N_{\langle a_1 \cdots a_{s-1} a_{s+1} \cdots a_l \rangle}$$

$$+ \frac{2}{(2l-1)(2l+1)} \sum_{s<s'} \delta_{a_s a_{s'}} N_{\langle i a_1 \cdots a_{s-1} a_{s+1} \cdots a_{s'} a_{s'+1} \cdots a_l \rangle} \ .$$

2. Differentiation formulas

The following formula is often used:

$$\partial_{A_l}\left(\frac{1}{r}\right) = (-1)^l (2l-1)!! \frac{\hat{N}_{A_l}}{r^{l+1}} .$$

3. Angular integration formulas

It can be shown that

$$\int N_{\langle K_l \rangle} N_{\langle A_m \rangle} N_{\langle B_n \rangle} d\Omega = 4\pi I_0(K_l, A_m, B_n) , \tag{A3a}$$

$$I_0(K_l, A_m, B_n) \equiv \sum_s^{\min(m,n)} \frac{1}{(l+m+n+1)!!} C(m,s) C(n,s) s! l!$$

$$\times \delta(A_m, A_{m-s} C_s) \delta(B_n, B_{m-s} C_s) \delta(K_l, A_{m-s} B_{m-s}) , \tag{A3b}$$

where

$$C(m,s) = \frac{m!}{(m-s)!s!} , \quad \delta(A_m, B_m) \equiv \delta_{a_1 b_1} \delta_{a_2 b_2} \cdots \delta_{a_m b_m} . \tag{A4}$$

Similarly,

$$\int N_{\langle K_l \rangle} N_{\langle A_m \rangle} N_{\langle B_n \rangle} n_j d\Omega = 4\pi I_1(K_l, A_m, B_n, j) , \tag{A5a}$$

$$I_1(K_l, A_m, B_n, j) \equiv \sum_s^{\min(m,n)} \frac{1}{(l+m+n+2)!!} l! C(m,s) C(n,s) s!$$

$$\times \Big\{ \delta(A_m, A_{m-s} C_s) \delta(B_n, B_{n-s}, C_s) \delta(K_l, A_{m-s} B_{n-s} j)$$

$$+ (m-s) \delta(A_m, j A_{m-s-1} C_s) \delta(B_n, B_{n-s} C_s) \delta(K_l, A_{m-s-1} B_{n-s})$$

$$+ (n-s)\delta(A_m, A_{n-s}\, C_s)\delta(B_n, jB_{n-s-1}C_s)\delta(K_l, A_{m-s}B_{n-s-1})\Big\} .$$

(A5b)

Also,

$$\int N_{\langle K_l\rangle} N_{\langle A_m\rangle} N_{\langle B_n\rangle} n_i n_j \, d\Omega = 4\pi I_2(K_l, A_m, B_n, i, j) , \qquad \text{(A6a)}$$

$$I_2(K_l, A_m, B_n, i, j) = \sum_{s}^{\min(m,n)} \frac{1}{(l+m+n+3)!!} l!\, C(m,s)\, C(n,s)\, s!$$

$$\times \Big\{\delta(A_m, A_{m-s}\, C_s)\delta(B_n, B_{n-s}\, C_s)[\delta(K_l, A_{m-s}\, B_{n-s} ij) + \delta(K_l, A_{m-s}\, B_{n-s})\delta_{ij}]$$

$$+ (m-s)\delta(A_m, jA_{m-s-1}C_s)\delta(B_n, B_{n-s}\, C_s)\delta(K_l, iA_{m-1-s}\, B_{n-s}) + (\text{exchange } i, j)$$

$$+ (n-s)\delta(A_m, A_{m-s}\, C_s)\delta(B_n, jB_{n-s-1}C_s)\delta(K_l, iA_{m-s}\, B_{n-s-1}) + (\text{exchange } i, j)$$

$$+ (m-s)(m-s-1)\delta(A_m, ijA_{m-s-1}C_s)\delta(B_n, B_{n-s}\, C_s)\delta(K_l, A_{m-s-2}B_{n-s})$$

$$+ (n-s)(n-s-1)\delta(A_m, A_{m-s}\, C_s)\delta(B_n, ijB_{n-s-2}C_s)\delta(K_l, A_m\, B_{n-s-2})$$

$$+ (m-s)(n-s)\delta(K_l, A_{m-s-1}B_{n-s-1}) \times [\delta(A_m, iA_{m-s-1}C_s)\delta(B_n, jB_{n-s-1}C_s)$$

$$+ \delta(A_m, jA_{m-s-1}C_s)\delta(B_n, iB_{n-s-1}C_s)] \qquad \text{(A6b)}$$

These complicated formulas can be easily understood: In $\int d\Omega$, the integral is zero unless all n_a are contracted. In Eq. (A3), this means that the largest l is given by $m+n$, so that $N_{\langle K_l\rangle}$ can be contracted with $N_{\langle A_m\rangle} N_{\langle B_n\rangle}$.

Smaller l are possible: some a_i can dot with b_j. Hence we have the sum over s. In Eqs. (A4) and (A5) more terms arise since the indices i and j can dot freely with K_l, A_m, B_n and among themselves.

4. Solution of Poisson's equation

The three formulas (A3)–(A5) take care of all the angular integrations that may ever be needed to carry out the algorithm for calculations up to G^2 order. Indeed the calculation of $\Delta^{-1}W_{\mu\nu}^2$ is straightforward with these formulas. Here by $\Delta^{-1}W_{\mu\nu}$ we mean a special solution to the Poisson equation

$$\nabla^2\bar{h}_{\mu\nu} = W_{\mu\nu} . \tag{A7}$$

Solving this equation is the most involved part of the algorithm.

The Poisson equation appears in the algorithm in the following forms, and only in these forms to G^2 order. (For higher-order calculations, the reductions to these forms are sometimes tedious.) The specific solutions given are precisely the Poisson integral, except in the cases of $\ln r$ terms where we have chosen simpler expressions.

$$\Delta^{-1}(Q_{\langle A_m\rangle}I_{\langle B_n\rangle}N_{A_m}N_{B_n}r^p)$$

$$= -\sum_{l=0}^{\infty} I_r(l,p)I_0(K_l,A_m,B_n)N_{\langle K_l\rangle}Q_{\langle A_m\rangle}I_{\langle B_n\rangle} , \tag{A8}$$

$$\Delta^{-1}(Q_{\langle A_m\rangle}I_{\langle B_n\rangle}N_{A_m}N_{B_n}n_jr^p)$$

$$= -\sum_{l=0}^{\infty} I_r(l,p)I_1(K_l,A_m,B_n,n_j)N_{\langle K_l\rangle}Q_{\langle A_m\rangle}I_{\langle B_n\rangle} , \tag{A9}$$

$$\Delta^{-1}(Q_{\langle A_m\rangle}I_{\langle B_n\rangle}N_{A_m}N_{B_n}n_in_jr^p)$$

$$= -\sum_{l=0}^{\infty} I_r(l,p)I_2(K_l,A_m,B_n,n_in_j)N_{\langle K_l\rangle}Q_{\langle A_m\rangle}I_{\langle B_n\rangle} . \tag{A10}$$

Here Q_{A_m} and I_{B_n} are arbitrary constant tensors, and

$$I_r(l,p) \equiv \frac{(2l-1)!!}{l} r^{2+p} \times \begin{cases} \ln r & \text{if } l+p+3=0 \\ -\ln r & \text{if } 2+p-l=0 \\ \left(\dfrac{1}{l+3+p} - \dfrac{1}{2+p-l}\right) & \text{otherwise .} \end{cases} \tag{A11}$$

With the foregoing formulas, each step of the algorithm is straightforward, though sometimes tedious.

APPENDIX B

In this appendix we give $\bar{h}_{\mu\nu}$ to first order in the coupling of multipoles, for the lowest few multipoles. With the formulas in appendix A and $W_{\mu\nu}$ as given in Sec. 5 [Eqs. (5.1)–(5.3)], the calculation is straightforward. It is also clear that to first order in the coupling we can separate the discussion into two moments at one time. Since only the coupling of external moments with internal moments gives rise to interesting results, we will not list the terms that arise from internal-internal or external-external coupling. Some expressions for internal-internal coupling can be found in Ref. 9 and Ref. 15.

The requirement that $\bar{h}_{\mu\nu}$ take up the forms (2.27)–(2.29) has greatly restricted the coordinate freedom. After these restrictions, we have left only the freedom of choosing the origin of the coordinates and the orientation of the axis (i.e., a Euclidean motion, see Sec. 2C). We could have used this freedom to make our coordinates be mass centered, i.e., $I_i=0$. However this results in no substantial simplification in our treatment. In fact I_i behave just like other multipoles but with a simpler structure. Hence it serves as a good example for studying the general behavior of multipole moments. This point will be clarified by the following examples.

(a) For $\mathcal{Q}_a$ with M:

$$\gamma^1_{00} = 4M\frac{1}{r} + 4\mathcal{Q}_a n_a r \ , \quad \gamma^1_{0j} = 0 \ , \quad \gamma^1_{ij} = 0 \ ; \tag{B1a}$$

$$\gamma^2_{00} = 14\ \mathcal{Q}_a M n_a + 2\ M\mathcal{Q}_a \frac{n_a}{r^2} t^2 + \{-2M\mathcal{Q}_a n_a\} \ , \tag{B1b}$$

$$\gamma^2_{0i} = -4M\mathcal{Q}_i \frac{t}{r} \ , \ \gamma^2_{ij} = 2\ \delta_{ij}\mathcal{Q}_a M n_a - 4M\mathcal{Q}_{(i}n_{j)} \ . \tag{B1c}$$

The terms with t are forced into $\bar{h}_{\mu\nu}$ by the gauge condition (see the discussion in Secs. 3C and 5). From these terms we can read out the force on the central body, which arises from the failure of our coordinates to be locally inertial with respect to the external universe ($\mathcal{Q}_i \neq 0$). The term in $\{\ \}$ in γ^2_{00} is forced into existence by Eq. (2.9) and the presence of the t^2 term. In later expressions, terms in $\{\ \}$ have the same origin.

(b) For $\mathcal{Q}_a$ with M_b:

$$\gamma^1_{00} = 4M_b \frac{n_b}{r^2} + 4\mathcal{Q}_a n_a r \ , \quad \gamma^1_{0j} = 0 \ , \quad \gamma^1_{ij} = 0 \ ; \tag{B2a}$$

$$\gamma^2_{00} = 14\ \mathcal{Q}_a M_b \frac{n_a n_b}{r} \ , \tag{B2b}$$

$$\gamma^2_{0i} = -2\ \frac{t}{r^2}(\mathcal{Q}_i M_b - \mathcal{Q}_b M_i) n_b = -2\ \varepsilon_{ipq} n_p \frac{t}{r^2}(\varepsilon_{qab}\mathcal{Q}_a M_b) \ , \tag{B2c}$$

$$\gamma^2_{ij} = 2\ \delta_{ij} M_a \mathcal{Q}_b \frac{n_a n_b}{r} - 4\ M_a \frac{\mathcal{Q}_{(i}n_{j)}n_a}{r} + \left[-2\delta_{ij}\frac{M_a\mathcal{Q}_a}{r}\right] . \tag{B2d}$$

From the γ_{0i} term we can read out the torque on the central body, i.e., the increase of the body's orbital angular momentum with respect to the coordinate system, which results from the acceleration of our coordinates with respect to the external universe ($\mathcal{Q}_i \neq 0$) together with the failure of our coordinates to be mass-centered in the body ($M_i \neq 0$). The term in square

brackets is a homogeneous term, i.e, ∇^2 free, which is forced into existence by the gauge requirement [step (iii) of algorithm A]. In later expressions, terms in square brackets have the same origin.

(c) For Q_a with I_{ab}:

$$\gamma^1_{00} = 6I_{ab}\frac{n_a n_b}{r^3} + 4\,Q_a n_a r\ ,\quad \gamma^1_{0j} = 0\ ,\quad \gamma^1_{ij} = 0\ ; \tag{B3a}$$

$$\gamma^2_{00} = 21\,Q_a I_{bc}\frac{n_a n_b n_c}{r^2}\ ,\quad \gamma^2_{0i} = 0\ , \tag{B3b}$$

$$\gamma^2_{ij} = 3\,\delta_{ij}Q_a I_{bc}\frac{n_a n_b n_c}{r^2} - 6\,I_{bc}Q_{(i}n_{j)}\frac{n_b n_c}{r^2}$$

$$+\left[-2\delta_{ij}Q_a I_{ab}\frac{n_b}{r^2} + 2Q_b I_{ij}\frac{n_b}{r^2}\right]\ . \tag{B3c}$$

In this case we have no time-dependent term. Indeed, only when the external moment has the same number or one more number of indices than the internal moment, do we obtain secular evolution.

(d) For Q_{ab} with I:

$$\gamma^1_{00} = 4I\frac{1}{r} + 6\,Q_{ab}n_a n_b r^2\ ,\quad \gamma^1_{0j} = 0\ ,\quad \gamma^1_{ij} = 0\ ; \tag{B4a}$$

$$\gamma^2_{00} = 21\,Q_{ab}In_a n_b r\ ,\ \gamma^2_{0i} = 0\ ; \tag{B4b}$$

$$\gamma^2_{ij} = 3\,\delta_{ij}IQ_{ab}n_a n_b r - 6IQ_{a(i}n_{j)}n_a r + 6IQ_{ij}r\ . \tag{B4c}$$

(e) For Q_{ab} with I_c:

$$\gamma^1_{00} = 4I_a\frac{n_a}{r^2} + 6\,Q_{ab}n_a n_b r^2\ ,\quad \gamma^1_{0j} = 0\ ,\quad \gamma^1_{ij} = 0\ ; \tag{B5a}$$

$$\gamma^2_{00} = 21\,Q_{ab}I_c n_a n_b n_c + 6Q_{ba}I_a\frac{n_b t^2}{r^2} + \{-6\,Q_{ba}I_a n_b\}\ , \tag{B5b}$$

$$\gamma^2_{0i} = -12 Q_{ia} V_a \frac{t}{r}, \tag{B5c}$$

$$\gamma^2_{ij} = 3\,\delta_{ij} Q_{ab} V_c n_a n_b n_c - 6\, V_b Q_{a(i} n_{j)} n_a n_b - 6\, Q_{ij} V_a n_a$$

$$- 6\, V_a Q_{a(i} n_{j)} + 6\, Q_{a(j} V_{i)} n_a \tag{B5d}$$

(f) For Q_{ab} with V_{cd}

$$\gamma^1_{00} = 6 V_{ab} \frac{n_a n_b}{r^3} + 6\, Q_{ab} n_a n_b r^2\,, \quad \gamma^1_{0i} = 0\,, \quad \gamma^1_{0j} = 0\,; \tag{B6a}$$

$$\gamma^2_{00} = \frac{63}{2} Q_{ab} V_{cd} \frac{n_a n_b n_c n_d}{r} \tag{B6b}$$

$$\gamma^2_{0i} = -6\, \varepsilon_{ipq} \frac{n_p t}{r^2} (\varepsilon_{qab} Q_{ac} V_{cb})\,, \tag{B6c}$$

$$\gamma^2_{ij} = -9\, V_{bc} Q_{a(i} n_{j)} \frac{n_a n_b n_c}{r} + \frac{9}{2} \delta_{ij} Q_{ab} V_{cd} n_a n_b n_c n_d \frac{1}{r}$$

$$- 6\, V_{ab} Q_{a(i} n_{j)} \frac{n_b}{r} - 3\, Q_{ij} V_{ab} \frac{n_a n_b}{r} + 6\, Q_{a(i} V_{j)b} \frac{n_a n_b}{r}$$

$$+ \left[-3\, \delta_{ij} Q_{ab} V_{ab} \frac{1}{r} - 6\, Q_{a(i} V_{j)a} \frac{1}{r} \right]. \tag{B6d}$$

The time-dependent term in γ^2_{0i} is due to the torque produced by coupling the body's quadrupole moment, V_{ab}, to the quadrupole mass moment (electric part of Riemann curvature) of the external universe, Q_{ac}.

(g) For $(V, \mathcal{S}_i)$ with $\mathcal{C}_i$:

$$\gamma^1_{00} = 4 V \frac{1}{r}, \quad \gamma^1_{0i} = -2 \varepsilon_{ipq} \mathcal{S}_p \frac{n_q}{r^2} - 2\, \varepsilon_{ipq} \mathcal{C}_p n_q r\,, \quad \gamma^1_{ij} = 0\,. \tag{B7a}$$

We again will write down only those terms which arise from the coupling of internal and external moments (V with $\mathcal{C}_i$, $\mathcal{S}_i$ with $\mathcal{C}_j$):

$$\gamma^2_{00} = -4\mathcal{C}_a \mathcal{S}_b \frac{n_{\langle a} n_{b\rangle}}{r}, \tag{B7b}$$

$$\gamma^2_{0i} = 8\varepsilon_{ikq}\mathcal{C}_q \mathcal{M}_k + 4\varepsilon_{iap}\frac{n_a t}{r^2}(\varepsilon_{pmn}\mathcal{C}_m \mathcal{S}_n), \tag{B7c}$$

$$\gamma^2_{ij} = 8\mathcal{S}_n \mathcal{C}_{(i} n_{j)}\frac{n_a}{r} - 4\delta_{ij}\mathcal{S}_a \mathcal{C}_b \frac{n_a n_b}{r} + 4\delta_{ij}\mathcal{C}_a \mathcal{S}_a \frac{1}{r}. \tag{B7d}$$

The time-dependent term arises because our coordinates are rotating relative to the local inertial frames of the external universe with angular velocity $\mathcal{C}_m$, and the body's angular momentum $\mathcal{S}_n$ refuses to rotate with them (it insists on remaining inertial).

(h) For $(M,\mathcal{S}_i)$ with $\mathcal{C}_{ab}$:

$$\gamma^1_{00} = 4\frac{M}{r}, \quad \gamma^1_{0i} = -2\varepsilon_{ipq}\mathcal{S}_p \frac{n_q}{r^2} - 4\varepsilon_{ipq}\mathcal{C}_{pa} n_{\langle a} n_{q\rangle} r^2, \quad \gamma^1_{ij} = 0; \tag{B8a}$$

$$\gamma^2_{00} = -16\mathcal{C}_{ab}\mathcal{S}_a n_b - 2\mathcal{C}_{ab}\mathcal{S}_c n_a n_b n_c - 12 n_b \frac{t^2}{r^2}\mathcal{C}_{ab}\mathcal{S}_a$$

$$+ \{12 n_b \mathcal{C}_{ab}\mathcal{S}_a\}, \tag{B8b}$$

$$\gamma^2_{0i} = 24\varepsilon_{ipq}\mathcal{C}_{aq}\mathcal{M}_a n_p r + 24\mathcal{C}_{aj}\mathcal{S}_a \frac{t}{r}, \tag{B8c}$$

$$\gamma^2_{ij} = 12(\mathcal{S}_a \mathcal{C}_{a(j} n_{i)} - \mathcal{C}_{a(i}\mathcal{S}_{j)} n_a + \mathcal{C}_{ij}\mathcal{S}_a n_a)$$

$$+ 6(2\mathcal{S}_b \mathcal{C}_{a(i} n_{j)} n_a n_b - \delta_{ij}\mathcal{C}_{ab}\mathcal{S}_c n_a n_b n_c). \tag{B8d}$$

The time-dependent terms are due to the force on the body caused by coupling of its spin angular momentum $\mathcal{S}_a$ to the external universe's curvature.

With these examples, it is clear that the algorithm A can be used easily to construct model spacetimes. The metric in the weak-field region can be written down in a straightforward manner once the multipoles of the chosen

spacetime have been specified. For example, for a Kerr black hole in an external universe (say, a quadrupolar external gravitational field), the metric can easily be written down showing explicitly the precession of the angular momentum of the hole.[12] This is the subject of an accompanying paper.

REFERENCES

[1] R. Beig, Acta. Phys. Austrian **53**, 249 (1981).

[2] V. A. Belinsky and V. E. Zakharov, Zh. Eksp. Teor. Fiz. **77**, 3 (1979) [Soc. Phys. JETP **50**, 1 (1979)]; I. Hauser and F. J. Ernst, J. Math. Phys. **21**, 1126 (1980); C. M. Cosgrove, J.Math. Phys. **21**, 2417 (1980); and references cited therein.

[3] A. I. Janis and E. T. Newman, J. Math. Phys. **6**, 902 (1965); N. G. J. Van der Burg, Proc. Roy. Soc. **A303**, 37 (1968); C. J. S. Clarke and D. W. Sciama, Gen. Rel. & Grav. **2**, 331 (1971).

[4] R. Geroch, J. Math. Phys. **11**, 2580 (1970); R.D. Hansen, J. Math. Phys. **15**, 46 (1974).

[5] R. Beig and W. Simon, Proc. R. Soc. London **A376**, 333 (1981); P. Kundu, J. Math. Phys. **22**, 1236 (1981); **22**, 2006 (1981); Y. Tanabe, Progr. Theor. Phys. **52**, 294 (1980).

[6] R. Beig and W. Simon, Gen. Rel. & Grav. **12**, 1003 (1980); R. Beig and W. Simon, Commun. math. Phys. **78**, 75 (1980); B.C. Xanthopoulos, J. Phys. A **12**, 1025 (1979).

[7] K.S. Thorne, Rev. Mod. Phys. **52**, 299 (1980).

[8] R. Beig and W. Simon, J. Math. Phys. **24**, 1163 (1983).

[9] Y. Gürsel, Gen. Rel. & Grav. **15**, 737 (1983).

[10] B.L. Schumaker and K.S. Thorne, Mon. Not. Roy. Astron. Soc. **203**, 457 (1983); K.S. Thorne and Y. Gürsel, Mon. Not. Roy. Astron. Soc. **205**, 809 (1983); L. S. Finn and K. S. Thorne, (in preparation); K. S. Thorne and J. B. Hartle, Phys. Rev. D. in press.

[11] Z.H. Zhang (in preparation).

[12] K.S. Thorne and J. B. Hartle, Ref. 10.

[13] Z.H. Zhang, Phys. Rev. D. submitted; also available as Caltech preprint GR.P-030.

[14] L. Blanchet and T. Damour (in preparation).

[15] L. Blanchet, Ph.D. thesis, 1984 (unpublished).

[16] F. A. E. Pirani, in *Lectures on General Relativity*, edited by A. Trautman, F. A. E. Pirani and H. Bondi, (Prentice-Hall, Englewood Cliffs, 1964)

[17] C.B. Morrey, Amer. J. Math. **80**, 198 (1958).

[18] See, e.g., W. B. Campbell and T. A. Morgan, Am. J. Phys. **44**, 356 (1975).

[19] H. Müller zum Hagen, Proc. Comb. Phil. Soc. **67**, 415 (1970).

[20] K.S. Thorne, R.H. Price, W.-M. Suen, D.A. Macdonald, I.H. Redmount, R.J. Crowley, X.-H. Zhang, Rev. Mod. Phys. (to be submitted).

[21] L.A. Mysak and G. Szekeres, Can. J. Phys. **44**, 617 (1966).

[22] R. Geroch and J.B. Hartle, J. Math. Phys. **23**, 4 (1982).

[23] W. Israel and K.A. Khan, Nuovo Cimento **33**, 331 (1964); W. Israel, Lett. Nuovo Cimento **6**, 267 (1973).

[24] H. Weyl, Ann. Phys. **54**, 117 (1917); J.L. Synage, *Relativity: The General Theory* (North Holland, Amsterdam, 1964).

[25] S. Weinberg, *Gravitation and Cosmology: Principles and Applications of the General Theory of Relativity* (John Wiley and Sons, New York, 1972).

[26] L. L. Smarr, Ph. D. Thesis, (unpublished).